ABSTRACT

CHAO, JINGYI. Transport Properties of Strongly Interacting Quantum Fluids: From CFL Quark Matter to Atomic Fermi Gases. (Under the direction of Thomas Schäfer.)

Kinetic theory is a theoretical approach starting from the first principle, which is particularly suit to study the transport coefficients of the dilute fluids. Under the framework of kinetic theory, two distinct topics are explored in this dissertation.

CFL Quark Matter We compute the thermal conductivity of color-flavor locked (CFL) quark matter. At temperatures below the scale set by the gap in the quark spectrum, transport properties are determined by collective modes. We focus on the contribution from the lightest modes, the superfluid phonon and the massive neutral kaon. We find that the thermal conductivity due to phonons is $\sim 1.04\times10^{26}\,\mu_{500}^{8}\,\Delta_{50}^{-6}$ erg cm^{-1} s^{-1} K^{-1} and the contribution of kaons is $\sim 2.81\times10^{21}\,f_{\pi,100}^{4}\,T_{\rm MeV}^{1/2}\,m_{10}^{-5/2}$ erg cm^{-1} s^{-1} K^{-1}. Thereby we estimate that a CFL quark matter core of a compact star becomes isothermal on a timescale of a few seconds.

Atomic Fermi Gas In a dilute atomic Fermi gas, above the critical temperature, T_c, the elementary excitations are fermions, whereas below T_c, the dominant excitations are phonons. We find that the thermal conductivity in the normal phase at unitarity is $\propto T^{3/2}$ but is $\propto T^2$ in the superfluid phase. At high temperature the Prandtl number, the ratio of the momentum and thermal diffusion constants, is 2/3. The ratio increases as the temperature is lowered. As a consequence we expect sound attenuation in the normal phase just above T_c to be dominated by shear viscosity.

Finally, We calculate the viscosity spectral function of the dilute atomic Fermi gas in three different channels. We find the expected structure consisting of a diffusive peak in the transverse shear channel and a sound peak in the longitudinal channel. At zero

momentum the width of the diffusive peak is $\omega_0 \simeq (2\varepsilon)/(3\eta)$ where ε is the energy density and η is the shear viscosity. At finite momentum the spectral function approaches the collisionless limit and the width is of order $\omega_0 \sim k(T/m)^{1/2}$.

Transport Properties of Strongly Interacting Quantum Fluids: From CFL Quark Matter to Atomic Fermi Gases

by
Jingyi Chao

A dissertation submitted to the Graduate Faculty of
North Carolina State University
in partial fulfillment of the
requirements for the Degree of
Doctor of Philosophy

Physics

Raleigh, North Carolina

2011

APPROVED BY:

John Blondin	Chueng Ji
Dean Lee	Wenbin Lu (ST)

Thomas Schäfer
Chair of Advisory Committee

BIOGRAPHY

The author was born in Yifeng, Jiangxi, China.

ACKNOWLEDGEMENTS

First and foremost I would like to express my deepest gratitude to my advisor Dr. Thomas Schaefer, for his thoughtful guidance during my graduate study. I would like to thank Dr. Schaefer, who led me to experience research from intuitive physics pictures to solid mathematic skills. I thank him for his patience, encouragement and support. I also thank him for the financial support as graduate student.

I would like to thank Dr. Dean Lee for helping me practice the presentation.

I would also like to thank Dr. John Blondin, Dr. Chueng Ji, Dr. Dean Lee and Dr. Wenbin Lu for serving on my oral defense committee and my dissertation reading committee. I greatly appreciate their time and effort.

I would like to thank Dr. Matt Braby for discussions and close collaborations.

Thank all my officemates. It would be a lonely office without you guys.

Thank all my friends for helping me go through the hardest time in my life; for helping me have a regular dinner schedule.

Thank my sisters for believing and bearing, and for everything that taken for me.

Last, but most important, I thank my father for him letting me know how to be a tough person; I thank my mother for her caring, worrying and considering. Thank my parents for their unconditional love and endless support.

TABLE OF CONTENTS

LIST OF TABLES

LIST OF FIGURES

Chapter 1

Introduction

1.1 Quantum Liquids

A fluid is, liquid or gas, a many body system in whose behavior not only determined by microscopic mechanics, but also those of statistics. In physics, with many particles, it is usually impossible to know the wave function of the whole system. As a result, it is often more useful to think in terms of macroscopic observable, such as transport coefficients, rather than microscopic states. Before calculating the magnitude of transport coefficients, below we will give some briefly introduction about several known fluids.

The main tool for studying the behavior of macroscopic systems in thermal equilibrium is thermodynamics. Away from equilibrium the two most important tools are hydrodynamics and kinetic theory. In this thesis we will use these tools to study non-equilibrium properties of strongly correlated quantum fluids. Quantum fluids are many body systems in which quantum mechanics not only governs the structure of the constituents (molecules, atoms, nuclei, etc.), but also their collective behavior. A rough criterion for the importance of quantum effects can be obtained from the particle-wave

correspondence. The quantitative relation is given by the de Broglie relation:

$$\lambda = \hbar/p \tag{1.1}$$

where p is the particle's momentum and λ is the particle's wavelength of the associated wave. In the case of a many-body particle system, another reasonable microscopic length is the interparticle distance, $d \sim n^{-1/3}$, where n is the density. Roughly speaking, the condition to see particle-wave effects is,

$$\lambda \geq d \tag{1.2}$$

On the other hands, the typical particle's momentum is determined by the thermal energy, $k_B T$, where

$$p \sim \sqrt{m k_B T} \tag{1.3}$$

Combing Eq. 1.1 and Eq. 1.3, we find out the condition for quantum mechanical effects to be important is below the temperature

$$k_B T \leq n^{2/3} \hbar^2 / m \tag{1.4}$$

where m is the mass of the atom, molecule or particle in question. With the estimation $n \sim 10^{23} \mathrm{cm}^{-3}$, it requires temperatures at a very low order of 20 K$/A$, much lower than the room temperatures, where A is the atomic or molecular weight.

As we have mentioned before, liquid is a composed system of particles which must be in either the gas or the liquid phase. Collecting these conditions, we have already known, in universal, the class of quantum liquids include:

1. electrons gases [11] in any solid or liquid metal.

2. the new state of hot, dense matter out of the quarks and gluons created by heavy ion collider, such as RHIC at BNL and LHC at CERN [12, 13, 14, 15].

3. atoms or molecules in their liquid or gaseous phase, which the known member are helium [16, 17, 18, 19] and the dilute alkali gases [20, 21, 22, 23].

4. in some regions of neutron stars, including nuclear and quark matter [24, 25, 26, 27].

The last two classes liquids, dilute alkali gases and the quark matter in neutron stars are our research topics in this thesis. I will detailed study them in chapter 4, 5 and 6. Therefore, I will briefly introduce the properties of the former two classes liquids and helium in the immediate next.

1.1.1 Fermi Liquids, Electron Gases

It is known that the kinetic energy of electron goes as $n^{3/2}$, whereas the Coulomb interaction between the electrons goes as $n^{1/3}$. We see that the ratio $V_{Coulomb}/E_K = n^{-1/3}$, named as the coupling constant in question. Hence, at high densities regime, $n \gg 1$, the interaction between electrons is neglected, then we have the free-electron (Fermi) gas. Or, perturbation theory can be used in discussed the properties of weakly interacting electron systems. The behavior of electrons in a white dwarf [28, 29] or neutrons in a neutron star can be approximated by treating them as an ideal Fermi gas. Something similar take place in the periodic systems, such as electrons moving in the crystal lattice of metals and semiconductors [30]. The notable features of this kind weakly interacting degenerate Fermi gases are: specific heat is proportional to T, the spin susceptibility is temperature independent and the shear viscosity $\sim T^{-2}$, as pointed out by Leggett [19].

However, for typical metals, $6 \leq n \leq 2$, in atom unit, the interactions are not weak enough. Fermi liquid theory [31, 32] (also known as Landau-Fermi liquid theory) is a theoretical model of interacting fermions that describes the normal state (in contrary to super state) of most metals at sufficiently low temperatures. Landau phenomenologically developed the idea of "quasiparticle" excitations in the context of interacting Fermi systems, and later Abrikosov and Kalatnikov [33] gave a formal derivation through perturbative method to higher orders. Landau suggested describing the excited states of the interacting system as a correspondence of the excited states of the noninteracting system. Starting from this noninteracting system with one particle added in state $\mathbf{p}$; to the ground state Fermi sea, then "switching on" the pair interactions adiabatically. The interactions do not effect on the total particle number, spin, and momentum. Thereby the particle become a quasiparticle with some effective mass m^* and must obey the Pauli exclusion. We note there that there is a finite lifetime of quasiparticles since the state given by this switch-on process will eventually decay into a collection of more complicated states. The energy of course is not preserved because the Hamiltonian is changed. The energy of a single quasiparticle state is just

$$\varepsilon_p = \frac{p^2}{2m^*} \tag{1.5}$$

We can see from the above equations that there is a one-to-one mapping of the quasiparticles with the single particles of the free electron gas.

Except this assumption, in the Fermi liquid theory, Landau made another important one: the interaction of the quasiparticles can be taken into account as a self-consistent field of surrounding particles, which leads to the fact that the total energy of the system does not equal the sum of energies of the N quasiparticles, but it is a functional of its

distribution function. This is reflected in the form,

$$\begin{aligned}\varepsilon(\mathbf{p},\sigma) &= \varepsilon_0(\mathbf{p},\sigma)+\delta\varepsilon(\mathbf{p},\sigma)\\ &= \varepsilon_0(\mathbf{p},\sigma)+\frac{1}{2}\mathrm{Tr}\int \mathrm{d}\Gamma f(\mathbf{p},\sigma;\mathbf{p}^{'},\sigma^{'})\delta n(\mathbf{p}^{'},\sigma^{'})\end{aligned} \tag{1.6}$$

where $\delta n = n - n_{T=0}$, σ is the notation of spin, $\varepsilon_0(\mathbf{p},\sigma)$ is the energy of the quasiparticles at zero temperature, and the second is the mean-field effect of the interactions with other quasiparticles. The function f is a very important characteristic of a Fermi liquid. Today, Landau's Fermi liquid theory is the foundation for the modern standard model of the weekly repulsive interactions fluid.

1.1.2 Nearly Perfect Fluid, Strongly Coupled QGP

It is predicted that if heat up the nuclei beyond the critical temperature, the quarks should come out from their parent hadrons and form a gas of hot and dense quark matter. Meanwhile, because of pair annihilation processes within the hot QGP system, there will be a lot of thermal gluons. This whole system is expected to behave like a plasma of quarks (anti-quarks) and gluons, called quark-gluon plasma (QGP) [34]. To date, the quark-gluon plasma has been created in heavy-ion collider. At RHIC, when two gold nuclei moving at nearly light speed, colliding, the amount of energy that dump in the microscopic fireball is about 2.0×10^4GeV, with an approximation of order 4×10^{12}K. The conditions of the early universe was recovered on a tiny scale.

Motivated by the asymptotic freedom of QCD at high energies, QGP was expected to behave like a weakly coupled gas. However, this hot and dense quark matter, instead of a gas, was confirmed to behave like a liquid in RHIC experiments [12, 13, 14, 15]. The anisotropic "elliptic" flow observed in non-central collisions is generated mostly during

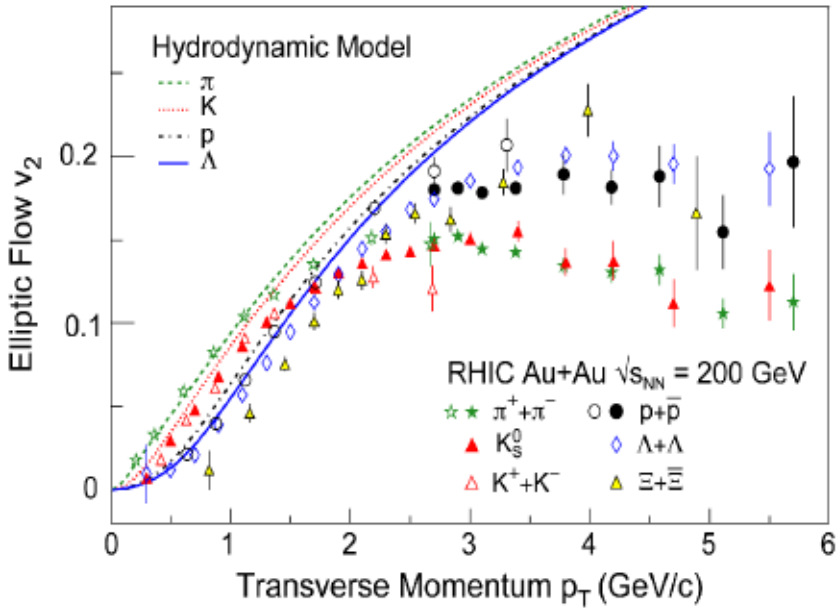

Figure 1.1: Elliptic flow v_2 for different hadron species [1, 2, 3], plotted as a function of transverse momentum, compared with ideal hydrodynamics predictions [4, 5]

the hot early stage, and thus provides the information about the QGP phase. The elliptic flow v_2 [35, 36, 37, 38] is defined as the 2nd Fourier coefficients of the azimuthal distribution of hadron spectra:

$$v_2(p_T) = \langle \cos(2\phi_p) \rangle \equiv \frac{\int \mathrm{d}\phi_p \cos(2\phi_p) \frac{\mathrm{d}N}{p_T \mathrm{d}y \mathrm{d}p_T \mathrm{d}\phi_p}}{\int \mathrm{d}\phi_p \frac{\mathrm{d}N}{p_T \mathrm{d}y \mathrm{d}p_T \mathrm{d}\phi_p}} \tag{1.7}$$

where $\frac{\mathrm{d}N}{p_T \mathrm{d}y \mathrm{d}p_T \mathrm{d}\phi_p}$ is the angular distribution of the transverse momentum (p_T) dependent spectra, and $y = \frac{1}{2} \ln \frac{E+p_L}{E-p_L}$ is the rapidity of the particles. Figure 1.1.2 compares the experimental elliptic flow data $v_2(p_T)$ with ideal hydrodynamic predictions For $p_T <$ 1.5GeV, where most (more than 98%) of the particles are produced, ideal hydrodynamics shows excellent agreement with the experimental data and correctly predicts the observed

splitting for different hadron species. Thus, such strongly coupled QGP behaves like not a gas but an almost perfect fluid. Besides, why the QGP is strongly coupled at RHIC energies is yet unknown.

1.1.3 Helium

Since the helium mass is very small and the attractive interaction between two atoms very weak, the pairing energy is $\sim 10^{-7}$ K at temperature of the order of 10^{-3} K, the helium atoms cannot form a lattice due to zero point energy even at zero temperature. In fact, solid helium requires a temperature of $1 \sim 1.5$ K and about 2.5 MPa pressure. This characteristic allows us to observe quantum effects on a macroscopic scale. There are eight known isotopes of helium, but only helium-3 and helium-4 are stable. Meanwhile, that Bose-Einstein statistics is important for understanding the behavior of superfluid ^{4}He, while Fermi-Dirac statistics is important for exploring that of ^{3}He.

Helium-3

Experiments show that between 100 mK and 3 mK the normal phase of liquid ^{3}He behaves like a weakly interacting degenerate Fermi gas. Landaus Fermi liquid theory, as we introduced above, provide a good description. However, ^{3}He form rich phases other than the ordinary weekly coupled Fermi gases at different conditions. As shown by Leggett [16], the atoms in ^{3}He form a pair, which has many similarities with the condensation of Cooper pairs in superconductivity. The main difference is that in superconductors, the attractive interaction between the two electrons is due to the exchange of phonon. Whereas in ^{3}He, there are no phonons available. To overcome the strong hard core repulsive interaction at short distances, the Cooper pairs composed by two ^{3}He atoms must be in a state with non-zero angular momentum L. The direct consequence is that

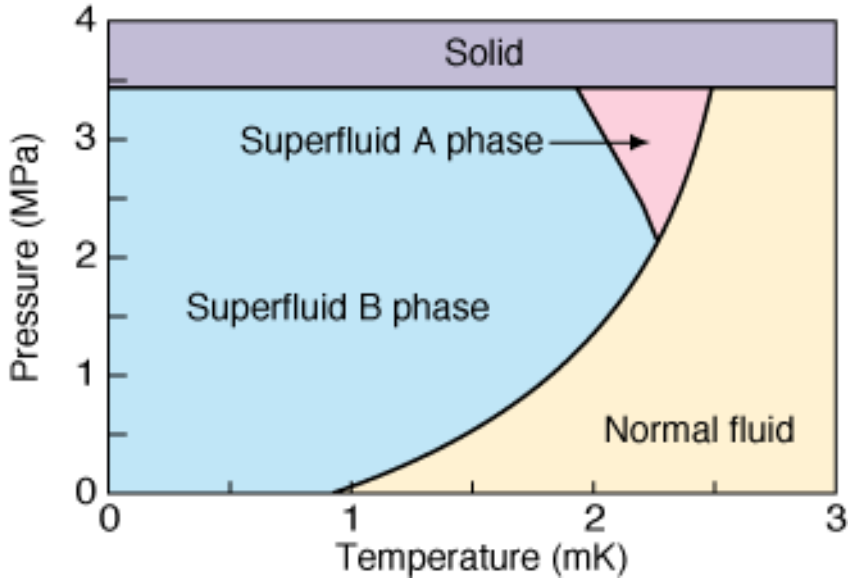

Figure 1.2: Helium Three, the phase diagram plotted as a function of temperature and pressure[6].

p-wave pairing is favorable. It also leads to a remarkable feature of ^{3}He that an each atom (quasiparticle) can be seen as carrying two vectors, one for spin, $SO(3)_S$, and one for orbital momentum, $SO(3)_L$. Hence, there has two distinct superfluid phases due to the different breaking patterns. If you think that both degrees of freedom as independent of each other, symmetries are broke by themselves in a common sense. This particular symmetry breaking pattern is named as A phase. But, if keep the relative orientation of spin and angular momentum being always the same, remaining a $SO(3)_{L+S}$ group after even both the symmetries of angular momentum and spin broken. This type of symmetry breaking is so-called B phase in ^{3}He. Only the phase with the lowest free energy will be realized in practice. It was shown by Balian and Werthamer [39], using the weak coupling approach, that the B-phase is the most stable one. Only at some higher temperatures and pressures regime, A phase is the most stable one determined by

strong coupling effects. This was shown by Anderson and Brinkman [40]. We show the phase diagram of ^{3}He in the Figure 1.1.3

Table 1.1: Phases in ^{3}He

	B phase	A phase
conditions	at lowest T and P	$T \sim 2$ mk, $P > 20$ MPa
spin states	$\|\uparrow\uparrow\rangle$, $\|\uparrow\downarrow\rangle + \|\downarrow\uparrow\rangle$, $\|\downarrow\downarrow\rangle$	$\|\uparrow\uparrow\rangle$, $\|\downarrow\downarrow\rangle$
gap	isotropic	anisotropic, $\Delta = 0$ in some directions
symmetry	Lock phase between L and S	L and S break individually

Helium-4

Helium four is the more common isotope of helium. Figure 1.1.3 shows the phase diagram of ^{4}He at low temperatures. ^{4}He remains liquid at zero temperature if the pressure is below 25 atmospheres. The liquid has a phase transition to a superfluid phase, also known as He-II, at the temperature of 2.17 K (at vapor pressure). The solid phase has either Hexagonal Close Packed (HCP) or Body Centered Cubic (BCC) symmetry.

At low temperatures($T_c = 2.17$ K), helium atoms condense into the ground state and enter a superfluid state due to Bose-Einstein condensation. The characteristic phenomena of superfluidity were experimentally discovered in the 1930s by Kapitza and Allen et al. [41, 42]. The idea of the two-fluid model was proposed by Landau [43] and Tisza [44], which has successfully explained the phenomena of superfluidity. According to the two-fluid model, the system consists of a superfluid (density ρ_s) and a viscous normal fluid (density ρ_n) with two independent velocity fields $\mathbf{v}_s$ and $\mathbf{v}_n$, respectively. The mixing ratio of the two fluids depends on the temperature. As the temperature is reduced below about 1 K, the ratio of the superfluid component increases, and the fluid becomes entirely

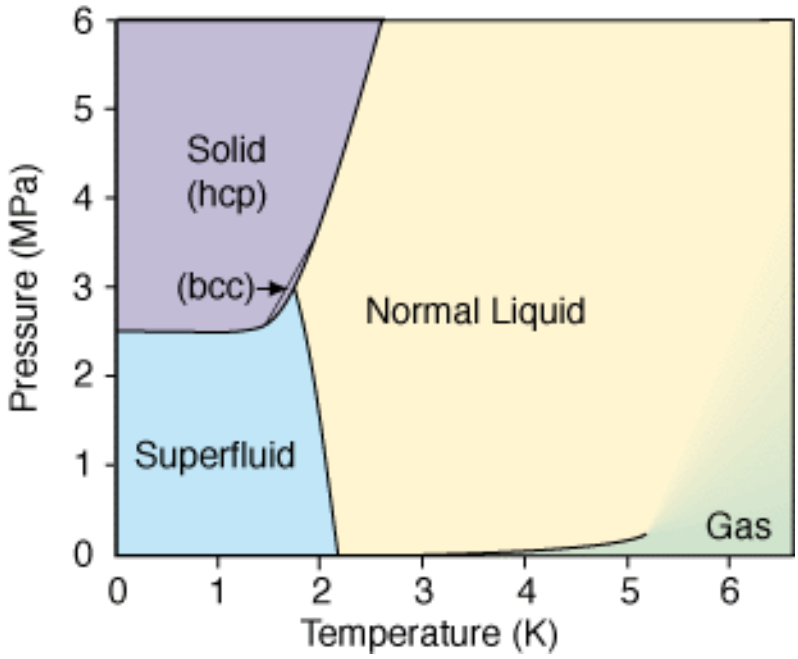

Figure 1.3: Helium Four, the phase diagram plotted as a function of temperature and pressure[6].

superfluid below.

1.2 Response to Gradient Perturbations

Consider that a fluid is in equilibrium at given uniform values of temperature, pressure and velocity. Gradients of these variables are controlled under perturbation. Meanwhile, the fluid responds to these gradients in a manner to restore equilibrium. Such coefficients, the ratio of the response to gradients of the perturbation, are called as transport coefficients, which are defined as follows.

1.2.1 Shear Viscosity

Classically, the shear viscosity is defined as the ratio between the friction force F per area and the transverse flow gradient, $\nabla_y V_x$,

$$\frac{F}{A} = \eta \nabla_y V_x \tag{1.8}$$

Microscopically, shear viscosity is associated with momentum transfer between particles in different fluid elements. For a dilute gas of non-relativistic particles, the shear viscosity η and entropy s are estimated as

$$\eta \sim \frac{m\bar{v}}{\sigma}, \qquad s \sim n, \tag{1.9}$$

where n is the particle density, m is the particle mass, σ is the cross section, and the entropy density s is proportional to the particle density n. The shear viscosity of a non-relativistic dilute gas increases with temperature with temperature $\eta \sim \sqrt{mT}$ and is approximately independent of density. Using the ideal gas EOS, $P = nk_BT$, thus, for fixed pressure, η/s increases with temperature approximately as

$$\eta/s \sim T^{3/2} \tag{1.10}$$

in the high temperature gas phase.

The density of a liquid decreases with temperature, which leads to an increase of shear viscosity due to the growth of mean free path. Detailed calculation [45, 46] shows that

$$\eta \sim n\hbar \mathrm{e}^{E/k_BT}, \qquad \eta/s \sim \hbar \mathrm{e}^{E/k_BT}, \tag{1.11}$$

where E is an activation energy and $\hbar$ is the Planck constant, and again entropy s is the typical function of density n. This result shows that for a liquid the ratio of η to s increases with decreasing temperature. Taking the liquid phase and gas phase together, Eq. 1.10 and Eq. 1.11 imply that η/s is likely to reach a minimum during the liquid-gas phase transition. This is confirmed by experimental results in three kinds fluids of helium, nitrogen and water.

1.2.2 Bulk Viscosity

In a dense gas, bulk viscosity is associated with the internal friction force arising from the change of volume at constant shape. Naively, we expect the bulk viscosity (like the shear viscosity) to be proportional to the mean free path. There are however, a number of scattering processes that do not contribute to bulk viscosity. An example is elastic $2 \Leftrightarrow 2$ scattering. As a consequence bulk viscosity is controlled by inelastic or particle number changing reactions.

In both monatomic and ultra-relativistic gases, the bulk viscosity vanishes or tends to zero. It also has been proved that the bulk viscosity must vanish in a scale invariant system [47], such as $N = 4$ SYM field. The reason is that the tensor space of bulk viscosity is not conformal invariant which is not allowed in a conformal system. In a mixed fluid, such as normal-super fluid model, there has additional three bulk viscosities. Similarly, following the same argument, two of them, ζ_1 and ζ_2, have to be vanish either, while the third one ζ_3 is allowed to be nonzero [47].

In contrast to shear viscosity arrive in a minimum in the vicinity of the gas-liquid phase transition, the bulk viscosity shows a peak near the phase transition. Such behavior of the bulk viscosity of spherical molecules was studied by Meier, Laesecke and Kabelac using molecular-dynamics simulations with Lennard-Jones potentials [48]. Recently work

[49] confirms that the same holds true for relativistic QCD matter.

1.2.3 Thermal Conductivity

Thermal conductivity, κ, is the property of a material describing its ability to conduct heat, which defined as

$$\mathbf{q} = -\kappa \nabla T \tag{1.12}$$

The negative sign inherits from the reason that the heat flow would persist until a state of uniform temperature is reached. The higher the conductivity, the shorter the time for this relaxation. Classically, the estimate with mean free path l gives [50]

$$\kappa \sim c_V \bar{v} / \sigma \tag{1.13}$$

where c_V is the specific heat. For the non-relativistic dilute gas, we have

$$\kappa \sim \frac{\sqrt{T/m}}{\sigma} \tag{1.14}$$

At a given temperature, the thermal conductivity is seen to be independent of the gas density, i.e. of the gas pressure. It must be emphasized that this important property is not related to the assumptions used in making the estimate, but is an exact consequence of the kinetic theory, which only takes account of collision between pairs of particles in the dilute gases.

1.3 Organization of the Thesis

In chapter 2 a short overview of the phenomena mathematical models, hydrodynamic, is presented. This chapter serves to orient the reader in the relevant method of collective mode, conservation laws and continuity equations. Chapter 3 introduce the systematical framework that is used in our recent works, kinetic theory. The following three chapters address our research topics, and can be read independently of each other. Chapter 4 introduces the cooling mechanism of neutron stars and estimate the thermal conductivity of the quark matter, which possibly exists in the core of neutron stars. In chapter 5, the thermal conductivity of a cold, dilute atomic gas is explored; an improved experimental way is proposaled to help extracting observation data more explicitly. In chapter 6 the contributions toward the development of the viscose spectral function are reported. A short summary and outlook is provided in chapter 7.

Chapter 2

Mathematical Models

The mathematical description of the state of a fluid is determined by five macroscopic variables, the fluid velocity $\mathbf{v} = \mathbf{v}(t, \mathbf{r})$ and any two thermodynamic quantities of the fluid, for example the pressure $P(t, \mathbf{r})$ and the density $\rho(t, \mathbf{r})$. It must be true that five hydrodynamics equations appear as the existence of the conservation laws of mass, momentum and energy. Together with the equation of state, the macroscopic state of the fluid is completely known without detailed information of the microscopic dynamics. Hence, hydrodynamics is a well suited macroscopic approach for studying strongly coupled systems while the underlying microscopic theory is unknown.

2.1 Hydrodynamic Equation

We briefly summarize how to derive the fundamental equations of fluid dynamics. These conservation equations typically arise from the form [51]

$$\frac{\partial A}{\partial t} + \nabla \cdot \mathbf{\Gamma}_A = 0 \tag{2.1}$$

where $\mathbf{\Gamma}_A = A\mathbf{v}$ is a flux vector corresponding to the quantity A. The quantity A of fluid in given volume is $\int A\mathrm{d}V$, which flowing in unit time through the surface element $\mathrm{d}\mathbf{S}$ is $A\mathbf{v}\cdot\mathrm{d}\mathbf{S}$, where the magnitude of the vector $\mathrm{d}\mathbf{S}$ is equal to the area of the surface element, and its direction is along the normal. Therefore, the total quantity A of fluid flowing out of the volume V in unit time is

$$\oint A\mathbf{v}\cdot\mathrm{d}\mathbf{S} \tag{2.2}$$

where the integration is taken over the whole of the closed surface surrounding the volume in question.

Next, the decrease per unit time in the quantity A of fluid in the volume V can be written

$$-\frac{\partial}{\partial t}\int A\mathrm{d}V \tag{2.3}$$

Taking the integration over the volume V and employing Gauss's theorem

$$\oint A\mathbf{v}\cdot\mathrm{d}\mathbf{S} = \int \nabla\cdot(A\mathbf{v})\mathrm{d}V \tag{2.4}$$

thus, it lead the general continuity equation.

$$\int\left[\frac{\partial A}{\partial t} + \nabla\cdot(A\mathbf{v})\right]\mathrm{d}V = 0 \tag{2.5}$$

Since this equation must hold for any volume, the integration must vanish, i.e. Eq. 2.1 is present.

Consider the mass density, $\rho(\mathbf{x},t)$ and macroscopic fluid density, $\mathbf{v}(\mathbf{x},t)$, which defined

by

$$\begin{aligned} \rho &= \int m f \mathrm{d}V \\ \rho \mathbf{v} &= \int \mathbf{p} f \mathrm{d}V \end{aligned} \tag{2.6}$$

where $\mathbf{p}$ is the momentum of fluid cells and f is the distribution function of fluid cells. It obey the mass continuity equation:

$$\frac{\partial \rho}{\partial t} + \nabla \cdot \mathbf{j} = 0 \tag{2.7}$$

where the vector $\mathbf{j} = \rho \mathbf{v}$ is called the mass flux density. Its direction is that of the motion of the fluid.

Similarly, consider the energy density, $\varepsilon(\mathbf{x}, t)$, pressure tensor P^{ij} and macroscopic heat flux, $\mathbf{q}(\mathbf{x}, t)$, which given by

$$\begin{aligned} \varepsilon &= \int \frac{m v^2}{2} f \mathrm{d}V \\ \Pi^{ij} &= \int v^i p^j f \mathrm{d}V \\ q^i &= \int \frac{m v^2 v^i}{2} f \mathrm{d}V \end{aligned} \tag{2.8}$$

Conservation of momentum yields

$$\frac{\partial}{\partial t}\left(\rho v^i\right) + \nabla_j \Pi^{ji} = \rho \, Q^i \tag{2.9}$$

where Q^i is the external force field. The conservation equation for energy is given by

$$\frac{\partial \varepsilon}{\partial t} + \nabla \cdot \mathbf{q} = \rho \, \mathbf{Q} \cdot \mathbf{v} \tag{2.10}$$

If the equilibrium distribution function f_0 is used in deriving the equations of motion, Eq. 2.7, Eq. 2.9 and Eq. 2.10 describe the motion of an ideal fluid, in which the dissipation terms ignored. In other words, no gradients of temperature or velocity are included in the conserved momentum or energy currents, which may occur in a moving fluid as the consequence of internal friction in the fluid and heat exchange between different parts of it. Therefore, a fluid is said to be ideal if its thermal conductivity and viscosity are tend to zero. It also means an ideal fluid must be adiabatic without the heat exchange between different parts of the fluid. In adiabatic motion the entropy of any particle of fluid remains constant. We can express the condition for adiabatic motion as

$$\mathrm{d}s/\mathrm{d}t = 0 \tag{2.11}$$

Using Eq. 2.1, we can write it as an equation of continuity for entropy

$$\partial(\rho s)/\partial t + \nabla \cdot (\rho s \mathbf{v}) = 0 \tag{2.12}$$

Here the product $\rho s \mathbf{v}$ is the entropy flux density.

2.2 Navier-Stokes Equations

When an external perturbation is applied to a simple fluid, the disturbance is damped by the relaxation processes in the system. In a macroscopic view, these dissipation

phenomena are diffusion, viscous flows, and thermal conduction. To obtain the equations of a viscous fluid, it is straight to include some dissipative terms in the equation of ideal fluid. Multiplying by $\mathbf{r}$ to the both sides of the equation of mass continuity Eq. 2.7 and integrating over the fluid volume, one have

$$\frac{\mathrm{d}\left(\int \rho\ \mathbf{r}\ \mathrm{d}V\right)}{\mathrm{d}t} = \int \mathbf{j}\ \mathrm{d}V \tag{2.13}$$

and since the L.H.S. of above equation determines the position of the center of mass. It is clear the R.H.S. is the momentum of fluid. In other words, Eq. 2.7 is equally valid for any fluid. On the other hand, the equations of momentum and energy motion are required to modify.

The Navier-Stokes (N-S) Equations [51] are the equations of motion of a viscous fluid. In the ideal momentum equation Eq. 2.9, the momentum flux Π_{ij} represents a completely reversible transfer of momentum. However, to describe the irreversible momentum transfer, caused by internal friction, an additional viscous tensor is therefore to be added to the "ideal" momentum flux. One obtains the momentum flux density in the form

$$\Pi_{ik} = P\delta_{ik} + \rho v_i v_k - \sigma_{ik} \tag{2.14}$$

The general form of σ_{ik} can be established as follows. 1) The internal friction transfer the momentum from the points where the velocity is large to those where it is small. Hence, σ_{ik} must depend on the space derivatives of the velocity and first order one is enough if the gradients of velocity are small. 2) There can be no term which independent of $\partial v_i/\partial x_k$, since σ_{ik} would vanish when velocity is same in everywhere. 3) Uniform rotation with angular velocity $\mathbf{\Omega}$ does not lead to viscous tensor σ_{ik} since no internal

friction occurs in the fluid. The sums

$$\frac{\partial v_i}{\partial x_k} + \frac{\partial v_k}{\partial x_i} \tag{2.15}$$

vanish when $\mathbf{v} = \mathbf{\Omega} \times \mathbf{r}$. Therefore, σ_{ik} must only contain these symmetrical combinations of the derivatives $\partial v_i / \partial x_k$. Hence, one write down the most general tensor of rank two satisfying above conditions,

$$\sigma_{ik} = \eta \left(\frac{\partial v_i}{\partial x_k} + \frac{\partial v_k}{\partial x_i} - \frac{2}{3} \delta_{ik} \frac{\partial v_i}{\partial v_i} \right) + \zeta \delta_{ik} \frac{\partial v_i}{\partial v_i} \tag{2.16}$$

where η and ζ are both positive and independent of the velocity, which are valid for most fluid. η and ζ are named as shear and bulk viscosities, respectively.

Thus, the equation of motion of a viscous fluid is obtained by adding σ_{ik} into Eq. 2.9. Combining with the mass continuity equation, after some simple algebra calculation, one produce the expression of N-S equation,

$$\rho \left[\frac{\partial v^i}{\partial t} + v^k \nabla_k v^i \right] = -\nabla^i P + \nabla_k \sigma^{ki} \tag{2.17}$$

2.2.1 Energy Dissipation from N-S equations

In an ideal fluid the energy conservation law is expressed by

$$\frac{\partial}{\partial t} \left(\frac{1}{2} \rho v^2 + \rho \varepsilon \right) = -\partial_i \left(\frac{\rho v^2 v^i}{2} + \rho w v^i \right) \tag{2.18}$$

where ε is the internal energy and $w = \varepsilon + P$ is the heat function. When the gradients of temperature in the fluid is not large, one can expand the heat flux q^i as a series of powers of the temperature gradients. The constant term always rules out since heat flux

vanish when $\partial^i T$ is zero. Therefore, to the first order, one have

$$q^i = -\kappa \partial^i T \tag{2.19}$$

where κ is positive, named as thermal conductivity. Thus, the total energy flux in a fluid is given by $\frac{\rho v^2 v^i}{2} + \rho w v^i - v_k \sigma^{ik} - \kappa \partial^i T$. Thereby, the conservation law of energy is rewrite as,

$$\frac{\partial}{\partial t}\left(\frac{1}{2}\rho v^2 + \rho\varepsilon\right) = -\partial_i\left(\frac{\rho v^2 v^i}{2} + \rho w v^i - v_k \sigma^{ik} - \kappa \partial^i T\right) \tag{2.20}$$

On the other hands, calculating the time derivative of the energy in unit volume of fluid, one have

$$\frac{\partial}{\partial t}\left(\frac{1}{2}\rho v^2 + \rho\varepsilon\right) = \frac{v^2}{2}\partial_t \rho + \rho v^i \partial_t v_i + \rho \partial_t \varepsilon + \varepsilon \partial_t \rho \tag{2.21}$$

Substituting the equations of continuity and the expression of $\partial v^i/\partial t$, which arisen from the N-S equation, one obtains

$$\frac{\partial}{\partial t}\left(\frac{1}{2}\rho v^2 + \rho\varepsilon\right) = -\frac{v^2}{2}\partial_i(\rho v^i) - \rho v^i \partial_i(\frac{v^2}{2}) - v^i \partial_i P + v_i \partial_k \sigma^{ik} + \rho \partial_t \varepsilon - \varepsilon \partial_i(\rho v^i) \tag{2.22}$$

Using the thermodynamic relation $\mathrm{d}\varepsilon = T\mathrm{d}s + P/\rho^2 \mathrm{d}\rho$, one finds $\frac{\partial \varepsilon}{\partial t} = T\frac{\partial s}{\partial t} - \frac{P}{\rho^2}\partial_i(\rho v^i)$. Next, from the thermodynamic relation $\mathrm{d}w = T\mathrm{d}s + \mathrm{d}P/\rho$, one has $\partial_i P = \rho \partial_i w - \rho \partial_i s$. It also very useful to rewrite the term $v_i \partial_k \sigma^{ik} = \partial_k\left(v_i \sigma^{ik}\right) - \sigma^{ik}\partial_k v_i$. Finally, one obtains

$$\begin{aligned}\frac{\partial}{\partial t}\left(\frac{1}{2}\rho v^2 + \rho\varepsilon\right) &= -\partial_i\left(\frac{\rho v^2 v^i}{2} + \rho w v^i - v_k \sigma^{ik} - \kappa \partial^i T\right) \\ &\quad + \rho T\left(\frac{\partial s}{\partial t} + v^i \partial_i s\right) - \partial_i v_k \sigma^{ik} - \kappa \partial_i \partial^i T\end{aligned} \tag{2.23}$$

Comparing with the equation of energy motion Eq. 2.20, it leads to the equation of the

entropy dissipative motion,

$$\rho T\left(\frac{\partial s}{\partial t}+v^{i}\partial_{i}s\right)=\partial_{i}v_{k}\sigma^{ik}+\kappa\partial_{i}\partial^{i}T \tag{2.24}$$

Expanding the term $\partial_i v_k \sigma^{ik}$ by substituting the expression of σ_{ik}, the entropy equation thus becomes

$$\rho T\left(\frac{\partial s}{\partial t}+v^{i}\partial_{i}s\right)=\kappa\partial_{i}\partial^{i}T+\frac{\eta}{2}\left(\partial_{i}v_{k}+\partial_{k}v_{i}\right)^{2}+\zeta\left(\partial_{i}v^{i}\right)^{2} \tag{2.25}$$

It is clearly that the R.H.S. of Eq. 2.25 is always positive, which implied by the second thermodynamic law

$$\frac{\mathrm{d}s}{\mathrm{d}t}\geq 0 \tag{2.26}$$

2.3 Israel-Stewart Equations

Together with equation of state and well formulated boundary conditions, the Navier-Stokes equations successfully model the fluid motion, even turbulent flows seem to agree with real world observations (on average). Unfortunately, the N-S equations suffer from the unphysical instability in relativistic fluids; the instability is attributed to the lack of the causality and lead to infinite speed of signal propagation. It is a necessary to invent a fluid dynamical equation which contains the second-order time-derivative as well as the first-order one. The new equation called Israel-Stewart equation [52, 53, 54] introduces new transport coefficients like the relaxation time yet to be determined microscopically or phenomenologically. The Israel-Stewart second order theory of relativistic fluids are derived basing on Grad's 14-moment expansion method, which will introduce in the Chapter 3. The resulting equations are hyperbolic and lead to causal propagations. The

formulation of relativistic hydrodynamics can be found in standard text books. Here I only list the results from the recently works by Muronga [55, 56].

Firstly, the notation of the macroscopic variables are present through a covariant way,

$$\begin{aligned}
\varepsilon & \quad \text{energy density}, \\
P & \quad \text{pressure}, \\
\mathcal{D} = u^\mu \partial_\mu & \quad \text{convection time depravation}, \\
\nabla^\mu & \quad \text{gradient operator}, \\
\theta & \quad \text{volume expansion}, \\
u^\mu & \quad \text{four velocity}, \\
a^\mu & \quad \text{four acceleration}, \\
\pi^{\mu\nu} & \quad \text{viscous stress tensor}, \\
q^\mu & \quad \text{heat flow},
\end{aligned} \tag{2.27}$$

where $\Delta^{\mu\nu} = g^{\mu\nu} - u^\mu u^\nu$ is the projection tensor orthogonal to the four velocity and $g^{\mu\nu} = \text{diag}(+1, -1, -1, -1)$ is the metric tensor in Minkowski space time. In the Eckart theory [57] the dissipative contribution to the bulk pressure, the heat flux and the shear viscous tensor are given by

$$\begin{aligned}
\langle \pi \rangle &= \zeta\theta, \\
q^\mu &= \kappa T(\nabla^\mu \ln T - a^\mu), \\
\pi^{\mu\nu} &= 2\eta\nabla^{\langle\mu} u^{\nu\rangle}
\end{aligned} \tag{2.28}$$

where ζ, κ and η are the bulk, thermal conductivity and shear coefficients respectively. T is the temperature of the system. The angular bracket notation is defined by

$$A^{\mu\nu} \equiv \frac{1}{2}\left(g^{\mu\alpha}g^{\nu\beta} + g^{\mu\beta}g^{\nu\alpha} - \frac{2}{3}g^{\mu\nu}g^{\alpha\beta}\right)A_{\alpha\beta} \tag{2.29}$$

The truncated energy equation governing fluid motion, called as Müller-Israel-Stewart [52, 53, 54] equations, is given by

$$\begin{aligned}
\mathcal{D}\langle\pi\rangle &= -\frac{1}{\tau_{\langle\pi\rangle}}\langle\pi\rangle + \frac{1}{2\beta_0}\langle\pi\rangle\left(\beta_0\theta + T\mathcal{D}\frac{\beta_0}{T}\right) - \frac{1}{\beta_0}\theta + \frac{\alpha_0}{\beta_0}\nabla_\mu q^\mu, \\
\mathcal{D}q^\mu &= -\frac{1}{\tau_q}q^\mu + \frac{1}{2\beta_1}q^\mu\left(\beta_1\theta + T\mathcal{D}\frac{\beta_1}{T}\right) + \frac{1}{\beta_1}\left(\frac{\nabla^\mu}{T} - a^\mu\right) - \frac{\alpha_1}{\beta_1}\nabla_\nu\pi^{\mu\nu} - \frac{\alpha_0}{\beta_1}\nabla^\mu\langle\pi\rangle, \\
\mathcal{D}\pi^{\mu\nu} &= -\frac{\pi^{\mu\nu}}{\tau_\pi} + \frac{1}{2\beta_2}\pi^{\mu\nu}\left(\beta_2\theta + T\mathcal{D}\frac{\beta_2}{T}\right) + \frac{1}{\beta_2}\nabla^{\langle\mu}u^{\nu\rangle} + \frac{\alpha_1}{\beta_2}\nabla^{\langle\mu}q^{\nu\rangle},
\end{aligned} \tag{2.30}$$

where

$$\tau_{\langle\pi\rangle} = \zeta\beta_0, \quad \tau_q = \kappa T\beta_1, \quad \tau_\pi = 2\eta\beta_2 \tag{2.31}$$

are the relaxation times, β_0, β_1 and β_2 are the relaxation coefficients and α_0 and α_1 are the coupling coefficients. These five new coefficients are functions of primary thermodynamic variables like pressure, number density and energy density and hence depend on the equation of state. Relaxation time is the distinguishing feature of hyperbolic causal theories which is not present in the first-order theories. Here τ is the time taken by the corresponding dissipative flux to relax to its steady-state value.

2.4 A Word at the End

Hydrodynamic equations have developed significant contributions to phenomenologically approach the non-equilibrium statistical mechanics of a dense and strongly coupled system through the evolution of macroscopic states. However, it is a fundamental task for theorists to investigate the physical systems from the knowledge of their underlying microscopic dynamics. In next chapter, we will introduce the kinetic theory, a method starting from the first principle. In fact, it was a central topic of kinetic theory to derive macroscopic descriptions, i.e., hydrodynamic equations, during its development.

Chapter 3

Kinetic Theory

3.1 Introduction

In a weakly coupled quantum or classical system, one would expect to be able to compute most physical observable by the fundamental knowledge of particle interactions. Kinetic theory does be the method which has natural advantages from the mathematical point of view. Thus, kinetic theory is particular well suited to studying the dynamical properties of dilute or moderately dense gases. However, this approach will break down in the dense regime. Therefore, it is an very important further work to establish a principle understanding to connect two approaches, hydrodynamics and kinetic theory.

An overview of kinetic theory that form the background of the thesis shall be provided in this chapter.

3.2 Quasi-particle Excitation

The purpose of kinetic theory is to model the time evolution of a collection of particles. The particles may be entirely different objects depending on the physical situation. For instance, the particles are atoms and molecules in a neutral gas or electrons and ions in a plasma. A great development of many body systems, was the concept of the quasiparticle, as a basic element to understand the low-energy excitations of many-body systems. Firstly, the term quasiparticle appears in Boguilubov's [58] paper on the theory of superfluidity in 1947. However, the idea of treating quasiparticle as the fundamental element in a complicated system is usually associated with Landau's pioneering work on the Fermi liquid theory [31], in 1957. Later, the concept of quasiparticle has become the fundamental assumption of kinetic theory.

A characteristic feature of kinetic theory is that the dynamical evolution of system are described by the Boltzmann's Equation in terms of the quasiparticle's distribution functions $f = f(t, \mathbf{r}, \mathbf{p})$, which represent the density of particles at given space-time position $(t, \mathbf{r})$ and momentum $\mathbf{p}$. In terms of a given potential function and known equilibrium distribution function, one obtains a directly calculation on any macroscopic states, by analyzing the microscopic details of particle collisions. In this respect, kinetic theory provides a microscopic trustable way to calculate observable quantities.

3.3 BBGKY Hierarchy

3.3.1 Liouville's Equation

In physics, Liouville's theorem [50, 59] is a key theorem in classical statistical and Hamiltonian mechanics. Assume we have a problem of N particles moving in the Hamiltonian,

it asserts that the phase-space distribution function f_N is constant along the trajectories of the system,

$$f_N = f_N(\mathbf{q}_1, \mathbf{p}_1, \mathbf{q}_2, \mathbf{p}_2, ...\mathbf{q}_N, \mathbf{p}_N, t) \tag{3.1}$$

In other words, the density of system in phase space remains constant along a dynamic trajectory. The time evolution of f_N obeys the Liouville's equation as

$$\begin{aligned} \frac{\mathrm{d}f_N}{\mathrm{d}t} &= \frac{\partial f_N}{\partial t} + [f_N, H] \\ &= \frac{\partial f_N}{\partial t} + \sum_{i=1}^{3N} \left(\frac{\partial f_N}{\partial q^i} \dot{q}^i + \frac{\partial f_N}{\partial p_i} \dot{p}^i \right) \end{aligned} \tag{3.2}$$

and in equilibrium:

$$[f_N, H] = 0 \tag{3.3}$$

where H is the Hamiltonian and the bracket is the Poisson bracket in classical physics. The density function f_N is contained in the infinitesimal volume element $\mathrm{d}^{3N}p\, \mathrm{d}^{3N}q$. And the expected total number of particles is expressed by:

$$N = \int f_N(\mathbf{q}_1, \mathbf{p}_1, \mathbf{q}_2, \mathbf{p}_2, ...\mathbf{q}_N, \mathbf{p}_N)\ \mathrm{d}^{3N}p\ \mathrm{d}^{3N}q \tag{3.4}$$

3.3.2 The BBGKY Hierarchy

In statistical physics, the BBGKY hierarchy [60, 50, 59, 61] (Bogoliubov-Born-Green-Kirkwood-Yvon hierarchy, sometimes called Bogoliubov hierarchy) is a set of equations describing the dynamics of a system of a large number of interacting particles. The equation in terms of the particle distribution function form a coupled chain of equations in the BBGKY hierarchy. Such infinite tower of coupled integro-differential equations are relating the joint distribution function $f_s(1, 2, ...s)$, $s < N$, to distribution function

f_{s+1} by integrating over the phase volume $\mathrm{d}\Gamma_{s+1}\mathrm{d}\Gamma_{s+2}...\mathrm{d}\Gamma_N$.

Assume that the Hamiltonian is of the form

$$\mathcal{H} = \sum_{i=1}^{N} \frac{p^2}{2m} + \sum_{i=1}^{N} U_i + \sum_{i<j}^{N} U_{ij} \tag{3.5}$$

The first two equation of the hierarchy read [60, 50]

$$\begin{aligned}
&\left(\frac{\partial}{\partial t} + \mathbf{v}_1 \cdot \nabla_{\mathbf{r}_1} + \mathbf{F}_1 \cdot \nabla_{p_1}\right) f_1(\mathbf{p}_1, \mathbf{r}_1, t) = -\int \mathrm{d}\Gamma_2 \mathbf{K}_{12} \cdot \nabla_{p_1} f_2(\mathbf{p}_1, \mathbf{r}_1, \mathbf{p}_2, \mathbf{r}_2, t) \\
&\equiv \widehat{A}_1 f_2(\mathbf{p}_1, \mathbf{r}_1, \mathbf{p}_2, \mathbf{r}_2, t), \\
&\left(\frac{\partial}{\partial t} + \mathbf{v}_1 \cdot \nabla_{\mathbf{r}_1} + \mathbf{F}_1 \cdot \nabla_{p_1} + \mathbf{v}_2 \cdot \nabla_{\mathbf{r}_2} + \mathbf{F}_2 \cdot \nabla_{p_2} + \frac{1}{2}\mathbf{K}_{12} \cdot (\nabla_{p_1} - \nabla_{p_2})\right) f_2(\mathbf{p}_2, \mathbf{r}_2, t) \\
&= -\int \mathrm{d}\Gamma_3 \left(\mathbf{K}_{13} \cdot \nabla_{p_1} + \mathbf{K}_{23} \cdot \nabla_{p_2}\right) f_3(\mathbf{p}_1, \mathbf{r}_1, \mathbf{p}_2, \mathbf{r}_2, \mathbf{p}_3, \mathbf{r}_3, t),
\end{aligned} \tag{3.6}$$

where

$$\begin{aligned}
\mathbf{F}_i &= -\nabla_{\mathbf{r}_i} U(\mathbf{r}_i), \\
\mathbf{K}_{ij} &= -\nabla_{\mathbf{r}_i} U_{ij}(|\mathbf{r}_i - \mathbf{r}_j|),
\end{aligned} \tag{3.7}$$

To date, existence and uniqueness results for the BBGKY hierarchy in nonrelativistic physics have been proved. The BBGKY hierarchy allows one to describe both equilibrium and non-equilibrium states of many-particle systems from a common point of view. Non-equilibrium states are characterized by the solutions of the initial condition for this hierarchy; and equilibrium states are characterized by the solutions of the steady BBGKY hierarchy.

If we truncate the chain of BBGKY hierarchy at some level s, expressing f_s in terms

of equal or lower order distributions, then we obtain a closed set of equations which in principle can be solved, at least numerically. Truncation of the BBGKY chain is the starting point of kinetic theory that can be used for derivation of classical or quantum kinetic equations. In particular, it is used to derive classical and quantum Boltzmann equations if truncating at the first equation; get the first order of density correction if truncating at the second equation.

3.4 The Boltzmann Transport Equation

3.4.1 Collisional Invariants

Truncate BBGKY hierarchy equation to the first sequence, we obtain the generic form for all kinetic equations. A kinetic equation is a closed equation since each particle molecule constitutes a closed subsystem. Performing the assumption

$$\widehat{A}_1 f_2(\mathbf{p}_1, \mathbf{r}_1, \mathbf{p}_2, \mathbf{r}_2, t) = C(f_1) \tag{3.8}$$

it leads to the Boltzmann equation, where C is the collisions integral involve only two particles. We now explicit write down the form of Boltzmann equation as:

$$\frac{\partial f}{\partial t} + \mathbf{v} \cdot \nabla \mathbf{f} + \mathbf{F} \cdot \nabla_p f = C[f] \tag{3.9}$$

Here we have ignore the script of 1 because of the closure.

The transport equation becomes meaningful only after the form of the collision integral has been established. Let us consider collision between two particles, one of which has phase space of Γ in a given range $\mathrm{d}\Gamma_1$ represented by distribution function f_1, and

the other one in a range $\mathrm{d}\Gamma_2$ represented byf_2, and which acquire in the collision values in the ranges $\mathrm{d}\Gamma_1'$ and $\mathrm{d}\Gamma_2'$, represented by $f_{1'}$ and $f_{2'}$, respectively. Subtracting the losses from the gains, thus the number of collisions $\Gamma_1\Gamma_2 \Leftrightarrow \Gamma_1'\Gamma_2'$ per unit time and volume have the following expression:

$$\int C[f_1]\mathrm{d}\Gamma_1 = \int W(f_1'f_2' - f_1f_2)\mathrm{d}\Gamma_1\mathrm{d}\Gamma_2\mathrm{d}\Gamma_1'\mathrm{d}\Gamma_2' \tag{3.10}$$

The function of W is given by solving the underlying mechanical collision of interacting particles. Therefore, the transport equation is written as

$$\partial f/\partial t + \mathbf{v}\cdot\nabla f = \int W(f_1'f_2' - f_1f_2)\mathrm{d}\Gamma_2\mathrm{d}\Gamma_{1'}\mathrm{d}\Gamma_{2'} \tag{3.11}$$

without the external force. This integro-differential equation is also called the Boltzmann-equation; it was first derived by Ludwig Boltzmann, the founder of the kinetic theory, in 1872.

The collision term in the Boltzmann equation violates time reversal invariance even if the underlying dynamics is invariant under time reversal. This, of course, is in agreement with the second law of thermodynamics, which in the context of kinetic theory is a consequence of Boltzmann's H theorem. The time reversal invariance of the microscopic dynamics is reflected in symmetries of the collision operator. We can show, for example, that for a any given function ϕ, it has a transformation rule [1],

$$\int \phi(\Gamma)\ C[f]\mathrm{d}\Gamma = \frac{1}{4}\int(\phi_1 + \phi_2 - \phi_{1'} - \phi_{2'})W f_1f_2(1+\alpha f_{1'})(1+\alpha f_{2'})\ \mathrm{d}^{(4)}\Gamma \tag{3.12}$$

[1]It is not all the collision process would have such symmetry. For example, the number is not conserved in the phonon's split process.

where $\alpha = -1$ is denoted for Bose, $\alpha = +1$ for fermi and $\alpha = 0$ for Maxwell statistical distribution functions.

3.4.2 Macroscopic Variables and Conservation Equations

We shall show how the transport equation can be converted into the usual equation of fluid mechanics, as we have introduced in chapter 2, macroscopic description of this time variation. The description is valid when the macroscopic properties (temperature, density, velocity, etc.) of the particle vary sufficiently slowly through its volume: the vary distance L of system must be much greater that free mean path l of the collision. Then, fluid dynamics can be systematically derived if this condition has been satisfied. Note the ration of l to L is named as Knudsen number, Kn.

If the number of the quasi-particle is conserved. The spatial distribution density of particles is,

$$n(t, \mathbf{r}) = \int f(t, \mathbf{r}, \Gamma) \, \mathrm{d}\Gamma \tag{3.13}$$

The product $\rho = mn$ is correspondingly the mass density of the particles. The macroscopic velocity of the particle denoted by $\mathbf{V}$; it is defined as the mean value of

$$\rho \mathbf{V} = \int \mathbf{p} f \mathrm{d}\Gamma \tag{3.14}$$

Collisions do not alter either the number of colliding particle or their energy and momentum. It is therefore clear that the collisional part of the changes in the distribution function cannot affect the macroscopic quantities in the corresponding volume of the

density, internal energy, and macroscopic velocity $\mathbf{V}$ of particles, i.e.

$$\int C[f]\ \mathrm{d}\Gamma = 0 \tag{3.15}$$

$$\int \epsilon\ C[f]\ \mathrm{d}\Gamma = 0 \tag{3.16}$$

$$\int \mathbf{p}\ C[f]\ \mathrm{d}\Gamma = 0 \tag{3.17}$$

These equation are easily derived by applying to the integrals the transformation Eq. 3.12 with $\phi = 1, \epsilon, \mathbf{p}$ respectively; the first integral is zero identically, the other two are zero by virtue of the conservation of energy and momentum in collisions.

Let us now take the transport equation in the form of

$$\frac{\partial f}{\partial t} + \frac{\partial}{\partial x_\alpha}(v_\alpha f) = C[f] \tag{3.18}$$

and integrate over $\mathrm{d}\Gamma$ after first multiplying by m, p_β or ϵ. In every case, the R.H.S. is zero, and we have continuity equations

$$\frac{\partial \rho}{\partial t} + \nabla \cdot (\rho \mathbf{V}) = 0 \tag{3.19}$$

$$\frac{\partial (\rho V_\alpha)}{\partial t} + \frac{\partial \Pi_{\alpha\beta}}{\partial x_\beta} = 0 \tag{3.20}$$

$$\frac{\partial \varepsilon}{\partial t} + \nabla \cdot \mathbf{q} = 0 \tag{3.21}$$

The first of these is the usual continuity equation of fluid mechanics, expressing the conservation of mass of the particles. The second equation expresses the conservation of momentum; the tensor $\Pi_{\alpha\beta}$ is defined as

$$\Pi_{\alpha\beta} = \int m v_\alpha v_\beta f \mathrm{d}\Gamma \tag{3.22}$$

and is the momentum flux tensor. Lastly, Eq. 3.21 is the equation of conservation of energy; the vector $\mathbf{q}$ defined as

$$\mathbf{q} = \int \epsilon \mathbf{v} f \mathrm{d}\Gamma \tag{3.23}$$

and ε is the energy flux in the system.

Two variant of perturbative methods are widely used for deriving the higher orders of fluid dynamic equations. The method of Grad's Momentum Expansion [62, 59, 61] stems from the BBGKY hierarchy. Another way, called as Chapman-Enskog Expansions Method [59, 61, 50], is related the expansion of small parameter Kn.

3.4.3 Grad's Momentum Expanding Method

In the Grad's momentum approach, the Boltzmann equation is replaced by a set of moment equations, i.e., the distribution function of the s order tensor is determined by the all other distribution function of higher order tensors $s+1, s+2, ...N$. Which and how many moments are needed depends on the particular process, but experience shows that the number of moments must be increased with increasing Knudsen number [59, 63, 64].

For the closure of the equations, the phase density is approximated by an expansion in Hermite polynomials about the equilibrium distribution, where the coefficients are related to the moments.

$$f = f_0 + f_0' \delta f, \qquad f_0' = \frac{\partial f_0}{\partial E_p} \tag{3.24}$$

where $\delta f \ll 1$,

$$\delta f = \epsilon(\mathbf{x}, t) + \epsilon_i(\mathbf{x}, t) p^i + \epsilon_{ij}(\mathbf{x}, t) p^i p^j + ... \tag{3.25}$$

Note that the scalar, vector and tensor ϵ, ϵ_i and ϵ_{ij} are related to the macroscopic

dissipative flows. It is convenient to define the nth moment by

$$f^{(n)} = \int \mathbf{c}^n f \mathrm{d}\Gamma \tag{3.26}$$

where all the measurement of higher momentums with respect to the intrinsic velocity

$$c^i(\mathbf{p}, \mathbf{x}, t) = \frac{p^i}{m} - u^i(\mathbf{x}, t), \tag{3.27}$$

where $u^i(\mathbf{x}, t)$ is the velocity of the fluid. For example, the second, third, fourth momentum are defined by

$$P_{ij}(\mathbf{x}, t) = \int c_i c_j f \mathrm{d}\Gamma \tag{3.28}$$

$$S_{ijk}(\mathbf{x}, t) = \int c_i c_j c_k f \mathrm{d}\Gamma \tag{3.29}$$

$$Q_{ijkl}(\mathbf{x}, t) = \int c_i c_j c_k c_l f \mathrm{d}\Gamma \tag{3.30}$$

By their definitions, the momentums are symmetric in their subscripts. There are $\frac{1}{2}(n+1)(n+2)$ distinct momentums of order n.

Substituting the expression of Eq. 3.25 into the Boltzmann equation, one find that the nth order tensor $f^{(n)}$

$$f^{(n)} = \int \mathbf{c}^{(n)} f \mathrm{d}\Gamma \tag{3.31}$$

satisfy the differential equations

$$\frac{\partial f^{(n)}}{\partial t} + \frac{\partial}{\partial x_i}\left(u_i f^{(n)} + f_i^{(n+1)}\right) + \frac{\partial \mathbf{u}}{\partial x_i} f_i^{(n)} - \frac{1}{\rho} f^{(n-1)} \partial^i f_i^{(2)} = J^{(n)} \tag{3.32}$$

where

$$J^{(n)} = \int \mathbf{c}^{(n)} W (f_1' f_2' - f_1 f_2) \mathrm{d}\Gamma_2 \mathrm{d}\Gamma_{1'} \mathrm{d}\Gamma_{2'} \tag{3.33}$$

While the full hierarchy of momentum equations should correspond to the original Boltzmann equation, it is too complicated to be treated exactly. However, an approximate evolution equation for systems not too far from equilibrium may be constructed. For simplicity, we consider a fluid with only shear viscosity, neglecting bulk viscosity and heat conductivity, which simplifies the expansion of δf as

$$\delta f(\mathbf{x}, t) = \tau_\pi \pi_{ij} p^i p^j \tag{3.34}$$

where π_{ij} is the shear viscosity. Asserting the first and third momentum $f^{(1,3)} = 0$, after employing the relaxation time approximation for the collision term:

$$C[f] = -\frac{f - f_0}{\tau_\pi} \tag{3.35}$$

and integrating out the phase space, one could read the Eq. 3.32 and therefore find the simplified second order I-S equations,

$$\delta\Pi_{ij} = \pi_{ij} - \tau_\pi \left(\dot{\pi}_{\langle ij \rangle} + V^k \nabla_k \pi_{ij} + \frac{4}{3} \pi^{ij} \nabla_k V^k + \frac{\pi^{ik}\omega_k^j}{2\eta} + \frac{\pi^{ik}\pi_k^j}{2\eta} \right) \tag{3.36}$$

where ω_{ij} is the vorticity tensor, $\omega_{ij} = 2\eta(\nabla_i V_j - \nabla_j V_i)$. The relaxation time τ_π and shear viscosity η are no longer independent from each other.

3.4.4 Chapman-Enskog Expansions Method

The possibility of an explicit calculation of viscosity and heat conductivity was realized in 1917, when Chapman and Enskog developed the Chapman-Enskog method [59] for solving the Boltzmann equation. In the Chapman-Enskog method, the distribution function is expanded in powers of the Knudsen number, i.e., $f = f_0 + \mathrm{Kn} \cdot f_1 + (\mathrm{Kn})^2 \cdot f_2 + ...$,

where f_0 is the local equilibrium distribution. To zeroth-order the expansion yields the Euler equations. A remarkable success of kinetic theory is recovering the macroscopic Navier-Stokes equations [60, 64, 65, 66]. The Navier-Stokes equations are based on the Chapman-Enskog expansion to the corresponding first-order correction of equilibrium distribution function. Moreover, the second-order expansion yields the Burnett equations [67, 68], and the third-order expansion yields the so-called Super-Burnett equations [63]. The Navier-Stokes equations cease to be accurate for Knudsen numbers above 0.05, and one is led to think that Burnett and Super-Burnett equations are valid for larger Knudsen numbers.

Chapman-Enskog method yields a linear integral equation for the deviation f_1, which is proportional to the gradients of T and u, and provides explicit expressions for the heat conductivity and viscosity. Below we will derive the solutions of the transport coefficients associated with demonstrating the procedure of Chapman-Enskog expansions method to the first order.

3.5 Transport Coefficients

3.5.1 Constrains on the Corrected Distribution Function

In order to take account of dissipative processes in a slightly inhomogeneous system, we must go to the next approximation beyond that treated in 3.4.2. In stead of regarding the distribution function in each region of the system as just the local-equilibrium function f_0, putting

$$f = f_0 + \delta f, \qquad \delta f = (\partial f/\partial \varepsilon_p)\chi(\Gamma) = f_0\chi/\ T \tag{3.37}$$

where f_0 is the Maxwell distribution function and δf is a small correction ($\ll f_0$). The correction δf is determined by solving the linearized Boltzmann transport equation. The function χ must satisfy not only the transport equation itself but also certain additional conditions. The reason is that f_0 is the equilibrium distribution function corresponding to given values of the system number, energy and momentum densities, i.e. to given values of the integrals

$$\int f_0 \mathrm{d}\Gamma, \qquad \int \varepsilon f_0 \mathrm{d}\Gamma, \qquad \int \mathbf{p} f_0 \mathrm{d}\Gamma \tag{3.38}$$

Therefore, to persist conservation laws of mass, momentum and energy, the function χ must satisfy the conditions

$$\int f_0 \chi \ \mathrm{d}\Gamma = 0, \qquad \int f_0 \chi \epsilon \ \mathrm{d}\Gamma = 0, \qquad \int f_0 \chi \mathbf{p} \ \mathrm{d}\Gamma = 0 \tag{3.39}$$

It is emphasized that the concept of the temperature becomes entirely rigorous only when the system as a whole is in complete equilibrium. To define the temperature in a non-equilibrium system, a further condition is necessary.

The above constrains also can be derived from another side. Let us transform the collision integral in the transport equation Eq. 3.11. When the function Eq. 3.37 are substituted, the terms not containing the small correction χ cancel, since the equilibrium distribution function makes the collision integral zero. The first order terms give

$$C[f] = f_0 I(\chi) / \ T \tag{3.40}$$

where $I(\chi)$ denotes the linear integral operators

$$I(\chi) = \int W f^{(1)} f^{(2)} (\chi_{1'} + \chi_{2'} - \chi_1 - \chi_2) \, \mathrm{d}\Gamma_2 \mathrm{d}\Gamma_{1'} \mathrm{d}\Gamma_{2'} \tag{3.41}$$

Here we have used equation $f^{(1)} f^2 = f^{(1')} f^{(2')}$. The integral Eq. 3.41 is identically zero for the functions

$$\chi = \text{constant}, \qquad \chi = \text{constant} \times \varepsilon \qquad \chi = \mathbf{p} \cdot \delta \mathbf{V} \tag{3.42}$$

where $\mathbf{V}$ is a constant vector.

3.5.2 The Solutions of Transport Coefficients

Write down the equilibrium distribution function

$$f_0 = \left(\exp \left[\frac{\varepsilon_p - \mathbf{V} \cdot \mathbf{p} - \mu}{T} \right] \pm 1 \right)^{-1} \tag{3.43}$$

where $+, -$ are for Fermi and Bose distribution respectively; μ is the chemical potential. In a slightly inhomogeneous system, f_0 depends on the coordinates and the time, as a result of the variation through the system of its macroscopic properties: the velocity $\mathbf{V}$, the temperature T and the pressure P (and therefore μ). Since the gradients of these quantities are assume small, it is sufficient (in this approximation) to replace f by f_0 on the left of the transport equation.

The calculation can be somewhat simplified by noting the obvious fact that the kinetic coefficients, our real subject of interest, do not depend on the magnitude of velocity $\mathbf{V}$, but its gradients. It is therefore simplified to choose the fluid velocity being $\mathbf{V} = 0$, but, of course, its derivatives is nonzero.

Differentiating the expression Eq. 3.43 with respect to time and then inserting $\mathbf{V} = 0$, we obtain

$$\frac{\partial f_0}{\partial t} = \frac{f_0(1 \pm f_0)}{T} \left\{ \left[\left(\frac{\partial \mu}{\partial T} \right)_P + \frac{\varepsilon_p - \mu}{T} \right] \frac{\partial T}{\partial t} + \left(\frac{\partial \mu}{\partial P} \right)_T \frac{\partial P}{\partial t} + m\mathbf{v} \cdot \frac{\partial \mathbf{V}}{\partial t} \right\} \tag{3.44}$$

By the familiar formulate of thermodynamics,

$$(\partial \mu / \partial T)_P = -s, \quad (\partial \mu / \partial P)_T = 1/n, \tag{3.45}$$

where s and $1/N$ are the entropy and volume per particle. Hence

$$\frac{\partial f_0}{\partial t} = \frac{f_0(1 \pm f_0)}{T} \left\{ \frac{\varepsilon_p - \mu - Ts}{T} \frac{\partial T}{\partial t} + \frac{1}{n} \frac{\partial P}{\partial t} + m\mathbf{v} \cdot \frac{\partial \mathbf{V}}{\partial t} \right\} \tag{3.46}$$

Similarly,

$$\mathbf{v} \cdot \nabla f_0 = \frac{f_0(1 \pm f_0)}{T} \left\{ \frac{\varepsilon_p - \mu - Ts}{T} \mathbf{v} \cdot \nabla T + \frac{1}{n} \mathbf{v} \cdot \nabla P + m v^\alpha v^\beta V_{\alpha\beta} + \frac{1}{3} m v^2 \nabla \cdot \mathbf{V} \right\} \tag{3.47}$$

where for brevity

$$V_{\alpha\beta} = \frac{1}{2} \left(\frac{\partial V_\alpha}{\partial x_\beta} + \frac{\partial V_\beta}{\partial x_\alpha} \right) - \frac{1}{3} \delta_{\alpha\beta} \nabla \cdot \mathbf{V}, \tag{3.48}$$

Here we remind the Eq. 3.19

$$\frac{\partial n}{\partial t} = -n \nabla \cdot \mathbf{V} \tag{3.49}$$

Combing with the continuity equation of motion of entropy, $\partial s / \partial t = 0$ for ideal fluids, one has

$$\frac{\partial T}{\partial t} = -\frac{T c_s^2 \alpha}{c_P} \nabla \cdot \mathbf{V} \tag{3.50}$$

under the help of the thermodynamic formula

$$\frac{\partial s}{\partial T}\Big|_n = \frac{c_V}{T}, \qquad \frac{\partial s}{\partial n}\Big|_T = -\frac{c_s^2}{n\gamma}\alpha \tag{3.51}$$

where α is the thermal expansion coefficient, c_s^2 is the speed sound of fluid, c_V, c_P are specific heat of constant volume and pressure, respectively, and $\gamma = c_P/c_V$. At the same time, from Eq. 3.20, one has

$$\frac{\partial \mathbf{V}}{\partial t} = -\frac{1}{mn}\nabla P \tag{3.52}$$

A straightforward calculation leads to the result

$$\begin{aligned}\frac{\partial f_0}{\partial t} + \mathbf{v}\cdot\nabla f_0 &= \frac{f_0(1\pm f_0)}{T}\left\{\frac{\varepsilon_p - w}{T}\mathbf{v}\cdot\nabla T + mv^\alpha v^\beta V_{\alpha\beta}\right\} \\ &\quad + \frac{f_0(1\pm f_0)}{T}\left[\varepsilon_p\left(\frac{2}{3} - \frac{c_s^2\alpha}{c_P}\right) + c_s^2\frac{w\alpha - c_P}{c_P}\right]\nabla\cdot\mathbf{V}\end{aligned} \tag{3.53}$$

where $w = \mu + Ts$ is the heat function.

Since the Boltzmann equation must be valid for any magnitude of vector, the gradients of velocity and/or temperatures, its solutions must only reply on their own corresponding vector spaces. In another words, the Boltzmann equation decouples to several independent equations according to the existence of external inhomogeneous sources. We benefit it if ignore all other vectors while trying to calculate one particular transport coefficients.

The Solution of Shear Viscosity

To calculate the shear viscosity, we read Eq. 3.52 as,

$$mv^\alpha v^\beta V_{\alpha\beta} = I[\chi] \tag{3.54}$$

It lead to the solution of this equation is sought in the form

$$\chi = g^{\alpha\beta} V_{\alpha\beta} \tag{3.55}$$

where $g^{\alpha\beta}$ is a symmetric and traceless tensor, for example, $g^{\alpha\beta} = a_0 \left(p^\alpha p^\beta - \delta^{\alpha\beta} p^2/3\right)$. Besides, this solution satisfy the constraint conditions Eq. 3.39 automatically. One can consider a fuller tensor to get a more accurate results, such as $g^{\alpha\beta} = \sum_{n=0} a_n p^{2n} \left(p^\alpha p^\beta - \delta^{\alpha\beta} p^2/3\right)$.

The Solution of Bulk Viscosity

To calculate the bulk viscosity, we read Eq. 3.52 as,

$$\left[\varepsilon_p \left(\frac{2}{3} - \frac{c_s^2 \alpha}{c_P}\right) + c_s^2 \frac{w\alpha - c_P}{c_P}\right] \nabla \cdot \mathbf{V} = I[\chi] \tag{3.56}$$

Before we explore the solution of this equation, we note the L.H.S. of above equation is zero in monotonic gases. It can be checked by use its thermodynamic properties: $c_P = 5/2$, $c_V = 3/2$, $c_s^2 = 5T/3$, $\alpha = 1/T$, and $w = c_P T$. The solution of equation $I[g] = 0$ is $g = 0$ and therefore $\zeta = 0$, as we have mentioned before. In other fluids while the L.H.S. is not zero, the form of solution is $\chi = \sum_{n=1} a_n p^{2n} p^2 \nabla \cdot \mathbf{V}$. The term start from $n = 1$ because of $a_0 p^2$ being ruled out by constraint conditions Eq. 3.39.

The Solution of Thermal Conductivity

To calculate the thermal conductivity, we read Eq. 3.52 as,

$$\frac{\varepsilon_p - w}{T} \mathbf{v} \cdot \nabla T = I[\chi] \tag{3.57}$$

Hence, the solution is in the form

$$\chi = \mathbf{g} \cdot \nabla \mathbf{T} \tag{3.58}$$

To satisfy the constrain condition

$$\int f_0 \mathbf{v} \cdot \mathbf{g} = \mathbf{0} \tag{3.59}$$

the suitable form is $\mathbf{g} = \sum_{n=1} a_n p^{2n} \mathbf{v}$.

If the transported equation has been solved and the function of χ is known. The transport coefficients can be determined by the corresponding tensor flux, for instance, momentum flux and heat flux.

Chapter 4

Quark Matter in the CFL Phase

4.1 Introduction

In this chapter, we will explore the thermal conductivity of quark matter in the regime of large baryon density and low temperature. It is expected that cold dense quark matter is a color superconductor, and that at asymptotically high density the ground state of three-flavor quark matter is the color-flavor locked (CFL) phase [7]. The work described in this chapter is part of an ongoing research effort with the goal of determining the transport properties of not only the CFL phase, but also of other, less dense, phases of quark matter. Previous work has focused on the shear viscosity [69], bulk viscosity [70, 71], and neutrino emissivity of the CFL phase [72, 73]. A general discussion of the kinetics of a CFL superfluid is given in [74]. There are also calculations of the transport properties of unpaired quark matter [75, 76, 77], and some results for the transport properties of a kaon condensed CFL phase [70]. The long term goal is to connect these calculations of transport properties to possible observational signatures of high density quark matter phases in the core of compact stars.

The thermal conductivity of dense matter plays an important part in the cooling of compact stars [78, 79, 80]. The cooling history of a star depends on the rate of energy loss by neutrino emission from the bulk and, at very late times, photon emission from the surface, on the specific heat, and on the thermal conductivity. Thermal conductivity determines how quickly different layers of the star become isothermal. It is generally assumed that the core of the star becomes isothermal very quickly, but that the outer crust is a poor conductor of heat and may take several hundreds of years to reach the temperature of the inner core [81, 82, 83]. In order to verify that this is true for CFL quark matter core we have to compute the thermal conductivity of CFL matter. There is an earlier calculation of the thermal conductivity of the CFL phase [84]. This calculation was based on a simple mean free path estimate. In the present chapter we will perform a more definitive calculation based on the linearized Boltzmann equation. We will show that while the mean free path estimate is not reliable, the main conclusion of [84] is valid, i.e., a CFL quark matter core becomes isothermal on a very short time scale.

This chapter is organized as follows. In section 4.2, We will briefly review the phase diagram of QCD matter, as a function in terms of temperature and density. In section 4.3, the formation of Color Superconductor is discussed. We will sketch the properties of CFL phase and the cooling mechanism of neutron star in section 4.4 and 4.5, respectively. In Section 4.6 and 4.7, We will outline the calculation of the thermal conductivity in kinetic theory, in Section 4.8 we will discuss the interaction among the light excitations and derive the associated collision terms, and in Section 4.9 We will present numerical results. We will end with some conclusions in Section 4.10.

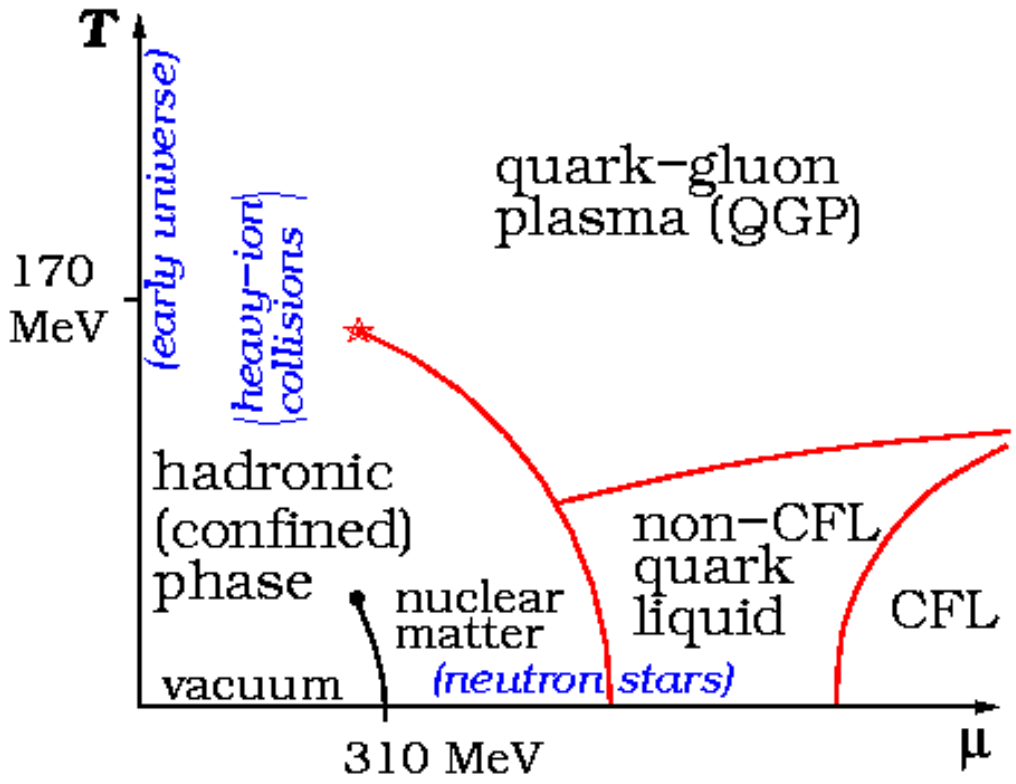

Figure 4.1: Sketched phase diagram of QCD matter as the function of temperature and density [7].

4.2 QCD Matter

4.2.1 Overview of the Quark Matter Phase Diagram

Our universe stared from a very hot, dense state according to the Big Bang theory. After cooling down, the universe transited through a cross-over into the normal hadronic phase. This is the main reason why we are so interested in investigating the extreme systems of Quantum ChromoDynamics (QCD) matter, where quarks are out of the ordinary hadronic phase. The phase diagram of quark matter is not well known, either experimentally or theoretically. A commonly sketched phase diagram, Figure 4.1, of quark matter

is shown in the work of [7]. In this diagram, every point represents a thermal equilibrium system of quarks and gluons at given temperature T and a quark chemical potential μ, where $\rho \sim \mu^3$ and ρ is the particle number density.

Hot QCD Matter

When the universe was only a few tens of microseconds old, the phase of matter was in a hot phase of quark matter, quark-gluon plasma, which is a gas of quarks, anti-quarks, gluons, and some lighter particles such as photons, electrons, positrons, etc. Predicted by the lattice gauge theory [85], the confined quark matter could be heat up and pass through a phase transition to the quark gluon plasma state around $T = 170$ MeV. As we introduced in section of 1.1.2, through collisions of heavy nuclei at ultra-relativistic energies one accomplished to rebuild the situation of the early universe in the laboratory [13, 14, 15].

Dense QCD Matter

Let us now turn to the region of phase diagram, a special interest in this thesis, moving along the horizontal line to explore the cold and dense matter in Figure 4.1. There is a first-order nuclear liquid-gas phase transition [86] around $\mu = 310$MeV. If one keeps squeezing matter further and further, nucleons will overlap. Eventually, nuclear matter transit to quark matter associated with chiral symmetry restore. Color Super-Conductivity, (CSC) [7], another stage of quark matter appears in the cold and dense region. At the highest densities, one found the Color-Flavor-Locking (CFL) phase [87], a state of Color Super-Conductivity involving in paring among three flavors quarks. CFL phase features chiral symmetry breaking, which distinguishes with two flavors quark CSC. Unlike QGP can be created in laboratory, the cores of neutron stars are the only

the places where the color conductor quark matter could exist in universal.

4.3 Color Super-Conductivity

Following the Landau fermi liquid theory, it is a first guess that quarks form a degenerate fermi gases at very cold but dense state. However, the interaction between quarks must be weak at the large densities, which is determined by asymptotic freedom. Furthermore, there of course has some special channels that the interaction between quarks is attractive, since quarks are able to combine together and form bound states, such as baryons. Therefore, it is more sensible to expect Color Super-Conductivity will onset at cold dense QCD matter.

The idea of color superconductivity was detailed studied by Bailin and Love [88], in 1984. In the recent years, a major upsurge of interest were performed in dense quark matter and color superconductivity (for recent reviews see ref. [7, 89]). The phase structure of QCD at high density depends on the number of flavors and there are two very interesting cases, corresponding to two flavors [90, 91] and to three flavors [87] quark matter, respectively.

4.3.1 Attracting Forces in QCD

The fundamental interaction between electrons (Coulomb interaction) is repulsive. Superconductivity show up as a consequence due to the effective attractive phonon interactions at very low temperatures. In the cuprate superconductors with high critical temperature, the mechanism is yet unknown. In color superconductivity, by contrast, the attractive interaction is a primary force in $\bar{\mathbf{3}}$ channel. This leads to two benefits: 1) the form of the condensate and associated energy spectrum can be calculated from first

principles. 2) the ratio of the gap scale to the Fermi surface energy will be much greater than the ordinary metal superconductor. Therefore, we predicted that the observing signals of Color Superconductor is stronger than in metals [7].

The thermodynamics of a quark matter at nonzero baryon density is described by QCD Lagrangian with a nonzero chemical potential μ

$$\mathcal{L}_{QCD} = \bar{\psi}_i^\alpha(\mathrm{i}\gamma^\mu\partial_\mu + \gamma^0\mu - m_i)\psi_i^\alpha + gA_\mu^l\bar{\psi}_i^\alpha\gamma^\mu T_{\alpha\beta}^l\psi_i^\beta - \frac{1}{4}\mathrm{Tr}F_{\mu\nu}^l F_{\mu\nu}^l \tag{4.1}$$

where $A_\mu = A_\mu^l T_l$, $F_{\mu\nu}$ is the gauge field strength with T_l as the $SU(N_c)$ generator in its fundamental representation, and ψ is a Dirac spinor with both color and flavor indices. The mass matrix m of quarks is diagonal with respect flavor indices. The running coupling constant is evaluated at the chemical potential,

$$g = \frac{24\pi^2}{(11N_c - 2N_f)\ln\frac{\mu}{\Lambda_{QCD}}} \tag{4.2}$$

where $N_f < \frac{11}{2}N_c$ and $\mu \gg \Lambda_{QCD}$.

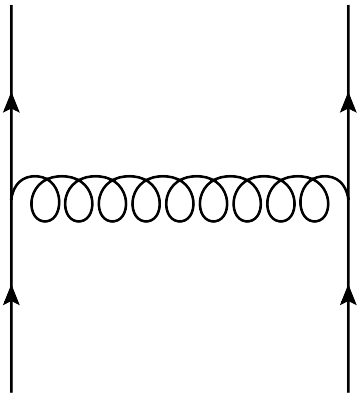

Figure 4.2: The one-gluon exchange vertex.

Single gluon exchange dominate the process between two quarks at the vicinity of Fermi surface, as shown in Figure 4.2. Decompose the group factor $T_l^{c_1 c_{1'}} T_l^{c_2 c_{2'}}$ into a color anti-symmetric channel ($\bar{\mathbf{3}}$) and a color symmetric one ($\mathbf{6}$),

$$T^l_{c_1 c_{1'}} T^l_{c_2 c_{2'}} = -\frac{N_c+1}{4N_c}(\delta_{c_1 c_{1'}}\delta_{c_1 c_{1'}} - \delta_{c_1 c_{2'}}\delta_{c_2 c_{1'}}) + \frac{N_c-1}{4N_c}(\delta_{c_1 c_{1'}}\delta_{c_1 c_{1'}} + \delta_{c_1 c_{2'}}\delta_{c_2 c_{1'}}) \quad (4.3)$$

which clearly indicate that the color anti-symmetric channel of one-gluon exchange interaction is attractive because of the negative sign of the group theoretic factor. The color $\bar{\mathbf{3}}$ is the dominant interaction at high densities QCD matter. The instanton interaction, among light quarks discovered by 't Hooft [92], is also attractive in the $\bar{\mathbf{3}}$ channel, which is important at lower densities. In a word, we should expect the formation of a condensate in a color $\bar{\mathbf{3}}$ channel.

4.3.2 Pairing Symmetry

The gap parameter appearing in the quark spectrum, depend on the Dirac, chiral, color and flavor indices of pairing quarks. Zero angular momentum Cooper pairs [93], $\langle \psi^{c_1}_{f_1} C\gamma_5 \psi^{c_2}_{f_2} \rangle$, allow quarks to participate in the pairing at all angles on the entire Fermi-sphere. Hence, it is the most favorite diquark condensate and the pairs of quark of equal helicity is antisymmetric in exchanging Dirac indices. Since the condensate should acquire a negative sign with respect to interchanging all quantum numbers, the sign under the exchange of their color and flavor indices must be positive, i.e.

$$\psi^{c_1}_{f_1}\psi^{c_2}_{f_2} = \psi^{c_2}_{f_1}\psi^{c_1}_{f_2} \quad (4.4)$$

Given three colors and three flavors in the chiral limit, in which the masses of the u, d

and s quarks are set to zero, if one define a $SU(3)$ rotation among flavor indices combining with that among color indices, the representation contents of the diquark condensate can be decomposed into a set of irreducible representations under a simultaneous $SU(3)$ rotation of both color and flavor indices. This pairing symmetry is called as the color-flavor locking (CFL). The diquark condensate of CFL pairing takes the form [87]

$$\langle \psi^{c_1}_{f_1} C\gamma^5 \psi^{c_2}_{f_2} \rangle = \phi_A \epsilon^{c_1 c_2 A} \epsilon_{f_1 f_2 A} + \phi_S (\delta^{c_1}_{f_1} \delta^{c_2}_{f_2} + \delta^{c_2}_{f_1} \delta^{c_1}_{f_2}) \tag{4.5}$$

The two invariants $\phi_{A,S}$ correspond to the two unit representation. It was found in that the magnitude of ϕ_S is smaller than ϕ_A, which is suppressed by the coupling constant.

Overall, the symmetry breaking pattern is

$$SU(3)_c \otimes \underbrace{SU(3)_R \otimes SU(3)_L}_{\supset U(1)_Q} \otimes U(1)_B \to \underbrace{SU(3)_{c+R+L}}_{\supset U(1)_{\widetilde{Q}}} \otimes Z_2 \tag{4.6}$$

The gauge potential corresponding to this unbroken $U(1)_{\widetilde{Q}}$ plays a role of the electromagnetic field in the superconductivity phase. Since both right handed flavor indices and left handed ones are locked to the color indices together. A spontaneous chiral symmetry breaking is therefore induced in the CFL condensate associated with an octet Goldstone bosons, meson.

4.3.3 Gap Equation

If one writes down a self-consistency equation, using the self energy as the parameter inside, and solves it, the actual self energy (the gap) is obtained. Denote the quark

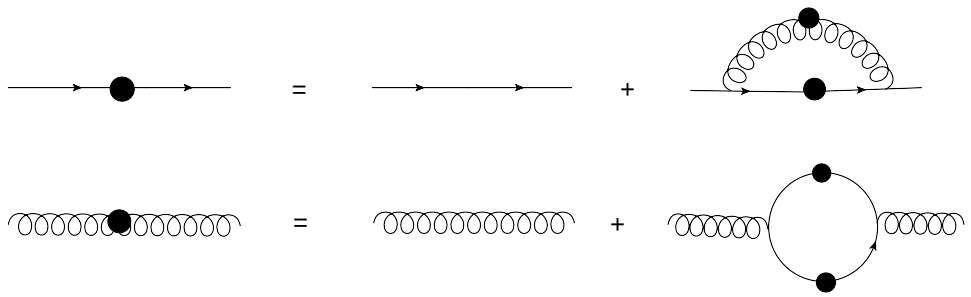

Figure 4.3: The graphical representation of the Schwinger-Dyson equation in the improved rainbow approximation. The quark propagator in the Nambu-Gorkov basis and the gluon propagator are denoted by the solid lines and the wavy lines, respectively.

self-energy Σ in Nambu-Gorkov space as

$$\Sigma \equiv \begin{pmatrix} \Sigma^{+} & \phi^{-} \\ \phi^{+} & \Sigma^{-} \end{pmatrix} \tag{4.7}$$

QCD dynamics are well described by the improved rainbow approximation at high densities, the bare quark-gluon vertices could be used directly, but the gluon propagator should include the screening effects from the approximation of High-Density-Loop (HDL) [94]. Upon making this approximation, the Schwinger-Dyson equations is presented in Figure 4.3. Plus, the analytical form of this equation reads

$$\phi^{+}(K) = g^2 \int_Q \gamma^{\mu} T_a^T F^{+}(Q) \gamma^{\nu} T_b D_{\mu\nu}^{ab}(K-Q) \tag{4.8}$$

where the so-called anomalous propagator are given by

$$F^{\pm} = -((G_0^{\pm})^{-1} + \Sigma^{\pm})^{-1} \phi^{\pm} G^{\pm} \tag{4.9}$$

Neglecting the momentum dependence of the gap and performing the momentum integration, one obtains the following approximate form of the gap equation in Euclidean space ($k_4 = \mathrm{i}k_0$)

$$\Delta(k_4) \simeq \frac{\alpha_s}{9\pi} \int \frac{\mathrm{d}p_4 \Delta(p_4)}{\sqrt{p_4^2 + \Delta^2}} \ln \frac{\Lambda}{\left|k_4 - p_4\right|} \tag{4.10}$$

In weak-coupling QCD calculations, where the full single gluon exchange vertex complete with gluon propagator is used, the gap equation takes the form

$$\Delta \sim \frac{\mu}{g^5} \exp\left(\frac{-3\pi^2}{\sqrt{2}g}\right) \tag{4.11}$$

This result of gap equation has two interesting features. First, the magnetic gluons propagator, which are only dynamically damped but not screened, induce $\Delta \sim \exp(-1/g)$ which is greater than the naively expect from the NJL model, $\Delta \sim \exp(-1/g^2)$. Second, in Eq. 4.11, it is natural to use the energy scale of the coupling constant $g(\mu)$ and assume that it is determined by the one-loop formula $1/g^2 \sim \ln \mu$ thus then the exponential factor in Eq. 4.11 gives very weak suppression. This means that color superconductivity will dominate the physics at high enough densities.

4.3.4 Two Flavors Color Superconductivity

As long as the density of strange quark can be neglected, the 2SC pattern is $\phi_B^A = \delta_3^A \delta_B^3$, in which only u and d quarks of two colors pair. According to the number of flavors, the superconducting phase in this system is commonly called the 2SC phase. The 2SC pairing pattern is $\langle \psi_{f_1}^{c_1} C\gamma^5 \psi_{f_2}^{c_2} \rangle \propto \Delta_{2SC} \epsilon^{c_1 c_2 3} \epsilon_{f_1 f_2 3}$, where the symmetry breaking pattern

is

$$\begin{aligned} & SU(3)_c \otimes \underbrace{SU(2)_R \otimes SU(2)_L}_{\supset U(1)_Q} \otimes U(1)_B \otimes U(1)_s \\ \rightarrow \quad & SU(2)_{rg} \otimes \underbrace{SU(2)_R \otimes SU(2)_L}_{\supset U(1)_{\widetilde{Q}}} \otimes U(1)_{\widetilde{B}} \otimes U(1)_s \end{aligned} \tag{4.12}$$

In this phase, there is an additional $U(1)_s$ introduced by the un-pairing strange quarks. All the symmetries remain except the the color gauge group $SU(3)_c$ breaking down to $SU(2)_{rg}$ gauge symmetry. Therefore, no order parameter distinguish 2SC phase from QGP state since no global symmetry are broken, even though 2SC phase is a color superconductor.

4.4 Color-Flavor-Locked Phase

It may happen that dense baryonic matter is made not only of up and down quarks, but also strange quarks. Thus, three flavor quark matter and paring patterns are more interesting. It has been confirmed in weak-coupling QCD calculations that the CFL phase has the highest condensation energy, thus it is the favored pairing pattern in high density quark matter. CFL pairing is the only patter that pairs all the quarks but leave a global $SU(3)$ symmetry unbroken. Though the energy gap $\Delta_{2SC} > \Delta_{CFL}$ by a factor of $2^{1/3}$, a varieties calculation have shown that the CFL condensation energy is $12\Delta_{CFL}^2\mu^2/(4\pi^2)$ which is greater than the condensation energy in 2SC phase, $4\Delta_{2SC}^2\mu^2/(4\pi^2)$, by a factor of 1.8899.

4.4.1 Properties of CFL

We briefly summarize the main features of CFL phase here.

Light quark

All the quark modes are gapped. The nine quark quasi-particles separate into $8 \oplus 1$ representations of the unbroken global $SU(3)_{c+L+R}$, thus lead to two gap parameters, Δ_1 and Δ_8. The corresponding singlet quasi-particles has a larger gap than the octet one.

Color gauge group

The color gauge group is completely broken. All eight gluons acquire magnetic mass via Higgs mechanism, which guarantee the gluon propagators are not infrared divergences.

Electromagnetism

One gauged generator is contained in the unbroken $SU(3)_{c+L+R}$ symmetry group, corresponding to an unbroken $U(1)_{\widetilde{Q}}$, which is a linear combination of gluon-photon and the mix angle is $\cos\theta = g/\sqrt{g^2 + 4e^2/3}$. Hence, CFL phase matter is an electromagnetic insulator.

Global symmetries

Two global symmetries are broken, the approximation chiral symmetry $SU(3)_L \otimes SU(3)_R$ and the exact global baryon number symmetry $U(1)_B$, associated with an octet chiral Goldstone boson, referring to these modes as pions, kaons, etc., and a singlet scalar Goldstone boson, respectively. Therefore, there are two gauge-invariant order parameters that distinguish the CFL phase from the QGP phase. After switch on the light quark

mass, we note here that the mass hierarchy of the meson octet in CFL is different, [95], such that the kaons are the lightest excitations.

Superfluidity

After switch on the current quark mass, the mass term would explicitly break the chiral symmetry and the order parameter of QGP would not be zero. The small quark mass also introduce a mass term in the energy spectrum of the chiral octet Goldstone bosons. However, the breaking of the exact baryon number symmetry makes the CFL phase a superfluid, helping the CFL phase be distinguished from QGP state.

Quark-hadron continuity

The hypernuclear phase is a hadron phase characterized by proton Ξ^-, neutron Ξ^0 and $\Sigma^+\Sigma^-$ paring, wherein the hyperons pair in an $SU(3)_{\text{flavor}}$ singlet. The symmetries of the three flavor CFL phase are same as the three flavor hypernuclear matter [96]. Therefore, there is no phase transition from hypernuclear phase to CFL phase.

4.4.2 Effective Field Theory

Effective Lagrangian for Goldstone Bosons

In the CFL phase, quarks pair together thus condensate. Goldstone fields are introduced as the phase of the condensation [97, 94]. Start from the high density effective Lagrangian with a gap term, Δ appearing in the quark spectrum

$$\mathcal{L} = \mathrm{Tr}\left[\psi_L^\dagger(\mathrm{i}v^\mu D_\mu \psi_L)\right] + \frac{\Delta}{2}\left\{\mathrm{Tr}\left(X^\dagger \psi_L X^\dagger \psi_L\right) - \left[X^\dagger \psi_L\right]^2 + h.c.\right\} + (L \leftrightarrow R, X \leftrightarrow Y) \tag{4.13}$$

where $v_\mu = (1, \mathbf{v}_F)$ with $\mathbf{v}_F$ being the Fermi velocity, D_μ the covariant derivative, $\psi_{L,R}$ are left and right hand quark fields and X, Y are defined as

$$X^i_\alpha = \epsilon^{ijk}\epsilon_{\alpha\beta\gamma}\langle\psi^j_{\beta L}\psi^k_{\gamma L}\rangle, \quad Y^i_\alpha = \epsilon^{ijk}\epsilon_{\alpha\beta\gamma}\langle\psi^j_{\beta R}\psi^k_{\gamma R}\rangle \tag{4.14}$$

Since quarks belong to the representation of $SU(3)_c \otimes SU(3)_{L(R)}$, they transform as under chiral and color transformation

$$\psi_L \to \mathrm{e}^{\mathrm{i}(\alpha+\beta)} g_c \psi_L g_L^T, \quad \psi_R \to \mathrm{e}^{\mathrm{i}(\alpha+\beta)} g_c \psi_R g_R^T, \quad \mathrm{e}^{\mathrm{i}\alpha} \in U(1)_B, \quad \mathrm{e}^{\mathrm{i}\beta} \in U(1)_A. \tag{4.15}$$

It is convenient to replace $X = \widehat{X}\mathrm{e}^{2\mathrm{i}(\phi+\theta)}$, $Y = \widehat{Y}\mathrm{e}^{2\mathrm{i}(\phi-\theta)}$. Therefore, the fields X and Y transform as $\widehat{X} \to g_c \widehat{X} g_L^T$, $\widehat{Y} \to g_c \widehat{Y} g_R^T$ under the total chiral, color, baryon and anomaly symmetry group. The fields ϕ and θ can be described through the determination of $\widehat{X}$ and $\widehat{Y}$,

$$d_X = \det(X) = \mathrm{e}^{6\mathrm{i}(\phi+\theta)}, \quad d_Y = \det(Y) = \mathrm{e}^{6\mathrm{i}(\phi-\theta)} \tag{4.16}$$

where we have assumed that the vacuum expectation is $\langle X\rangle = \langle Y\rangle = 1$. Check out the transformation properties of the field $\Sigma = \widehat{Y}^\dagger\widehat{X}$, one find that it transforms as an usual chiral field, $\Sigma^T \to g_L \Sigma^T g_R^\dagger$. It is straight to recognize that Σ field represents the octet Goldstone bosons corresponding to the breaking of the global symmetry. To get the effective Lagrangian of Goldstone bosons, one redefine the fermion fields as

$$\chi_L = \psi_L \widehat{X}^\dagger, \qquad \chi_R = \psi_R \widehat{Y}^\dagger \tag{4.17}$$

which help to rewrite the Lagrangian in the form of

$$\begin{aligned}\mathcal{L} &= \mathrm{Tr}\left[\chi_L^\dagger(\mathrm{i}v^\mu\partial_\mu\chi_L)\right] - \mathrm{iTr}\left[\chi_L^\dagger\chi_L\widehat{X}v^\mu(\partial_\mu - \mathrm{i}A_\mu^T)\widehat{X}^\dagger\right] \\ &\quad + \frac{\Delta}{2}\left\{\mathrm{Tr}\left(\chi_L\chi_L\right) - [\mathrm{Tr}(\chi_L)]^2 + h.c.\right\} + \left(L \leftrightarrow R, \widehat{X} \leftrightarrow \widehat{Y}\right) \end{aligned} \tag{4.18}$$

At low energies below the gap, we can integrate out the heavy quarks. Hence, it generates a kinetic term involving in the fields $\widehat{X}$ and $\widehat{Y}$

$$\mathcal{L}_{eff} = \frac{f_\pi^2}{2}\mathrm{Tr}\left[(\widehat{X}^\dagger D_0\widehat{X})^2 - v_\pi^2(\widehat{X}^\dagger D_i\widehat{X})^2\right] + (\widehat{X} \leftrightarrow \widehat{Y}) \tag{4.19}$$

At asymptotically high density, the pion decay constant f_π, v, can be determined by matching the effective theory to perturbative QCD [95, 98, 99]

$$f_\pi^2 = \frac{21 - 8\ln 2}{18}\frac{\mu^2}{2\pi^2}\,, \qquad\qquad v = \frac{1}{\sqrt{3}}\,, \tag{4.20}$$

where Δ is the energy gap at zero temperature.

The gluon is heavy either. Generally, gluon A_0^a and A_i^a, $a = 1, ...8$, acquire Debye and Meissner masses, which is given by

$$m_D^2 = g^2 f_\pi^2, \qquad m_M^2 = v_\pi^2 m_D^2 \tag{4.21}$$

Since the gluon is heavy, we also can integrate them out,

$$A_\mu = \frac{\mathrm{i}}{2}\left(X^\dagger\partial_\mu X + Y^\dagger\partial_\mu Y\right) \tag{4.22}$$

In the chiral limit, the effective action of Goldstone bosons only enter into in terms of the

derivatives of the fields. Therefore, up to two derivative terms, the most general effective Lagrangian for the Goldstone modes is derived through substituting this expression of Eq. 4.22 into the Lagrangian term Eq. 4.19, it is easy to show,

$$\begin{aligned}\mathcal{L}_{eff} &= \frac{f_\pi^2}{4}\mathrm{Tr}\left(\partial_0\Sigma\partial_0\Sigma^\dagger - v_\pi^2\partial_i\Sigma\partial_i\Sigma^\dagger\right) \\ &\quad +\frac{1}{2}\left(\partial_0\phi\partial_0\phi - v_B^2\partial_i\phi\partial_i\phi\right) + \frac{1}{2}\left(\partial_0\vartheta\partial_0\vartheta - v_{\eta'}^2\partial_i\vartheta\partial_i\vartheta\right) \end{aligned} \tag{4.23}$$

where the fields ϕ and ϑ describe the baryon number and the $\eta^{'}$ bosons. The above results have include the global symmetry breaking of the exact $U(1)_B$ and approximate $U(1)_A$ symmetries.

Dispersion Laws for Goldstone Bosons

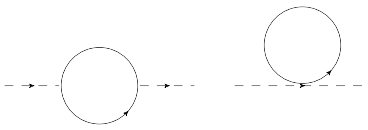

Figure 4.4: One-loop diagrams. External dashed lines represent the NG boson field; solid lines are fermion propagators.

To found the quasiparticle propagator, one diagonalize the color-flavor structure of the gap matrix by separating fermion fields $\chi_{L(R)}$ to the octet and the singlet representations of the unbroken $SU(3)$ group.

$$\mathbf{\Delta} = \Delta\mathbf{Q} + 2\Delta\mathbf{P}_1 \tag{4.24}$$

where

$$\begin{aligned} \mathbf{Q}_{ab}^{ij} &= \frac{1}{3}\delta_a^i\delta_b^j - \delta_b^i\delta_a^j \\ \mathbf{P}_1 &= \frac{1}{3}\delta_a^i\delta_b^j \\ \mathbf{Q}_{ab}^{ij}\mathbf{Q}_{bc}^{jk} &= \mathbf{P_8}_{ac}^{ik} \end{aligned} \tag{4.25}$$

The Dirac structure of the quasiparticle Lagrangian is diagonalized with the help of the helicity projector

$$H_\pm = \frac{1 \pm \gamma^0\gamma^5\gamma^i n_i}{2}, \qquad \mathbf{n} = \frac{\mathbf{p}}{|p|} \tag{4.26}$$

it leads the propagator of right quasiparticles as,

$$S_R(p) = H_+\left(\frac{\not{p}_- - \Delta\mathbf{Q}}{p_-^2 - \Delta^2}\mathbf{P}_8 + \frac{\not{p}_- - 2\Delta}{p_-^2 - 4\Delta^2}P_1\right) + H_-\left(\frac{\not{p}_+ - \Delta\mathbf{Q}}{p_+^2 - \Delta^2}\mathbf{P}_8 + \frac{\not{p}_+ - 2\Delta}{p_+^2 - 4\Delta^2}P_1\right) \tag{4.27}$$

where

$$p_\pm = (p_0, \mathbf{p} \pm \mu\mathbf{n}) = (p_0, (|\mathbf{p}| \pm \mu)\mathbf{n}) \tag{4.28}$$

The propagator for the left quasiparticles is obtained by flipping signs of μ and Δ. Furthermore, the inverse propagators of the Goldstone bosons are given by longitudinal components of the polarization operators:

$$\Pi(k) = k_\mu\Pi^{\mu\nu}k_\nu, \qquad K(k) = k_\mu K^{\mu\nu}k_\nu \tag{4.29}$$

Using quasiparticle propagators Eq. 4.27, one find out the octet and singlet polarization operator. After extracting the longitudinal part, the inverse pion and phonon propagator

are

$$\begin{aligned}
\Pi(\omega,k) &= -\frac{\mu^2\Delta^2}{24\pi^2 k}\int_0^1 \mathrm{d}x \int_0^k \mathrm{d}\alpha(\alpha^2-\omega^2) \\
&\quad \left[\frac{5}{x(1-x)(\alpha^2-\omega^2)+\Delta^2}+\frac{4-6x}{x(1-x)(\alpha^2-\omega^2)+(4-3x)\Delta^2}\right] \\
k(\omega,k) &= -\frac{\mu^2\Delta^2}{\pi^2 k}\int_0^1 \mathrm{d}x \int_0^k \mathrm{d}\alpha(\alpha^2-\omega^2) \\
&\quad \left[\frac{2}{x(1-x)(\alpha^2-\omega^2)+\Delta^2}+\frac{2}{x(1-x)(\alpha^2-\omega^2)+4\Delta^2}\right]
\end{aligned} \tag{4.30}$$

The poles of the propagators determine dispersion relations for the Goldstone bosons, pions and phonon, respectively. At low momenta,

$$\begin{aligned}
\omega(k) &= \frac{1}{\sqrt{3}}k\left(1-\frac{1}{135}\frac{123-112\ln 2}{21-8\ln 2}\frac{k^2}{\Delta^2}\right) \\
\omega_s(k) &= \frac{1}{\sqrt{3}}k\left(1-\frac{11}{540}\frac{k^2}{\Delta^2}\right)
\end{aligned} \tag{4.31}$$

4.4.3 Kaon Condensation

Switching on the quark mass in CFL phase, one find a correction to the ψ_L field of the form $MM^\dagger/(2p_F)$ which is generated while integrating out the ψ_R field, vice versa. If we treat these terms, $X_L = MM^\dagger/(2p_F)$, $X_R = M^\dagger M/(2p_F)$ as a favor dependent chemical potential for left and right handed fermions, respectively. We can redefine the time derivatives of Goldstone bosons field Σ to a covariant way

$$\nabla_0\Sigma = \partial_0\Sigma + \mathrm{i}\left(\frac{MM^\dagger}{2p_F}\right)\Sigma - \mathrm{i}\Sigma\left(\frac{M^\dagger M}{2p_F}\right) \tag{4.32}$$

Thus, the dispersion law of the flavored Goldstone bosons change to

$$\begin{aligned} E_{\pi^\pm} &= \mu_{\pi^\pm} + \left[v_\pi^2 p^2 + \frac{4A}{f_\pi^2}(m_u + m_d)m_s \right]^{1/2} \\ E_{K^\pm} &= \mu_{K^\pm} + \left[v_\pi^2 p^2 + \frac{4A}{f_\pi^2}(m_u + m_s)m_d \right]^{1/2} \\ E_{K^0,\bar{K}^0} &= \mu_{K^0,\bar{K}^0} + \left[v_\pi^2 p^2 + \frac{4A}{f_\pi^2}(m_s + m_d)m_u \right]^{1/2} \end{aligned} \tag{4.33}$$

where

$$\mu_{\pi^\pm} = \mp\frac{m_d^2 - m_u^2}{2\mu}, \qquad \mu_{K^\pm} = \mp\frac{m_s^2 - m_u^2}{2\mu}, \qquad \mu_{K^0,\bar{K}^0} = \mp\frac{m_s^2 - m_d^2}{2\mu}, \qquad A = \frac{3\Delta^2}{4\pi^2}. \tag{4.34}$$

Goldstone bosons will condensate if their energy become negative. And it is possible to be true if the favor dependent chemical potential in Eq. 4.33 are larger than the corresponding mass term in Eq. 4.34. Considering the known physical knowledge, $m_s \gg m_u \sim m_d$, such condensation is particular to take place in the K^0 and the K^+. Note that in CFL phase matter, it is not easy to switch on s quarks into d quarks since all quarks are gapped. Instead, one can recognize the mesons as a composition of d quarks and s holes.

Including the mass terms, the effective lagrangian for the meson octet is given by [97, 95, 98]

$$\mathcal{L} = \frac{f_\pi^2}{4}\mathrm{Tr}\left[\nabla_0\Sigma\,\nabla_0\Sigma^\dagger - v^2\nabla\Sigma\,\nabla\Sigma^\dagger\right] + \frac{a f_\pi^2}{2}\mathrm{Tr}\left[M^{-1}|M|(\Sigma + \Sigma^\dagger)\right] \tag{4.35}$$

where Σ is the chiral field, f_π is the pion decay constant, $M = \mathrm{diag}(m_u, m_d, m_s)$ is the quark mass matrix, and $|M|$ is the determinant of the mass matrix. a is calculate by by matching the effective theory to perturbative QCD [95, 98, 99], with $a = 3\Delta^2/(\pi^2 f_\pi^2)$.

Since kaons are the lightest excitations in the theory, ones give the leading terms in the effective theory involving kaons are $\mathcal{L}_0 + \mathcal{L}_{int}$ with

$$\begin{aligned} \mathcal{L}_0 &= \frac{1}{2}(\partial_\mu K^0)(\partial^\mu \bar{K}^0) + \frac{1}{2}(\partial_\mu K^+)(\partial^\mu K^-) - \frac{1}{2}m_{K^0}^2 K^0 \bar{K}^0 - \frac{1}{2}m_{K^+}^2 K^+ K^- \,, \\ \mathcal{L}_{int} &= -\frac{1}{24}\left[\lambda_0 \left(K^0\bar{K}^0\right)^2 + \lambda_+ \left(K^+K^-\right)^2 + (\lambda_0 + \lambda_+)\left(K^0\bar{K}^0\right)\left(K^+K^-\right)\right], \end{aligned} \tag{4.36}$$

where $\lambda_{0,+} = m_{K^{0,+}}^2 / f_\pi^2$ and

$$m_{K^0}^2 = a m_u (m_d + m_s)\,, \qquad m_{K^+}^2 = a m_d (m_u + m_s)\,. \tag{4.37}$$

We have not included kaon interactions that involve derivatives of the kaon field. These terms arise from expanding the first term in Eq. 4.35, see [100]. For energies and momenta that are small compared to the kaon mass these terms are suppressed as compared to the terms in Eq. 4.36.

4.5 Neutron star

Neutron stars are compact stellar objects that originate from supernova explosions. Typically, the radius of neutron stars is about 10 km and whose mass is of the order of the suns mass M_S, $0.1M_S \sim 2M_S$. Note here that the suns radius is $6.7 \cdot 10^5$ km. Consequently, the matter what a neutron star is made of is extremely dense. Hence, neutron stars are golden mine fields to investigate the dense matter in universal.

It is a thin crust of iron at the surface of the neutron star; the next followed layer is the one that is composed of neutron-rich nuclei. Moreover, neutrons start to coexist individually in equilibrium with nuclei and electrons at the regime where density become higher. Even closer to the center of the star, closing nuclear matter density ρ_0,

the preferred state of matter are expressed by the particles of neutrons, protons, and electrons. This is the phase why neutron stars are named as neutron stars. Approaching even higher densities, the contained particles are pions, muons, and hyperons. In the core of the neutron star, matter density might reach an order of magnitude larger than ρ_0. Therefore, it is predicted that pure quark matter could be found in the core of neutron star.

The first fundamental concept to explore the properties of neutron stars is the equation of state, which connects pressure with temperature and energy density. Theoretical models are essentially based on the astrophysical observations. For example, neutron stars emit electromagnetic radiation in periodic pulses due to rotation. The rotating periods are in the range of milliseconds. Observations have shown that the spinning-down of the star (the rotation frequency decreases due to radiative energy loss) is interrupted by sudden spin-ups, called glitches. From the spectra and frequency of the radiation pulses, properties of the neutron star can be deduced. However, the only active fermions, which involving in pairing, are those lying in the thin shell around the Fermi surface. In fact, equation of state itself is not much sensitive to different paring patter, i.e. phase state, since it is deduced from the integration of all fermi momentum space. But, transport coefficients are characterized by the low energy quasi-particles, which is the good signature to differentiate between the phase and phase.

Investigating the cooling mechanism is another important topic of studying neutron stars. The temperature of neutron stars right after their creation is in the range of 10^{11} K, or 10 MeV. During its evolution, the star cools down. This decrease of temperature is dominated by neutrino emission. After a time of about a million years, photons arrive in the surface layer and their emission become the dominant way to cool down the stars to temperatures $\sim 10^5$ K, or 10 eV. Consequently, matter in the interior of neutron stars

indeed is cold and dense. Temperatures inside of old neutron stars are lower than the critical temperatures of color superconductors. Therefore, it is expected that the cores of neutron stars are made of CFL phase quark matter. It also is the second main reason why we are interested in calculating the thermal conductivity of CFL phase quark matter.

4.6 Thermal Conductivity and Transport Theory

The thermal conductivity, like other transport properties, depends on the properties of quasi-particle excitations. In the CFL phase up, down, and strange quarks are all gapped, with the gaps typically much larger than the appropriate temperature of the compact stars. Hence, the quarks are unlikely to have any significant contribution to transport properties. The remained lightest excitation are phonons and kaons in the CFL phase, which is the basic consideration of our calculation.

4.6.1 Estimations from Mean Free Path

Firstly, we quickly summarize the results from Shovkovy and Ellis [84]. The authors point out that photons and phonons dominantly contribute to the thermal conductivity, κ. Using the estimated relation from classical Boltzmann kinetic theory,

$$\kappa \sim \frac{1}{3} c_V l \tag{4.38}$$

where c_V is the specific heat. κ is very large due to their very large mean free path.

The mean free path of phonons are coming from two kinds of processes: one is the decay into a pair of quark quasiparticles, another one is the scatter between themselves.

Confirmed by the microscopic calculation, one has:

$$\begin{aligned} l_{H\to qq} &\sim \frac{v}{T}\exp\left(\sqrt{\frac{3}{2}}\frac{\Delta}{T}\right) \\ l_{H\to HH} &\sim \frac{\mu^8}{T^8} \end{aligned} \tag{4.39}$$

where Δ was set as $\sim$ 50MeV. Both $l_{H\to qq}$ and $l_{H\to HH}$ depend very strongly on temperature, however, both of them are larger than the size of a compact star for temperatures T at the order of 1 MeV.

It was argued in [72] that the mean free path of photons is larger than the typical size of a compact star at all temperatures $T < 1$ MeV. Thus, the authors claim to use both the mean free path of photon and phonon being the size of the compact star $l \sim R_0$. Meanwhile, the total thermal conductivity is given by the sum of the two contributions, since the conductivity is additive. This yield the value

$$\kappa_{CFL} = \kappa_H + \kappa_\gamma = 1.2\times 10^{32}\ T^3 R_0\ \ \text{erg}\ \ \text{cm}^{-1}\ \ \text{sec}^{-1}\ \ \text{K}^{-1} \tag{4.40}$$

which is many orders of magnitude larger than the thermal conductivity of regular nuclear matter in a neutron star. It demonstrates that the thermal conductivity of dense quark matter in the CFL phase is very high. The authors roughly estimate that a temperature gradient of 1 MeV across a core of 1 km in size is washed away in a very short time interval of order 6×10^{-4} sec.

4.6.2 Subtle Results from Boltzmann Equation

However, comparing to above estimation, we have two main different arguments. The first one is, we agree on that the phonon is one of the dominant source to contribute

to the thermal conductivity, but its behavior is very subtle that one need to derive the Boltzmann equation more carefully. The second one is, the photon does not induce heat flux even its mean free path is finite. In our arguments, Kaon is another dominant contribution to the thermal conductivity. Below we will derive the microscopic expression of thermal conductivity from Boltzmann equation.

The thermal conductivity is defined in hydrodynamics as

$$\boldsymbol{q} = -\kappa \boldsymbol{\nabla} T \tag{4.41}$$

where $\mathbf{q}$ is the heat flow and κ is the thermal conductivity. In kinetic theory, the heat flux can be written in terms of the quasi-particle distribution function as

$$\mathbf{q} = \int \frac{d^3p}{(2\pi)^3} \mathbf{v_p} E_p \delta f_p \tag{4.42}$$

where $v_p = \partial E_p / \partial p$ is the particle velocity and $\delta f_p = f_p - f_p^0$ is the deviation of the distribution function from the form in local thermal equilibrium, given by

$$f_p^0 = \frac{1}{e^{(p_\mu u^\mu - \mu)/T} - 1} \,. \tag{4.43}$$

Here, u_μ is the local fluid velocity and μ is the chemical potential (which is zero in the case of phonons and equal to the hypercharge chemical potential in the case of the kaons). Since we are only interested in contributions to the stress-energy tensor arising from thermal gradients we can write δf_p as

$$\delta f_p = -\frac{f_p^0(1 + f_p^0)}{T^3} g(p) \boldsymbol{p} \cdot \boldsymbol{\nabla} T \,, \tag{4.44}$$

where $g(p)$ is a dimensionless function of the magnitude of the momentum (meaning $g(p)$ can always be written as $g(x)$ where $x = |\boldsymbol{p}|/\bar{E}$ where $\bar{E}$ is some appropriate energy scale in the problem like T or $\sqrt{mT}$). Inserting this into Eq. (4.42), we can then read off the heat flux as

$$\boldsymbol{q} = -\frac{\boldsymbol{\nabla} T}{3T^3} \int \frac{d^3p}{(2\pi)^3} \, f_p^0(1 + f_p^0) v_p \, E_p \, p \, g(p) \tag{4.45}$$

and the thermal conductivity as

$$\kappa = \frac{1}{3T^3} \int \frac{d^3p}{(2\pi)^3} \, f_p^0(1 + f_p^0) g(p) \, v_p \, E_p \, p \tag{4.46}$$

Kinetic theory also gives some constrains on the form that δf_p can take. Conservation of particle number, energy and momentum imply [50]

$$\int d\Gamma \delta f_p = \int d\Gamma E_p \, \delta f_p = \int d\Gamma \boldsymbol{p} \, \delta f_p = 0 \,, \tag{4.47}$$

where $d\Gamma = \frac{d^3p}{(2\pi)^3}$. Note that the number of phonons is not explicitly conserved. However, we will only consider $2 \leftrightarrow 2$ processes and the particle number constraint is expected to hold. We can show that for δf_p of the form given in Eq. (4.44) the first and second constraints (energy and momentum conservation) are automatically satisfied, but the third one (particle number conservation) is non-trivial. We get

$$0 = \int d\Gamma \, \boldsymbol{p} \, \delta f_p = \frac{\boldsymbol{\nabla} T}{3 \, T^3} \int d\Gamma \, f_p^0(1 + f_p^0) g(p) \, p^2 \,. \tag{4.48}$$

Note that if v_p is independent of p, then the contribution to the thermal conductivity vanishes due to the constraint. This implies that phonons with an exactly linear dispersion relation do not contribute to the thermal conductivity. This result was first derived

in connection with the transport properties of superfluid helium [101]. The thermal conductivity of superfluid helium is dominated by rotons and phonon-roton scattering. Note that the phonon and roton are part of the same excitation curve. The name roton refers to the part of the excitation curve in which the disperion relation is very non-linear and $E(p)$ develops a second minimum. In the following we will compute the thermal conductivity of the CFL phase due to non-linearities in the phonon dispersion relation, and due to massive kaons.

To solve for the thermal conductivity, we need to determine the form of $g(p)$. The quasi-particle distribution functions satisfies the Boltzmann equation,

$$\frac{df_p}{dt} = \frac{\partial f_p}{\partial t} + \boldsymbol{v}_p \cdot \frac{\partial f_p}{\partial \boldsymbol{x}} + \boldsymbol{F}_{ext} \cdot \frac{\partial f_p}{\partial \boldsymbol{p}} = C[f_p], \tag{4.49}$$

where $\boldsymbol{F}_{ext}$ is an external force and $C[f]$ is the collision term. In the case of binary scattering the collision integral is given by

$$C[f_p] = \frac{1}{2E_p} \int_{k,k',p'} (2\pi)^4 \delta(P + K - K' - P') |\mathcal{M}|^2 D_{2\leftrightarrow 2}, \tag{4.50}$$

where

$$\int_q = \int \frac{d^3q}{(2\pi)^3\, 2E_q} \tag{4.51}$$

is the one-particle phase space integral, and $D_{2\leftrightarrow 2} = f_p f_k (1 + f_{p'})(1 + f_{k'}) - (1 + f_p)(1 + f_k) f_{p'} f_{k'}$ is the term involving the distribution functions for $2 \leftrightarrow 2$ scattering. Linearizing in δf we can write $D_{2\leftrightarrow 2} = D_0 + \delta D$ where

$$\delta D = \frac{f_p^0 f_k^0 (1 + f_{k'}^0)(1 + f_{p'}^0)}{T^3} \boldsymbol{\Delta}_g \cdot \boldsymbol{\nabla} T, \tag{4.52}$$

and

$$\boldsymbol{\Delta}_g = g(p)\boldsymbol{p} + g(k)\boldsymbol{k} - g(k')\boldsymbol{k}' - g(p')\boldsymbol{p}' \,. \tag{4.53}$$

Note that the collision integral will vanish for $D = D_0$. This is a consequence of detailed balance, which implies that $|\mathcal{M}|^2$ is invariant under $(p,k) \leftrightarrow (p'\,k')$ and that $f^0_p f^0_k(1 + f^0_{k'})(1 + f^0_{p'}) = (1 + f^0_p)(1 + f^0_k) f^0_{k'} f^0_{p'}$. We can then write the collision integral as

$$C[f_p] \equiv \frac{\boldsymbol{F} \cdot \boldsymbol{\nabla} T}{T^2} \,, \tag{4.54}$$

where

$$\boldsymbol{F} = \frac{1}{2E_p} \int d\Gamma_{k,k',p'} \frac{f^0_p f^0_k (1 + f^0_{k'})(1 + f^0_{p'})}{T} \boldsymbol{\Delta}_g \tag{4.55}$$

and

$$\int d\Gamma_{k,k',p'} = \int_{k,k',p'} (2\pi)^4 \delta(P + K - P' - K') \, |\mathcal{M}|^2 \,. \tag{4.56}$$

We can simplify the left-hand side of the Boltzmann equation using our definition of the distribution function in Eq. (4.43). In general, we can write

$$\frac{df}{dt} = \alpha_p \frac{f^0_p (1 + f^0_p)}{T^2} \boldsymbol{p} \cdot \boldsymbol{\nabla} T \,, \tag{4.57}$$

where the form of α_p depends on the properties of the quasi-particles we are studying. In the following we will consider two cases. The first is phonons with a non-linear dispersion relation

$$E^{(P)}_p = vp \left(1 + \gamma p^2\right) \equiv vp \left(1 + \epsilon \frac{v^2\, p^2}{T^2}\right) \,, \tag{4.58}$$

where $v = 1/\sqrt{3}$ is the speed of sound, γ controls the curvature of the dispersion relation, and $\epsilon \equiv \gamma T^2 / v^2$ is a dimensionless measure of the non-linearity. The parameter γ was computed by Zarembo [102], showed in Eq. 4.31 with $\gamma = -11/(540\,\Delta^2)$, where Δ is the

gap in the fermion spectrum. The second case is massive kaons with

$$E_p^{(K)} = \sqrt{v_K^2 p^2 + m_K^2} \simeq \frac{v_k^2 p^2}{2m_K} + m_K \,, \tag{4.59}$$

where $v_K = v$. We will specify the kaon mass m_K in Section 4.8.2. The quasi-particle velocities, $v_p = \frac{\partial E_p}{\partial p}$, are given by

$$v_p^{(P)} = v\left(1 + 3\epsilon\frac{v^2 p^2}{T^2}\right) , \quad v_p^{(K)} = \frac{v^2 p}{m_K} \,. \tag{4.60}$$

The explicit form of α_p is derived in Appendix A.1. We find

$$\alpha_p^{(P)} = 4\,\epsilon\,v^2\,\left(\frac{v^2 p^2}{T^2} - \frac{20\pi^2}{7}\right) , \quad \alpha_p^{(K)} = \frac{v^4 p^2}{2m_K^2} - \frac{5\,v^2\,T}{2m_K}. \tag{4.61}$$

We have now expressed the LHS of the Boltzmann equation, Eq. (4.57), in terms of the function α_p. The RHS of the Boltzmann equation, Eq. (4.54), is given in terms of the unknown function $g(p)$. Once $g(p)$ is determined the thermal conductivity is given by Eq. (4.46). In practice we will solve the Boltzmann equation using a variational procedure. This procedure is based on an expression for the thermal conductivity in terms of a suitable integral over the collision term, which we will now derive. Consider the following integral over the LHS of the Boltzmann equation,

$$\frac{c}{T}\int d\Gamma\,\frac{df}{dt}g(p)\boldsymbol{p} = -\frac{c\boldsymbol{\nabla}T}{3\,T^3}\int d\Gamma\,f_p^0(1+f_p^0)p^2\alpha_p g(p), \tag{4.62}$$

where c is a constant. We observe that the RHS of this equation has the same structure

as Eq. (4.45) for the heat flux. For the two expressions to be equal, we need

$$c\int d\Gamma\, f_p^0(1+f_p^0)p^2\alpha_p g(p) = \int d\Gamma\, f_p^0(1+f_p^0)p^2\frac{v_p\,E_p}{p}\,g(p)\,. \tag{4.63}$$

The two sides of this equation can be matched by using the constraint Eq. (4.48). The constraint implies that constant terms in v_pE_p/p and α_p do not contribute to Eq. (4.63). We can then determine c by matching the p^2 terms in v_pE_p/p and α_p. We find $c = 1$ for both phonons and kaons. Using this fact together with the Boltzmann equation we can express the heat current in terms of the collision integral

$$\boldsymbol{q} = -\frac{\boldsymbol{\nabla} T}{3T^3}\int d\Gamma\, g(p)\,\boldsymbol{p}\cdot\boldsymbol{F}\,. \tag{4.64}$$

The corresponding expression for the thermal conductivity is

$$\kappa = \frac{1}{12T^4}\int d\Gamma_{p,k,k',p'}\,\Delta_g^2\,. \tag{4.65}$$

where

$$\int d\Gamma_{p,k,k',p'} = \int_{pkp'k'}(2\pi)^4\delta(P+K-K'-P')|\mathcal{M}|^2 f_p^0 f_k^0(1+f_{k'}^0)(1+f_{p'}^0) \tag{4.66}$$

and we have used Eq. (4.55) and the symmetries of the matrix elements to derive Eq. (5.27). We now have two expressions for the thermal conductivity, Eq. (4.46) and Eq. (5.27). Both equations depend on the unknown function $g(p)$, but the equivalence of the two equations rests on the fact that $g(p)$ satisfies the Boltzmann equation. As we will now show, this fact can be used to determine $g(p)$.

4.7 Variational Solution to the Boltzmann Equation

We will solve the Boltzmann equation by expanding $g(p)$ in a basis of orthogonal polynomials. The procedure is variational in the sense that the result for κ obtained in a truncated basis provides a lower bound on κ for the exact solution. The expansion has the form

$$g(p) = \sum_s b_s B_s(p^2)\,, \tag{4.67}$$

where $B_s(p^2)$ is a polynomial in p^2 of order s. The coefficient of the highest power is set to one. This means that $B_0 = 1$, $B_1 = p^2 + c_{10}$, etc. The polynomials $B_s(p^2)$ are orthogonal with regard to the inner product

$$\int d\Gamma\, f_p^0(1+f_p^0)p^2 B_s(p^2)B_t(p^2) \equiv A_s\delta_{st}\,. \tag{4.68}$$

The functions $B_s(p^2)$ are a generalization of the Laguerre polynomials used in solutions of the linearized Boltzmann equation in classical physics [50]. Starting with $B_0 = 1$, we can solve for all higher polynomials and their normalizations, A_s. This is laid out in more detail in Appendix A.2.

Inserting the expansion Eq. (4.67) into the constraint Eq. (4.48) we get

$$0 = \int d\Gamma\, f_p^0(1+f_p^0)p^2 B_s(p^2)B_0(p^2)\,, \tag{4.69}$$

where we have used $B_0 = 1$. We conclude that the constraint is satisfied if $b_0 = 0$. Using the polynomial expansion in the first expression for κ, Eq. (4.46), gives

$$\kappa = \frac{1}{3T^3}\sum_{s\neq 0} b_s \int d\Gamma\, f_p^0(1+f_p^0)\, p^2\, B_s(p^2)\,(a_0B_0 + a_1B_1) = \frac{a_1}{3T^3}b_1A_1\ , \tag{4.70}$$

where we have written $v_p E_p/p = a_0 B_0 + a_1 B_1$. The coefficients a_0 and a_1 are determined by Eq. (4.60). We get $a_1 = 4\epsilon v^4/T^2$ for phonons and $a_1 = v^4/2m_K^2$ for kaons. Substituting the polynomial expansion into the second expression for the thermal conductivity, Eq. (5.27), gives

$$\kappa = \frac{1}{12T^4} \sum_{s,t\neq 0} b_s b_t M_{st}, \tag{4.71}$$

where

$$M_{st} = \int d\Gamma_{p,k,k',p'} \boldsymbol{Q}_s \cdot \boldsymbol{Q}_t \,, \quad \boldsymbol{Q}_s = B_s(p^2)\boldsymbol{p} + B_s(k^2)\boldsymbol{k} - B_s(k'^2)\boldsymbol{k'} - B_s(p'^2)\boldsymbol{p'} \,. \tag{4.72}$$

Requiring Eq. (4.70) and Eq. (4.71) to be equal gives an equation for b_s

$$\frac{a_1}{3T^3} \sum_{s\neq 0} b_s A_s \delta_{s1} = \frac{1}{12T^4} \sum_{s,t\neq 0} b_s b_t M_{st} \,. \tag{4.73}$$

A sufficient condition to solve this equation is

$$\sum_{t\neq 0} M_{st} b_t = 4a_1 T \, A_1 \delta_{s1}. \tag{4.74}$$

which can be solved by inverting the matrix M to get

$$\begin{pmatrix} b_1 \\ b_2 \\ \vdots \end{pmatrix} = 4a_1 T \, A_1 M^{-1} \begin{pmatrix} 1 \\ 0 \\ \vdots \end{pmatrix} \tag{4.75}$$

This equation determines b_1 and, using (4.70), the thermal conductivity. We find

$$\kappa = \left(\frac{4a_1^2}{3T^2}\right) A_1^2 M_{11}^{-1}, \tag{4.76}$$

where M_{11}^{-1} is the $(1,1)$-element of the inverse of matrix M, the constants a_1 are given below Eq. (4.70) and A_1 is given in Appendix A.1. M is an infinite matrix, and in practice we solve for κ by restricting the dimension of the matrix to a finite number N. This procedure can be shown to be variational in the sense that [103]

$$\kappa \geq \left(\frac{4a_1^2}{3T^2}\right) \frac{(b_1 A_1)^2}{\sum_{s,t\neq 0}^{N} b_s b_t M_{st}} \tag{4.77}$$

for any value of N. This right hand side can be written as

$$\kappa \geq \left(\frac{4a_1^2}{3cT^2}\right) A_1^2 M_{11}^{-1}\,, \tag{4.78}$$

where M^{-1} is the the inverse of the truncated $N \times N$ matrix. The bound is saturated as $N \to \infty$.

4.8 Collision Terms

The matrix M depends on the $2 \leftrightarrow 2$ scattering amplitudes. In this Section we will compute the phonon and kaon scattering amplitude using a low energy effective lagrangian for the CFL phase.

4.8.1 Superfluid Phonon

The effective lagrangian for the phonon field ϕ is given by [104]

$$\mathcal{L} = \tfrac{1}{2}(\partial_0\phi)^2 - \tfrac{1}{2}v^2(\partial_i\phi)^2 - \frac{\pi}{9\mu_q^2}\partial_0\phi(\partial_\mu\phi\partial^\mu\phi) + \frac{\pi^2}{108\mu_q^4}(\partial_\mu\phi\partial^\mu\phi)^2 + \dots\,, \tag{4.79}$$

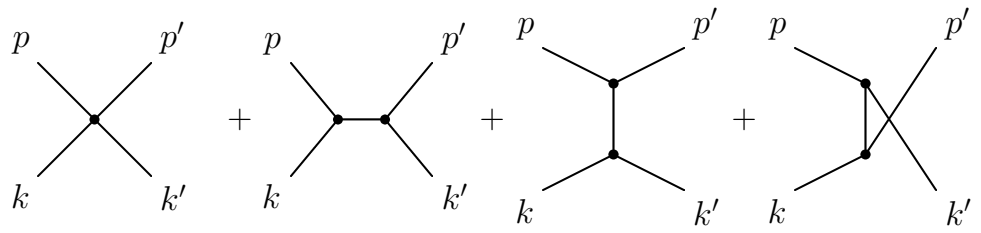

Figure 4.5: Lowest order Feynman diagrams for the 2-phonon scattering amplitude.

where $v = 1/\sqrt{3}$ is the speed of sound and μ_q is the quark chemical potential. We have displayed the leading three and four-phonon vertices. Higher order terms include higher powers of ϕ or additional derivatives. These terms are suppressed by powers of the typical momentum over the quark chemical potential. The speed of sound as well as the coefficients of the three and four-phonon vertices are given to leading order in the strong coupling constant. The lowest order diagrams that contribute to phonon-phonon scattering are shown in Figure 4.5.

The corresponding matrix elements were previously computed in connection with the phonon contribution to the shear viscosity of the CFL phase [69]. The matrix element $\mathcal{M}(P, K; P'K')$ where P, K and P', K' are the in and out-going four momenta can be written as the sum of the contact term $\mathcal{M}_c$ and the s, t, u-channel phonon exchange diagrams $\mathcal{M}_{s,t,u}$. The individual terms are

$$\begin{aligned}
i\mathcal{M}_c &= \lambda\left[(P\cdot K)(P'\cdot K)+(P\cdot K')(P'\cdot K)+(P\cdot P')(K\cdot K')\right] \\
i\mathcal{M}_s &= g^2\left[2(p_0+k_0)P\cdot K+p_0K^2+k_0P^2\right]\left[2(p_0'+k_0')P'\cdot K'+p_0'K'^2+k_0'P'^2\right]G(P+K) \\
i\mathcal{M}_t &= i\mathcal{M}_s(P\leftrightarrow K') \\
i\mathcal{M}_u &= i\mathcal{M}_t(P\leftrightarrow K),
\end{aligned} \tag{4.80}$$

where $G(Q)$ is the phonon propagator and the coupling constants λ and g are given by

$$\lambda = \frac{4\pi^2}{108\mu_q^4}\,, \qquad g = \frac{2\pi}{9\mu_q^2}. \tag{4.81}$$

At leading order the phonon propagator is given by $G(Q) = (q_0^2 - E_q^2)^{-1}$ with $E_q = vq$. The thermal conductivity is sensitive to non-linearities in the dispersion relation and we will use E_q as given in Eq. (4.58). We note that non-linear effects are generated by higher derivative terms in the effective lagrangian. Except for the non-linearities in the dispersion relation the structure of these terms has not been determined. We have verified that the matrix elements M_{st} are not sensitive to higher order corrections in the vertices. We also note that a non-linear dispersion (with $\epsilon < 0$) regulates a possible on-shell divergence of the matrix element, and as consequence there is no need to include self-energy corrections in the fermion propagator as in [69, 105].

We can now insert the scattering amplitude into Eq. (4.72) and compute the matrix elements M_{st}. Using the energy and momentum conserving delta functions as well as spherical symmetry the 12-dimensional phase space integral in Eq. (4.72) can be reduced to a 5-dimensional integral. First, we use the momentum conserving delta function to integrate over $\boldsymbol{p'}$. We can choose $\boldsymbol{p}$ to lie along the z-direction and perform the corresponding angular integrals. The energy conserving part of the delta function can be used to fix the magnitude of $\boldsymbol{k'}$. Finally, we note that the integrand only depends on the relative azimuthal angle of $\boldsymbol{k}$ and $\boldsymbol{k'}$ and we can trivially integrate over the other azimuthal angle. The remaining 5-dimensional integral is computed numerically using standard methods, such as the VEGAS routine [106].

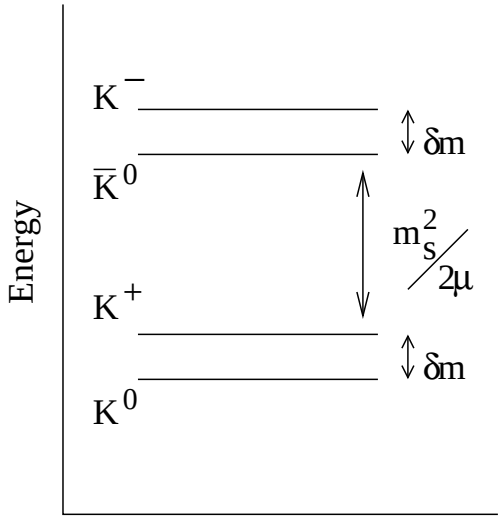

Figure 4.6: Spectrum of energies for the charged and neutral kaons. The mass splitting between K^0 and K^+ is given by δm and the larger splitting between the kaons containing $\bar{s}$ and those containing s is given by $m_s^2/2\mu_q$.

4.8.2 Massive Kaon

The spectrum of kaons is shown schematically in Figure 4.6. The mass difference between the isospin doublets (K^0, K^+) and $(\bar{K}^0, K^-)$ is proportional to $m_s^2/(2\mu_q)$, while the mass splitting with the doublets is $\delta m^2 = a m_s(m_d - m_u)$, with $a = 3\Delta^2/(\pi^2 f_\pi^2)$.

In the following we will only include the lightest kaon, the K^0. The relevant interaction term is read from the Eq. 4.36

$$\mathcal{L}_{int} = -\frac{m_{K^0}^2}{24 f_\pi^2}(K^0 \bar{K}^0)^2 \,, \tag{4.82}$$

and the corresponding scattering amplitude is

$$|\mathcal{M}|^2 = \frac{m_{K^0}^4}{f_\pi^4} \,. \tag{4.83}$$

This expression can be inserted into Eq. (4.72) in order to compute the matrix M_{st}. As in the case of phonon scattering, the phase space integral can be reduced to a 5-dimensional integral over the magnitudes of $\boldsymbol{p}$ and $\boldsymbol{k}$, the polar angles $\cos(\theta_k)$ and $\cos(\theta_{k'})$ describing the angles between $\boldsymbol{p}$ and the respective momenta, and one azimuthal angle.

4.9 Results

Before we show numerical results for the thermal conductivity, we would like to discuss the dependence of κ on the dimensionful parameters that appear in the problem, the temperature T, the quark chemical potential μ_q, the fermion gap Δ, and the mass of the kaon. We begin by studying the scaling of the matrix elements M_{st}. In the phonon case, we can rescale all momenta by the temperature and write M_{st} as a product of the dimensionful parameters and a dimensionless phase space integral. A subtlety arise due to the possible role of on-shell divergences. There is no on-shell sensitivity in the phonon contribution to the shear viscosity and the corresponding matrix elements exhibit the naive scaling behavior, but the phonon mean free path is sensitive to the phonon self energy near the on-shell point [105, 69]. We find that the thermal conductivity also depends on the behavior of the phonon propagator near the on-shell point. In the present calculation this behavior is governed by non-linearities in the dispersion relation. Consider the contribution to M_{st} from nearly on-shell phonons in the s, t or u-channel. We find

$$M_{st}^{(P)} \sim \frac{T^{2s+2t+14}}{\mu^8} \int \frac{dq^2 d\Gamma'}{(q^2 + \epsilon f(q,\Gamma'))^2} \sim \frac{T^{2s+2t+14}}{\mu^8} \frac{1}{|\epsilon|} \sim \frac{T^{2s+2t+12}\Delta^2}{\mu^8} \tag{4.84}$$

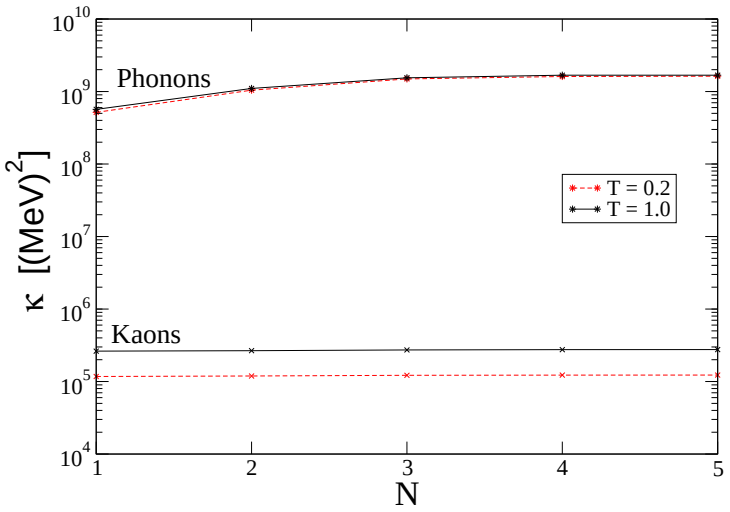

Figure 4.7: (Color online) Numerical results for the thermal conductivity of the CFL phase due to phonons and kaons as a function of the basis size N used in the variational procedure. Results are shown for two different temperatures $T = 0.2$ MeV and $T = 1$ MeV. We have used $\mu = 400$ MeV, $\Delta = 100$ MeV for the phonons and $m_K = 10$ MeV, $\mu_K = 5$ MeV and $f_\pi = 100$ MeV for the kaons. Numerical results are shown as stars and crosses, the lines are only serve to guide the eye.

where q represent the momentum transfer in the relevant channel, $d\Gamma'$ is a phase space integral over the remaining momenta, and $f(q, \Gamma')$ is a function of these variables.

In the kaon case we can assume that the temperature is smaller than all the other parameters and write the dispersion as $E_q = m_K + q^2/(2m_K)$. We rescale the momenta by $\sqrt{m_K T}$ and extract all dimensionful parameters from the phase space integral. We get

$$M_{st}^{(K)} \sim \frac{\lambda_0^2}{m_K^3}(m_K T)^{s+t+9/2} e^{-2\delta m/T} \sim \frac{m_K}{f_\pi^4}(m_K T)^{s+t+9/2} e^{-2\delta m/T} \tag{4.85}$$

Using Eq. (4.84) and Eq. (4.85), as well as the scaling of the normalization factor A_1

derived in Appendix A.2, we find

$$\kappa \sim \begin{cases} \frac{\mu_q^8}{\Delta^6} & \text{phonons,} \\ \frac{f_\pi^4}{m_K^2}\sqrt{\frac{T}{m_K}} & \text{kaons.} \end{cases} \tag{4.86}$$

We note that the contribution to the thermal conductivity from phonons is independent of temperature. The naive power counting gives $\kappa \sim \mu^8/T^6$, but the contribution from nearly on-shell phonons modifies the naive scaling behavior by a factor ϵ^3. Two powers of ϵ come from the a_1^2 term and one power of ϵ comes from the nonlinear dispersion cutting off the collinear regimes in the propagators. Using $\epsilon \sim T^2$ then leads to a thermal conductivity that is independent of temperature.

The thermal conductivity due to kaons is not exponentially suppressed by $\exp(-m_K/T)$ as one might naively expect, because the exponential factors in A_1^2 and M_{11} cancel at leading order. This result is analogous to the well known fact that the transport properties of a dilute gas are independent of the density of the gas. We should note, however, that in practice the range of validity of this result is limited to temperatures that are not too small. At very small temperature the kaon mean free path is bigger than the system size, and heat transport is no longer a diffusive process.

Numerical results for the thermal conductivity are shown in Figs. 4.7 and 4.8. In Fig. 4.7 we show the dependence of κ on the number of basis functions. We observe that the convergence in the case of the kaon contribution is excellent – using $N = 1, 2$ gives results within a few percent of the final result. Also, the rate of convergence is independent of the temperature. In the case of the phonon contribution the rate of convergence is slower, but going up to $N = 5$ appears to give converged results.

Fig. 4.8 shows the thermal conductivity as a function of temperature. We have used

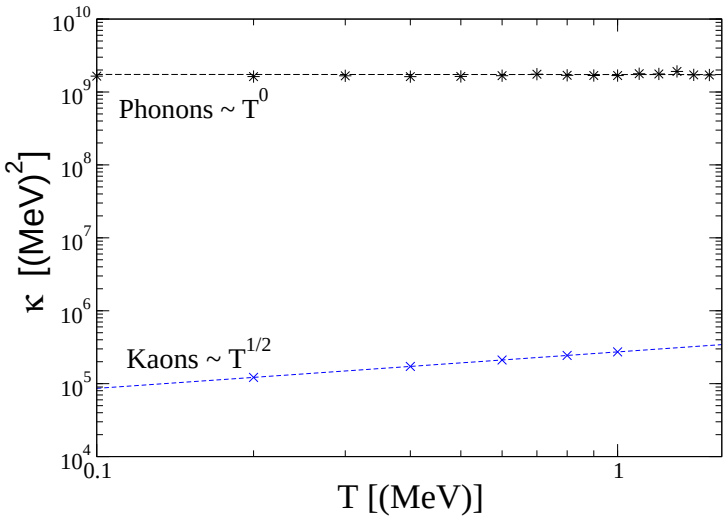

Figure 4.8: (Color online) Numerical results for the contribution of phonons and kaons to the thermal conductivity of the CFL as a function of temperature. The results shown in this figure were obtained using the variational method with $N = 5$. We have used $\mu = 400$ MeV, $\Delta = 100$ MeV for the phonons and $m_K = 10$ MeV, $\mu_K = 5$ MeV and $f_\pi = 100$ MeV for the kaons.

the results for $N = 5$. We observe that thermal conductivity due to kaons follows the square root dependence predicted by Eq. (4.86). Also, the thermal conductivity due to phonons is approximately temperature independent, in agreement with Eq. (4.86). The numerical results are well represented by

$$\kappa^{(P)} \gtrsim 4.01 \times 10^{-2} \, \frac{\mu^8}{\Delta^6} \, \mathrm{MeV}^2 \,, \qquad \kappa^{(K)} \simeq 0.86 \, \frac{f_\pi^4}{m_K^2} \sqrt{\frac{T}{m_K}} \, \mathrm{MeV}^2 \,. \tag{4.87}$$

We observe that for m_K in the few MeV range the phonon contribution is significantly larger than the kaon contribution.

4.10 Conclusions

We can convert these result into CGS units. We get

$$\kappa^{(P)} \gtrsim 1.04 \times 10^{26} \, \frac{\mu_{500}^8}{\Delta_{50}^6} \, \frac{\text{erg}}{\text{cm s K}} \,, \qquad \kappa^{(K)} \simeq 2.81 \times 10^{21} \, f_{\pi,100}^4 \, T_{\text{MeV}}^{1/2} \, m_{10}^{-5/2} \, \frac{\text{erg}}{\text{cm s K}} \,, \quad (4.88)$$

where μ_{500} is the quark chemical potential in units of 500 MeV, Δ_{50} is the gap in units of 50 MeV, $f_{\pi,100}$ is the pion decay constant in units of 100 MeV, T_{MeV} is the temperatures in units of MeV and m_{10} is the kaon mass in units of 10 MeV.

These numbers can be compared to a number of results in the literature. The thermal conductivity of the CFL phase was previously studied by Shovkovy and Ellis [84]. Based on a mean free path estimate they find that the contribution due to phonons is $\kappa^{(P)} \simeq 0.7 \times 10^{32} \, T_{\text{MeV}}^3 R_{0,\text{km}} \, \frac{\text{erg}}{\text{cm s K}}$, where $R_{0,\text{km}}$ is the phonon mean free path in units of 1 km. This particular number was chosen because the authors argued that the mean free path is so long that it is effectively cut off by the size of the quark matter core. In the present work we have demonstrated that in the framework of kinetic theory there is no simple connection between the phonon mean free path and the thermal conductivity. We note, however, that if one replaces the mean free path in the Shovkovy-Ellis estimate with a more accurate result from kinetic theory, which is on the order of millimeters rather than kilometers [69], one obtains a thermal conductivity which is close to our result. Shovkovy and Ellis also argued that there is a large contribution to κ from photons. The photon mean free path is indeed on the order of the size of the star [72]. This implies, however, that photons are not thermally coupled to the a CFL quark matter core.

The thermal conductivity of unpaired quark matter at low temperature is $\kappa = 0.5 m_D^2/\alpha_s^2$ [76], where m_D is the gluon screening mass and α_s is the strong coupling constant. Using $m_D \simeq 500$ MeV and $\alpha_s = 0.3$ this gives $\kappa \simeq 10^4 \, \text{MeV}^2$, about 5 orders

of magnitude larger than the thermal conductivity of the CFL phase. The thermal conductivity of nuclear matter was studied in [107, 108, 109, 110, 111]. A typical value at nuclear matter saturation density and $T \simeq 1$ MeV is $\kappa \simeq (10^{20} - 10^{21}) \frac{\mathrm{erg}}{\mathrm{cm\,s\,K}}$, which is about 5 orders of magnitude smaller than the thermal conductivity of the CFL phase.

We can convert the thermal conductivity to a timescale for thermal diffusion. The thermal diffusion constant is $\chi = \kappa / c_V$, where c_V is the specific heat. The time scale for thermal diffusion over a distance R is

$$\tau \simeq \frac{c_V R^2}{\kappa} \,. \tag{4.89}$$

Using $c_V = 2\pi^2 T^3/(15 v^3)$ for phonons, as well as $T = 1$ MeV, $\mu = 500$ MeV, $\Delta = 50$ MeV, and $R = 1$ km we get $\tau \simeq 10\,\mathrm{s}$, indicating that a CFL quark core will become isothermal rapidly.

In this work we have studied the thermal conductivity of the CFL phase using a linearized Boltzmann equation including a collision term that involves $2 \leftrightarrow 2$ scattering between phonons or kaons only. We have not studied a coupled transport equation for phonon-kaon scattering. Given that the relaxation times of phonons and kaons are quite different, it should be possible to find approximate solutions to the coupled problem. We have only provided a simple estimate for the relaxation time of temperature gradients. More accurate estimates will require a detailed model of the initial temperature profile, and a full solution of the dissipative two-fluid hydrodynamic equations for a CFL superfluid.

In the present work we have only considered a pure CFL phase without kaon condensation. This is the groundstate at asymptotically large density. Future work will be devoted to the effects of kaon condensation, and to the thermal conductivity of quark

phases at even lower density. Possible phases that are discussed in [7] include the curCFL phase, a color-flavor-locked phase supporting a non-zero Goldstone boson current, and the crystalline color superconducting phase.

Chapter 5

Trapped Atomic gases

5.1 Introduction

Cold, dilute Fermi gases in which the interaction between the atoms can be tuned using an external magnetic field provide a new paradigm for strongly correlated quantum fluids [22, 23]. Recently, there has been significant interest in the transport properties of these systems [112]. This interest was triggered by three independent developments. The first was the experimental observation of almost ideal hydrodynamic flow in the normal phase of a cold Fermi gas in the limit of infinite scattering length [113]. The second was the discovery of almost ideal flow in a completely different system, the quark gluon plasma created in heavy ion collisions at the Relativistic Heavy Ion Collider (RHIC) [12, 13, 14, 15]. Both of these experiments constrain the shear viscosity of the fluid. Remarkably, while the absolute value of the shear viscosity of the two systems differs by about 26 orders of magnitude, the ratio of shear viscosity η to entropy density s is very similar, $\eta/s \simeq (0.1 - 0.5)\,\hbar/k_B$, where $\hbar$ is Planck's constant and k_B is Boltzmann's constant [114, 115, 116, 117, 118].

The third development was the theoretical discovery of a new method to compute the shear viscosity of strongly coupled field theories [119, 120]. This method is based on the holographic duality between four dimensional field theory and string theory in higher dimensional spaces [121]. Using the holographic equivalence one can show that in a large class of field theories the strong coupling limit of η/s is equal to $\hbar/(4\pi k_B) \simeq 0.08\,\hbar/k_B$. This value is remarkably close to the experimental results for η/s quoted above. Initially the value $\hbar/(4\pi k_B)$ was derived only for scale invariant relativistic field theories, but it was later shown that the same value of η/s is obtained in the strong coupling limit of many non-conformal and non-relativistic field theories [122, 123].

The dilute Fermi gas at unitarity is a strongly correlated scale invariant quantum fluid [22, 23]. It provides a beautiful model system for testing ideas from many different areas of physics, including condensed matter physics, nuclear and particle physics, and quantum gravity. An important property of the Fermi gas at unitarity is nearly perfect fluidity [112]. Experiments with trapped Fermi gases in the vicinity of a Feshbach resonance indicate that [113, 114, 115, 116, 124, 125]

$$\frac{\eta}{s} \lesssim 0.5\,\hbar/k_B\,, \tag{5.1}$$

where η is the shear viscosity and s is the entropy density. This value is smaller than the viscosity to entropy density of any known fluid with the possible exception of the quark gluon plasma [117, 118, 126]. Equ. (5.1) approaches a bound $\eta/s = \hbar/(4\pi k_B)$ that has been proposed based on the AdS/CFT correspondence [127, 120].

In this work we will use kinetic theory to compute another important transport property of a dilute atomic Fermi gas, the thermal conductivity κ. We will consider both the high temperature as well as the low temperature, superfluid, phase. Our results

complement earlier studies of the shear viscosity in the high and low temperature phase [128, 105]. In the unitarity limit the bulk viscosity of the high temperature phase vanishes [47]. In the superfluid phase there are three bulk viscosities, one of which is non-vanishing in the unitarity limit. The bulk viscosities in the superfluid phase were recently computed in [129]. Combining our results for the thermal conductivity with the existing calculations of the shear viscosity we can study the relative size of momentum diffusion and thermal diffusion. The ratio of these quantities is known as the Prandtl number

$$Pr = \frac{c_P \eta}{\rho \kappa}\,, \tag{5.2}$$

where c_P is the specific heat at constant pressure and ρ is the fluid mass density.

The Prandtl number also controls the relative importance of shear viscosity and thermal conductivity in sound attenuation. Measurements of sound attenuation have the potential to provide new experimental constraints on transport properties of dilute atomic gases. Current estimates of the shear viscosity are based on the study of scaling flows, such as collective modes or the expansion out of a deformed trap [116]. These experiments do not directly constrain the density independent part of the shear viscosity. This is a problem, because kinetic theory predicts that the shear viscosity at high temperature is only a function of temperature, and not of density. Sound attenuation, on the other hand, is sensitive to this contribution. Using our results for the Prandtl number it is possible to use measurements of sound attenuation to constrain the shear viscosity. Conversely, in the regime where shear viscosity is well constrained it is possible to extract thermal conductivity from sound attenuation. First sound was observed in [130], and ideas for detecting second sound are discussed in [131].

This chapter is organized as follows. In section 5.2, we will outline introduce the ex-

perimental achievements and theoretical descriptions of unitarity Fermi gases. In Section 5.3, we will review the quasi-particle interactions in dilute atomic Fermi gases, and in Section 5.4 we outline the calculation of thermal conductivity using kinetic theory. In Sections 5.5 and 5.6 we compute the Prandtl number and sound attenuation length. We end with some conclusions in Section 5.7. We collect some formulas related to variational trial functions for the linearized Boltzmann equation in Appendix B.1, and the Virial expansion of thermodynamic functions at high temperature in Appendix B.2.

5.2 Unitarity Fermi Gas

5.2.1 Feshbach Resonances

Feshbach resonances [132] are quantum mechanical scattering resonances that were first discussed in the context of nuclear physics. Feshbach resonances have become important due to the developments of the techniques to cool and trap atoms [133]. In 2003-2005, a lots of ground-breaking experiments [113, 134, 135, 136] have been achieved by inducing magnetic Feshbach resonances in Bose condensates or Fermi degenerate gases. The interatomic interaction at ultracold temperature is dominated by binary s-wave collision, whose strength is characterized by scattering length a. In a ultracold atomic gas, a Feshbach resonance occurs when the bound molecular state in the closed channel energetically approaches the scattering state in the open channel, where the energy difference can be controlled by an external magnetic field B. Scattering length a is drastically altered near the Feshbach resonances. Such magnetically tuned Feshbach resonance can be described by a simple expression, introduced by Moerdijk et al. [137], for the s-wave scattering

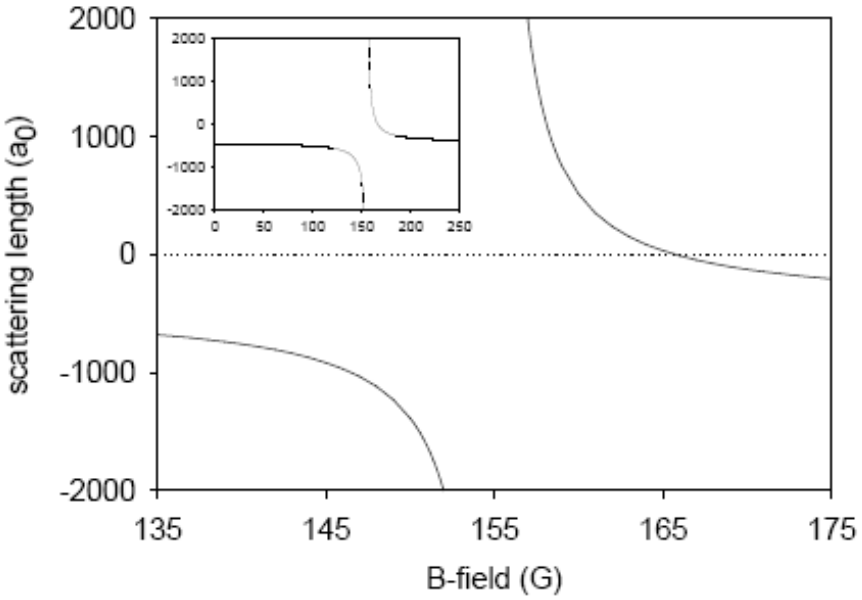

Figure 5.1: Magnetic field dependence of scattering length near the Feshbach resonance [8, 9]. The solid line is the scattering length, the horizontal dashed line indicates zero scattering length, which occurs at $B_{zero} = 165.75$G.

length a as a function of the magnetic field B,

$$a(B) = a_{bg}\left(1 - \frac{\Delta}{B - B_0}\right) \tag{5.3}$$

Figure 5.1 shows this resonance expression. The background scattering length a_{bg}, which is the scattering length associated with $V_{bg}(R)$, a background potential. We should remind an important feature of potential: the potential range is negligible compared to the de Broglie wavelength and the mean interparticle distance ($n^{1/3}$). The parameter B_0 denotes the resonance position and the parameter Δ is the resonance width. Note that both a_{bg} and Δ can be positive or negative. In the vicinity of the resonance position

at $B = B_0 + \Delta$, where the two channels are strongly coupled, the scattering length is going to diverges ($a \to \pm\infty$). The regime, where the infinite scattering length $a \to \pm\infty$ reached, is frequently referred to as the *unitarity limit*. The word "unitarity" refers to the fact that in this limit the s-wave scattering amplitude saturates the quantum mechanical unitarity bound. At unitarity the system displays universal properties. This can be seen by inspecting dimensionless parameters that characterize the many body system. One example of the dimensionless parameter is $k_F a$, where $k_F \equiv (3\pi^2 n)^{1/3}$ is the Fermi momentum. Here the effective range of the interaction r_0 is very small. It leads to the another typical dimensionless parameter $k_F r_0 \to 0$. Therefore, both parameters become invalid to describe such a strongly coupled system; the ratio of temperature to fermion density is the only dimensionless parameter. Hence, we conclude that the system behavior universal [138], i.e., independent of details of the interaction potential at unitarity limit. Note here, for large positive values of a, a "dressed" molecular state exists with a binding energy given by [139]

$$E_b = \frac{\hbar^2}{2\mu a^2} \tag{5.4}$$

where μ is the reduced mass of the atom pair.

In sum, the ultracold atomic gases provide an ideal system for studying quantum physics of interacting fermions from weak coupling to strong coupling. Below the critical temperature, T_c, the longstanding idea of the crossover from the Bardeen-Cooper-Schrieffer (BCS) state to the Bose-Einstein Condensation (BEC) also has been firstly realized in laboratories.

5.2.2 The Crossover from BCS to BEC

BCS mechanism [140] shows that if the Fermions' interaction is attractive, the Fermi surface is unstable toward to forming loosely bound Cooper pairs. Then, the bound states themselves form a condensate, exhibiting the superfluidity or superconductivity. Such phenomena have been observed in the metallic superconductor [141]; the superfluid ^{3}He [18]; the high-T_c superconductor [142]. Or possibilities of the superfluid nuclear matter [29]; the color superconductivity [7] and the neutrino superfluidity [143]. When the attraction between atoms is weak, where $k_F a$ is negative and $|k_F a| \ll 1$, the ultracold atomic gas, undergoes a phase transition and thus states in superfluid.

On the other hand, when the attraction is strong two fermions form a bound molecule and the system becomes a weakly interacting Bose gas in terms of molecules. The scattering length is positive and $0 < k_F a \ll 1$. Its ground state again exhibits superfluidity, but by the Bose-Einstein condensation of the tightly bound molecules. Thus, from the both sides, BCS and BEC, the gas transit from normal phase to superfluid phase below the critical temperature. The transition is smooth, which implies that the ground state of the system is a superfluid for any magnitude of $(k_F a)$, including $|k_F a| \to \infty$.

Such evolution from Cooper pairing (Fermi character) to condensation of composite bosons (Bose character) is named as BCS-BEC crossover, which firstly suggested in the dilute nuclear matter [144], where the neutron-neutron scattering length $a_{nn} \simeq -18.5$ fm is larger than the typical range of the nuclear force $r_0 \simeq 1.4$ fm. Ultracold atomic gases provide an experimental realization of BCS-BEC crossover [145, 146, 147, 148], where the unitarity limit exists in the middle of the BCS-BEC crossover. Through the standard perturbative expansion in terms of the small parameter $|k_F a| \ll 1$, one is able to quantitatively investigate the Fermi gas at both BCS and BEC limits. However, such

method break down in the unitarity limit because lack of a small expansion parameter, neither $k_F a$ nor $k_F r_0$. Therefore, theorists should establish another systematic approach to study the unitary Fermi gas and and its behavior at the BEC-BCS crossover.

5.2.3 Effective Field Theory at Superfluid Phase

The elegant approach of theoretical studying the unitarity gas was finished by D. Son and M. Wingate, see [138]. We will sketch how the effective action for the Goldstone bosons can be derived from the first principles in this section.

Considering a non-relativistic system is put in an external gauge field, A_μ, and curved three dimensional manifold with metric g_{ij}. If the particle interacting of system is described by a Yukawa two-body potential

$$V(r) = -\frac{q_0^2}{4\pi r}\mathrm{e}^{-r/r_0} \tag{5.5}$$

Note here, the infinity scattering length is achieved through tuning the parameters q_0 and r_0, when $mq_0^2 r_0 = 21.1$ Hence, the system can be described by the Lagrangian density

$$\mathcal{L} = \frac{\mathrm{i}}{2}\psi^\dagger\partial_t\psi - A_0\psi^\dagger\psi - \frac{g^{ij}}{2m}(\partial_i\psi^\dagger - \mathrm{i}A_i\psi^\dagger)(\partial_j\psi^\dagger + \mathrm{i}A_j\psi^\dagger) + q_0\psi^\dagger\psi\sigma - \frac{1}{2}g^{ij}\partial_i\sigma\partial_j\sigma - \frac{\sigma^2}{2r_0^2} \tag{5.6}$$

The gauge and manifold transformation rules read as

$$\begin{aligned}
\delta\psi &= \mathrm{i}\alpha\psi - \xi^k\partial_k\psi \\
\delta A_0 &= -\dot{\alpha} - \xi^k\partial_k A_0 - A_k\dot{\xi}^k \\
\delta A_i &= -\partial_i\alpha - \xi^k\partial_k A_i - A_k\partial_i\xi^k + mg_{ik}\dot{\xi}^k \\
\delta g_{ij} &= -\xi^k\partial_k g_{ij} - g_{ik}\partial_j\xi^j - g_{kj}\partial_i\xi^k \\
\delta\sigma &= -\xi^k\partial_k\sigma
\end{aligned} \tag{5.7}$$

where gauge parameter α and ξ^i are both time and space dependent. In fact, with particular choice of α and ξ^i, such transformation is describing a Galilean transformation if the space is flat, where

$$\alpha = mv^i x_i, \qquad \xi^i = v^i t. \tag{5.8}$$

The unitarity Fermi gas should be invariant under an additional transformation, which involves time scale, where

$$\begin{aligned}
\delta\psi &= -\beta\dot{\psi} - \frac{3}{4}\dot{\beta}\psi \\
\delta A_0 &= -\beta\dot{A}_0 - \dot{\beta}A_0 \\
\delta A_i &= -\beta\dot{A}_i \\
\delta g_{ij} &= -\beta\dot{g}_{ij} + \dot{\beta}g_{ij} \\
\delta\sigma &= -\beta\dot{\sigma} - \frac{3}{4}\dot{\beta}\sigma
\end{aligned} \tag{5.9}$$

with β being a linear function of time: $\beta = bt$.

The effective theory is generated by the general coordinate invariance, i.e., the effective action is invariant under the general coordinate transformations. It requires the

Lagrangian density to transform as

$$\delta\mathcal{L} = -\xi^k \partial_k \mathcal{L} \tag{5.10}$$

In the superfluid phase, the only physical freedom is the phase of condensate θ,

$$\psi = |\psi| \mathrm{e}^{-\mathrm{i}\theta} \tag{5.11}$$

where the chemical potential is encoded via $\theta = \mu t - \phi$. Note that ϕ is corresponding to phonons excitation. There is no other reason to forbid us to assume the microscopic theory is invariant under time, which means that the effective theory is invariant under

$$t \to -t, \qquad \text{and} \qquad \theta \to -\theta \tag{5.12}$$

Combining with rotational and parity symmetry, one has a constrain on the terms of time and space gradients after performing momentum expansion:

$$N[\partial_t] + N[\partial_i] - N[\theta] = \text{even} \tag{5.13}$$

Since θ is a Nambu-Goldstone field, it should always appear with derivatives in the effective Lagrangian. With respect to the gauge A_μ and manifold transformations, it limit the Lagrangian to be function of only two variables

$$\mathcal{L} = \mathcal{L}(D_t\theta, g^{ij} D_i\theta D_j\theta) \tag{5.14}$$

where

$$D_t\theta = \dot{\theta} - A_0 \qquad and \qquad D_i\theta = \partial_i\theta - A_i \tag{5.15}$$

Meanwhile, to satisfy the Eq. 5.10, there is only one combination of above two variables transforming as a scalar,

$$X = D_t\theta - \frac{g^{ij}}{2m} D_i\theta D_j\theta, \qquad \delta X = \xi^k \partial_k X \tag{5.16}$$

Therefore, to the first order, the lagrangian must be a function of this scaler, $\mathcal{L} = P(X)$. If we now set the metric to be flat and the external field to be zero, ones find the most general form of the Lagrangian for superfluid:

$$\mathcal{L} = P\left(\dot{\theta} - \frac{(\partial_i\theta)^2}{2m}\right) \tag{5.17}$$

Expanding the Lagrangian to quadratic order in ϕ, the Lagrangian is written as

$$\mathcal{L} = P(\mu) - n\dot{\phi} + \frac{\partial n}{2\partial\mu}\dot{\phi}^2 - \frac{n}{2m}(\partial_i\phi)^2 \tag{5.18}$$

where n is the particle density and the phonon speed is determined by the last two terms,

$$c_s = \sqrt{\frac{n}{m}\frac{\partial\mu}{\partial n}} \tag{5.19}$$

One finds in the Lagrangian to the Next-To-Leading(NTL) by repeating above argument: expand the term to higher order, choose the allowed invariant terms. Without external gauge field and sitting in a flat space, the NTL Lagrangian is read as

$$\mathcal{L}_{\text{NTL}} = \partial_i X \partial_i X f_1(X) + (\nabla^2\theta)^2 f_2(X) + m\nabla^2 A_0 f_3(x) \tag{5.20}$$

where

$$f_1(X) = c_1 m^{1/2} X^{-1/2}, \quad f_2(X) = c_2 m^{-1/2} X^{1/2}, \quad f_3(X) = c_2 m^{-1/2} X^{1/2}. \tag{5.21}$$

Here, to describe a conformal system, one requires $c_3 = -9c_2$. However, the real magnitude of c_1 and c_2 only can be decided by other microscopic computation. To get the phonon dispersion to NTL, one expands $\mathcal{L}_{\rm NTL}$ to quadratic order in ϕ, where

$$\mathcal{L}_{\rm NTL} = \frac{1}{\sqrt{\mu}} \left(\frac{15c_0}{8} \mu \dot{\phi}^2 - \frac{5c_0}{4} \mu^2 (\nabla\phi)^2 + c_1 (\partial_i \dot{\phi})^2 + c_2 \mu (\nabla^2 \phi)^2 \right) \tag{5.22}$$

Solving the above equation after Fourier transformation, the phonon dispersion relation is given by

$$\omega(q) = c_s q \left(1 - \pi^2 \sqrt{2\xi} \left(c_1 + \frac{3}{2} c_2 \right) \frac{q^2}{k_F^2} \right) \tag{5.23}$$

5.3 Elementary Excitations

Kinetic theory is based on the existence of well defined quasi-particle excitations. In the dilute Fermi gas quasi-particles exist both at very high and at very low temperature. In the high temperature limit the relevant degrees of freedom are spin 1/2 non-relativistic atoms with mass m. In the dilute limit the scattering cross section is dominated by elastic s-wave scattering. The scattering amplitude can be described in terms of a delta-function interaction $V(x - x') = C_0 \delta(x - x')$, see Fig. 5.2. Here, $C_0 = 4\pi a/m$ is related to the scattering length. The s-wave cross section is determined by sum of all two-body diagrams. The cross section is

$$\sigma = \int \mathrm{d}\Omega \, \frac{a^2}{1 + a^2 q^2} \,, \tag{5.24}$$

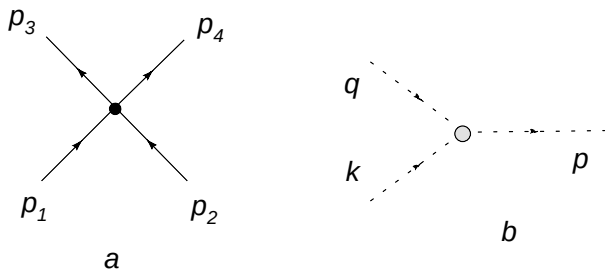

Figure 5.2: This figure shows the main processes that determine the thermal conductivity in high and low temperature phase, respectively. Fig. (a) shows the local four-fermion interaction, and Fig. (b) shows the three-phonon interaction.

where $\mathbf{p}_1, \mathbf{p}_2$ and $\mathbf{p}_3, \mathbf{p}_4$ are the ingoing and outgoing momenta and $\mathbf{q}$ is the relative momentum $\mathbf{q} = (\mathbf{p}_1 - \mathbf{p}_2)/2$. The relative momentum of the outgoing particles is $\mathbf{q}' = (\mathbf{p}_3 - \mathbf{p}_4)/2$ with $|\mathbf{q}'| = |\mathbf{q}|$. The solid angle is defined in terms of the angle between the relative momenta $\mathbf{q}$ and $\mathbf{q}'$, $d\Omega = d\cos(\theta_{\mathbf{q}\mathbf{q}'})d\phi_{\mathbf{q}\mathbf{q}'}$.

The characteristic temperature of the system is the Fermi temperature $T_F = k_F^2/(2m)$, where k_F is the Fermi momentum defined by $k_F^3 = 3\pi^2 n_{tot}$ and n_{tot} is the total density including both spin states. The strength of the interaction can be characterized by the dimensionless parameter $(k_F a)$. The regime of small and negative $(k_F a)$ is the BCS limit. In this limit the Fermi gas becomes a BCS superfluid at a critical temperature T_c which is exponentially small compared to T_F. The ratio T_c/T_F increases with $|k_F a|$. In the unitary limit $|k_F a| \to \infty$ the critical temperature is $T_c \simeq 0.15 T_F$ [149]. The regime of positive $(k_F a)$ is called the BEC limit. For small and positive $(k_F a)$ the system is composed of weakly interacting bosons with mass $2m$ and density $n_{tot}/2$. Superfluidity occurs at the Einstein temperature $T_c \simeq 0.21 T_F$.

In the superfluid phase the low energy excitations are phonons, Goldstone modes associated with the spontaneous breaking of the $U(1)$ phase symmetry. At unitarity

the effective lagrangian for the phonon field is strongly constrained by scale invariance. Expanding the Eq. 5.22, one has [138],

$$\begin{aligned}\mathcal{L}_\phi &= \frac{1}{2}(\partial_0\phi)^2 - \frac{1}{2}v_s^2(\boldsymbol{\nabla}\phi)^2 - g_3\big[(\partial_0\phi)^3 - 9v_s^2\partial_0\phi(\boldsymbol{\nabla}\phi)^2\big] \\ &\quad -\frac{3}{2}g_3^2\big[(\partial_0\phi)^4 + 18v_s^2(\partial_0\phi)^2(\boldsymbol{\nabla}\phi)^2 - 27v_s^4(\boldsymbol{\nabla}\phi)^4\big] + \dots ,\end{aligned} \tag{5.25}$$

where $g_3 = \pi v^{3/2}\xi^{3/4}/(3^{1/4}8\mu^2)$, μ is the chemical potential and v is the speed of sound with $v^2 = 2\mu/(3m)$. At unitarity $\mu = \xi E_F$ with $\xi \simeq 0.44$ [150]. At low momentum the phonon dispersion relation is linear, $\varepsilon_p = vp$. We will see that the thermal conductivity is sensitive to non-linearities in the dispersion relation. We will write the dispersion relation as $\varepsilon_p = vp(1+\gamma p^2)$, where the parameter γ can be expressed in terms of the coefficients of certain higher order terms in the lagrangian of Son and Wingate, $\gamma = -\pi^2\sqrt{2\xi}(c_1 + 1.5c_2)/k_F^2$. Rupak and Schäfer computed c_1 and c_2 using an epsilon expansion [151]. They find $c_1 \simeq -\sqrt{2}/(30\pi^2\xi^{3/2})$ and $c_2 \simeq 0$, corresponding to $\gamma = 1/(30m\mu)$. Other estimates of γ can be found in [152, 153].

We will study the contribution to thermal conductivity from the phonon splitting process $\varphi \rightleftharpoons \varphi + \varphi$, see Fig. 5.2. For $\gamma > 0$ this process is kinematically allowed. The matrix element for the three phonon process is

$$i\mathcal{M}_3 = g_3\Big(p_0[Q\cdot K] + k_0[Q\cdot P] + q_0[P\cdot K]\Big), \tag{5.26}$$

where we have defined the four vector product $Q\cdot K = q_0k_0 - 9v^2\boldsymbol{q}\cdot\boldsymbol{k}$. If γ is negative then the dominant contribution arises from $\varphi+\varphi \rightleftharpoons \varphi+\varphi$. We recently studied this process in a relativistic superfluid, the color-flavor-locked phase of QCD [154]. We found that the $2 \rightleftharpoons 2$ processes are controlled by s,t,u-channel exchanges with almost on-shell

intermediate state phonons. This means that the dominant process can be viewed as $1 \leftrightharpoons 2$ phonon splitting followed by $2 \leftrightharpoons 1$ phonon absorption.

5.4 Thermal Conductivity

Repeat the procedure in subsection 4.6.2, the thermal conductivity can then be written in two alternative ways

$$\kappa = T\langle\, \varepsilon_p \boldsymbol{v}_p | \boldsymbol{\chi}\rangle = T^2 \langle \boldsymbol{\chi} | \hat{C} | \boldsymbol{\chi}\rangle\,, \tag{5.27}$$

The function $\boldsymbol{\chi}$ is determined by the Boltzmann equation,

$$|\boldsymbol{\alpha}_p\rangle = \hat{C}|\boldsymbol{\chi}\rangle\,. \tag{5.28}$$

These two representations form the basis of the variational principle. Consider a trial state $|\boldsymbol{g}\rangle$. The Schwarz inequality implies that

$$\langle \boldsymbol{g}|\hat{C}|\boldsymbol{g}\rangle\langle\boldsymbol{\chi}|\hat{C}|\boldsymbol{\chi}\rangle \geq |\langle \boldsymbol{g}|\hat{C}|\boldsymbol{\chi}\rangle|^2\,. \tag{5.29}$$

Using Eq. (5.27) and Eq. (5.28), we can write this as

$$\kappa \geq T^2 \frac{|\langle \boldsymbol{g}|\boldsymbol{\alpha}_p\rangle|^2}{\langle \boldsymbol{g}|\hat{C}|\boldsymbol{g}\rangle} = \frac{|\langle \boldsymbol{g}|\varepsilon_p \boldsymbol{v}_p\rangle|^2}{\langle \boldsymbol{g}|\hat{C}|\boldsymbol{g}\rangle}\,. \tag{5.30}$$

We can then choose to expand the trial function $\boldsymbol{g}$ in orthogonal polynomials and take advantage of that fact that $\boldsymbol{g}$ is a dimensionless vector-valued function to write

$$\boldsymbol{g} = \boldsymbol{x} \sum_{s\neq 0}^{N} b_s^{(F,H)} B_s^{(F,H)}(x^2) \tag{5.31}$$

where $\boldsymbol{x} = \boldsymbol{p}/\Delta$, $x = |\boldsymbol{x}|$, and Δ is some characteristic energy scale in the problem (e.g. $\Delta = T/v$ for massless particles and $\Delta = \sqrt{2mT}$ for massive particles). The polymials are such that $B_0 = 1, B_1 = x^2 + a_{10}$, $B_2 = x^4 + a_{21}x^2 + a_{20}$, etc., and (F, H) labels the basis functions in the fermion and phonon case. The orthogonality condition is

$$A_s^{(F,H)}\delta_{st} = \int \mathrm{d}x f^0(x)(1 \pm f^0(x))x^4 B_s^{(F,H)}(x^2)B_t^{(F,H)}(x^2)\,. \tag{5.32}$$

The type of quasi-particle involved enters via the statistical factor $(1 \pm f^0(x))$ and through the dispersion relation in $f^0(x)$. The specific forms of $B_m^{(F,H)}(x^2)$ are given in Appendix B.1. Note that we have enforced the momentum constraint by excluding the $s = 0$ term in Eq. (5.31).

The thermal conductivity is now determined by solving Eq. (5.28) for $|\boldsymbol{\chi}\rangle$ and then adopting a variational procedure to compute κ by using Eq. (5.30). In practice, we will show that $\boldsymbol{\chi}$ satisfy the constrains inheriting from the conservation laws of mass, momentum and energy for both the fermions' and phonons' dispersion relation.

5.4.1 Normal Phase

In this section we will specify the matrix elements and the collision operator in the case of atom-atom scattering in the normal phase of the dilute Fermi gas. We will scale all the momenta as $x = p/\sqrt{2mT}$, use the Fermi-Dirac distribution functions and set $\nu = 2$.

The numerator of Eq. (5.30) is

$$\begin{aligned}\langle \boldsymbol{g}|\varepsilon_p \boldsymbol{v}_p\rangle &= \frac{2}{3T^3}\int \mathrm{d}\Gamma\, f^0(p)(1-f^0(p))\varepsilon_p \boldsymbol{v}_p\cdot\boldsymbol{g} \\ &= \frac{4m}{3\pi^2}\sum_{s\neq 0} b_s^F \int \mathrm{d}x\, f^0(x)(1-f^0(x))x^6 B_s^F(x^2) \\ &= \frac{4m}{3\pi^2}\sum_{s\neq 0} b_s^F A_{s1}^F \delta_{s1} = \frac{4m}{3\pi^2} b_1^F\, A_{11}^F\end{aligned} \tag{5.33}$$

where we have used the orthogonality condition. The matrix element of the collision operator is

$$\langle \boldsymbol{g}|\hat{C}|\boldsymbol{g}\rangle = \frac{2}{3T^4}\sum_{s,t\neq 0} b_s^F b_t^F \int \frac{\mathrm{d}^3P\mathrm{d}^3q}{(2\pi)^6}\,\mathrm{d}\Omega\,|\boldsymbol{v}_1-\boldsymbol{v}_2|\,\frac{a^2}{1+a^2q^2}\,D^0_{2\leftrightarrow 2}\,\boldsymbol{g}_1\cdot[\boldsymbol{g}_1+\boldsymbol{g}_2-\boldsymbol{g}_3-\boldsymbol{g}_4]\,. \tag{5.34}$$

Here we have written the transition probability in terms of the cross section Eq. (5.24) and the flux factor $|\boldsymbol{v}_1-\boldsymbol{v}_2|$. The integration variables are the pair momentum $\boldsymbol{P}=\boldsymbol{p}_1+\boldsymbol{p}_2$, the relative momentum $\boldsymbol{q}=(\boldsymbol{p}_1-\boldsymbol{p}_2)/2$, and the solid angle Ω is defined below Eq. (5.24). We have also defined $D^0_{2\leftrightarrow 2}=f^0(x_1)f^0(x_2)[1-f^0(x_3)][1-f^0(x_4)]$. We can write

$$\begin{aligned}\langle \boldsymbol{g}|\hat{C}|\boldsymbol{g}\rangle &= \frac{2^{11/2}m^{3/2}}{3T^{3/2}}\sum_{s,t\neq 0} b_s^F b_t^F \int \frac{\mathrm{d}^3x\mathrm{d}^3y}{(2\pi)^6}\,\mathrm{d}\Omega\,\frac{mTa^2y}{1+2mTa^2y^2}\,D^0_{2\leftrightarrow 2}\,\boldsymbol{B}_s^F\cdot\boldsymbol{B}_t^F \\ &= \frac{2^{11/2}m^{3/2}}{3T^{3/2}}\sum_{s,t\neq 0} b_s^F b_t^F M_{st}^F\end{aligned} \tag{5.35}$$

where $\boldsymbol{B}_t^F=\left[B_t^F(x_1)\boldsymbol{x}_1+B_t^F(x_2)\boldsymbol{x}_2-B_t^F(x_3)\boldsymbol{x}_3-B_t^F(x_4)\boldsymbol{x}_4\right]/2$. We finally get

$$\kappa_F \geq \frac{\langle \boldsymbol{g}|\varepsilon_p\boldsymbol{v}_p\rangle^2}{\langle \boldsymbol{g}|\hat{C}|\boldsymbol{g}\rangle} = \frac{\kappa_0}{3\cdot 2^{3/2}\pi^4}\left(\frac{T}{T_F}\right)^{\frac{3}{2}} D_F\left(k_F a, T/T_F\right) \tag{5.36}$$

where we have defined $\kappa_0 = m^{1/2} T_F^{3/2}$ and

$$D_F\left(k_F a, T/T_F\right) \equiv \frac{(b_1^F)^2 (A_{11}^F)^2}{\sum_{s,t\neq 0} b_s^F b_t^F M_{st}^F} \,. \tag{5.37}$$

We can now consider a finite basis and optimize the inequality with respect to the coefficients b_s^F. We obtain $D_F\left(k_F a, T/T_F\right) = (A_{11}^F)^2 (M^F)_{11}^{-1}$ where $(M^F)_{11}^{-1}$ refers to the (1,1)-component of the matrix inverse of M. Note that this result is equivalent to using the matrix form of the Boltzmann equation in the finite basis. The function D_F must typically be calculated numerically but we can analytically evaluate it in the limit of high temperature $T/T_F \gg 1$ and by keeping only the leading term in the polynomial expansion. We get

$$\kappa_F = \begin{cases} \frac{75}{128\sqrt{\pi}} \sqrt{\frac{T}{m}} \frac{1}{a^2} & |a| \to 0 \\ \frac{225}{128\sqrt{\pi}} m^{\frac{1}{2}} T^{\frac{3}{2}} & |a| \to \infty \end{cases} \tag{5.38}$$

We have tried to improve this result using higher order terms in the polynomial expansion, but the correction is very small, $\delta\kappa/\kappa < 2\%$. This is consistent with the results in [155], where the authors observed very rapid convergence for the shear viscosity in the high temperature phase. Numerical results are shown in Fig. 5.3. Note that the thermal conductivity depends only on the square of the scattering length so we plot the thermal conductivity as a function of $k_F|a|$. We observe that the thermal conductivity has a similar temperature dependence for all values of $(k_F a)$. At high temperature κ grows as $\kappa \sim T^{3/2}$ at unitarity and $T^{1/2}$ at small scattering length. The thermal conductivity then has a minimum at $T/T_F \simeq (0.2 - 0.3)$, and then increases for very small temperatures. This rise is related to Pauli blocking. We should note, however, that except in the BCS limit the results in this section are not reliable for $T \ll T_F$. The right panel shows that at fixed temperature κ decreases as the strength of the interaction increases, and that κ

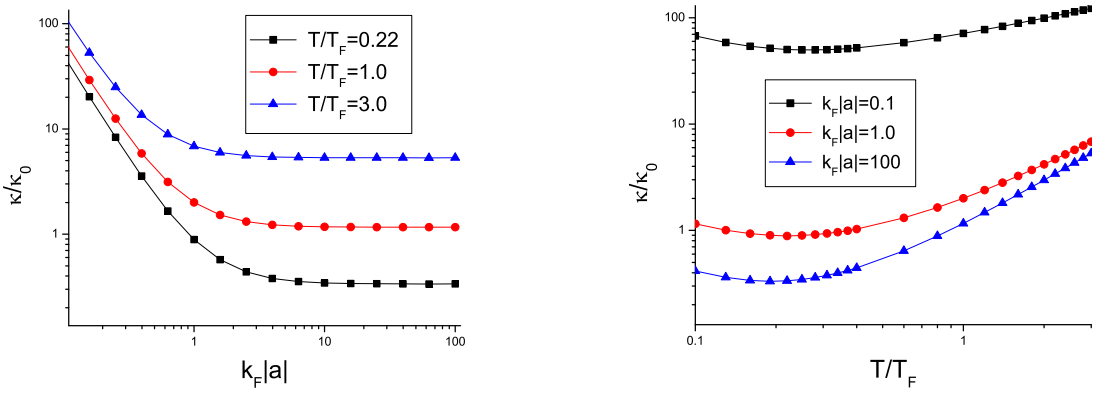

Figure 5.3: Thermal conductivity in the normal phase of a dilute Fermi gas in units of $\kappa_0 = m^{1/2}T_F^{3/2}$. In the left panel we show κ/κ_0 as a function of T/T_F for different values of $k_F a$. In the right panel we show κ/κ_0 as a function of $K_F a$ for different values of T/T_F.

becomes insensitive to $k_F a$ as we approach the unitarity limit $k_F a \to \infty$.

5.4.2 Superfluid Phase

In this section we study the thermal conductivity in the superfluid phase. We will concentrate on the unitarity limit $k_F a \to \infty$. In the BCS limit the critical temperature is exponentially small, and the thermal conductivity is dominated by fermionic quasi-particles even in the case $T < T_F$. In the extreme BEC limit the thermal conductivity reduces to that of an almost ideal Bose gas [156]. Following the procedure outlined in

the case the normal phase, we can write the numerator of Eq. (5.30) as

$$\begin{aligned}\langle \boldsymbol{g}|\varepsilon_p \boldsymbol{v}_p\rangle &= \frac{1}{3T^3}\int \mathrm{d}\Gamma f^0(p)(1+f^0(p))\varepsilon_p\, \boldsymbol{v}_p\cdot\boldsymbol{g} \\ &= \frac{2\gamma}{3\pi^2}\frac{T^3}{v^4}\sum_{s\neq 0} b_s^H \int \mathrm{d}x f^0(x)(1+f^0(x))x^6 B_s^H(x^2) \\ &= \frac{2\gamma}{3\pi^2}\frac{T^3}{v^4} b_1^H A_{11}^H\,,\end{aligned} \tag{5.39}$$

where we have used $\nu = 1$, scaled the momenta as $x = vp/T$ and kept only the leading order terms in the parameter γ that governs nonlinearities in the dispersion relation. We note that the result is indeed proportional to γ, and κ vanishes in the case of an exactly linear dispersion relation as discussed before. The matrix element of the collision operator is

$$\begin{aligned}\langle \boldsymbol{g}|\hat{C}|\boldsymbol{g}\rangle &= \frac{1}{3T^4}\sum_{s,t\neq 0} b_s^H b_t^H \int \mathrm{d}\Gamma_{pkq}\,|\mathcal{M}_3(p,k,q)|^2\,(2\pi)^4\delta^4(P+K-Q)\,D^0_{1\leftrightarrow 2}\,\boldsymbol{B}_s^H\cdot\boldsymbol{B}_t^H \\ &= \frac{g_3^2}{96\pi^3}\frac{T^5}{v^6}\sum_{s,t\neq 0} b_s^H b_t^H \int \mathrm{d}\Gamma_{xyz}\,|\mathcal{M}_3(x,y,z)|^2\,(2\pi)^4\delta^4(X+Y-Z)\,D^0_{1\leftrightarrow 2}\,\boldsymbol{B}_s^H\cdot\boldsymbol{B}_t^H \\ &= \frac{g_3^2}{96\pi^3}\frac{T^5}{v^6}\sum_{s,t\neq 0} b_s^H b_t^H M_{st}^H\,,\end{aligned} \tag{5.40}$$

where $\mathrm{d}\Gamma_{pkq}$ is the 3-particle Lorentz-invariant phase space, $D^0_{1\leftrightarrow 2} = f^0(x)f^0(y)(1+f^0(z))$ and $\boldsymbol{B}_t^H = \left[B_t^H(x)\boldsymbol{x} + B_t^H(y)\boldsymbol{y} - B_t^H(z)\boldsymbol{z}\right]/\sqrt{3}$. As before, we can define

$$D_H = (A_{11}^H)^2 (M_{st}^H)^{-1}_{11} \tag{5.41}$$

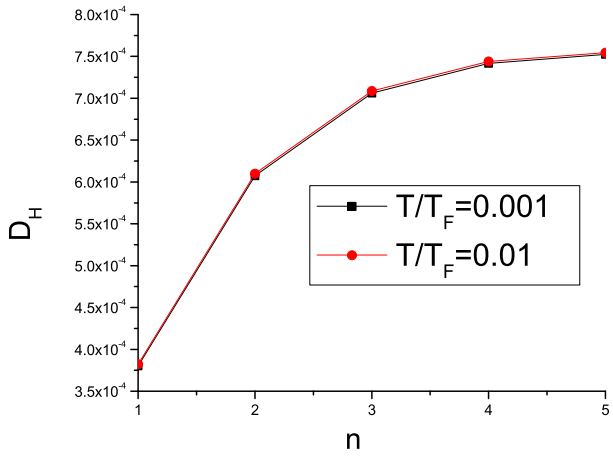

Figure 5.4: Variational function D_H as a function of the number of terms in the polynomial expansion of $\tilde{g}(x)$. We show D_H for two different temperatures.

which allows us to write the thermal conductivity as

$$\kappa_H \geq \frac{\langle \boldsymbol{g}|\varepsilon_p \boldsymbol{v}_p\rangle^2}{\langle \boldsymbol{g}|\hat{C}|\boldsymbol{g}\rangle} = \frac{128}{3\pi}\frac{\gamma^2}{g_3^2}\frac{T^2}{v^2}\,D_H = \frac{256\sqrt{2}}{25\pi^3\xi^2}\,\kappa_0\Big(\frac{T}{T_F}\Big)^2 D_H\,(T/T_F)\ . \tag{5.42}$$

where $\xi \simeq 0.44$ is defined in Section 5.3. D_H is a dimensionless function of T/T_F which has to be calculated numerically. The convergence of D_H with the number of terms in the trial function is shown in Fig. 5.4. We observe that the result in converging, but not nearly as fast as it did in the case of fermionic quasi-particles. The temperature dependence of D_H is very weak and $\kappa_H \sim T^2$. In Fig. 5.5 we combine our results for the thermal conductivity of the dilute Fermi gas at unitarity in the high and low temperature limits. The dashed line indicates the location of the phase transition. We note that the low and high temperature results do not match very well near T_c. This suggests that additional processes or excitations must become relevant in this regime. We also note that

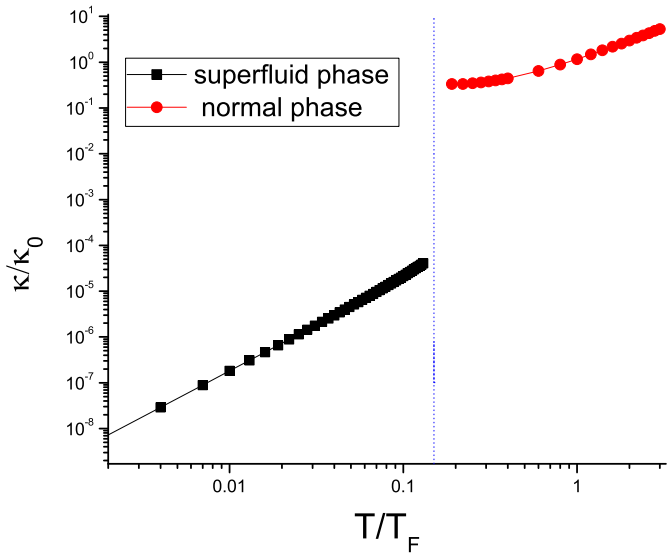

Figure 5.5: Thermal conductivity κ/κ_0 of the dilute Fermi gas at unitarity as a function of T/T_F. We show the calculations in the high and low temperature limit, extrapolated to $T \simeq T_c$. The position of the critical temperature is indicated by the dashed line.

at T_c critical fluctuations are expected to lead to a divergence in the thermal conductivity [157].

5.5 Shear Viscosity and the Prandtl Number

5.5.1 Shear Viscosity

We would like to make some comparisons of the thermal conductivity with the shear viscosity. The shear viscosity in both the high and low temperature regimes for the unitary gas have already been calculated, [128, 105]. Here, we summarize the results using the notation presented in this paper. First we write down the non-ideal part of the

stress-energy tensor in both a kinetic theory and hydrodynamic description as

$$\delta T_{ij} = \nu \int \mathrm{d}\Gamma v_p \frac{p_i p_j}{p} \delta f_p = -\eta V_{ij} \tag{5.43}$$

where $V_{ij} = \partial_i V_j + \partial_j V_i - 2/3\delta_{ij}\nabla \cdot V$ and V_i is the velocity of the fluid. Using an ansatz for δf_p similar to what we had in the thermal conductivity case as

$$\delta f_p = -\frac{f_p^0(1 \pm f_p^0)}{T} \chi_{ij} V_{ij}, \tag{5.44}$$

we can write down an expression for η as

$$\eta = \frac{\nu}{5T} \int \mathrm{d}\Gamma f_p^0(1 \pm f_p^0) \frac{v_p}{p} p_i p_j \chi_{ij} \equiv \frac{3T^2}{5} \langle \tilde{p}_{ij} | \chi_{ij} \rangle \tag{5.45}$$

where $\tilde{p}_{ij} = v_p(p_i p_j - 1/3\delta_{ij}p^2)/p$ and we have used the definition of the inner product defined previously. We can also write down the Boltzmann equation projected onto the shear component as

$$\begin{aligned} \frac{\mathrm{d}f}{\mathrm{d}t} &= \frac{f_p^0(1 \pm f_p^0)}{2T} |\tilde{p}_{ij}\rangle V_{ij} \\ &= C[f_p] \equiv \frac{f_p^0(1 \pm f_p^0)}{2T} \hat{C} |\chi_{ij}\rangle V_{ij} \end{aligned} \tag{5.46}$$

As before, we can combine these results into an exact form for the shear viscosity as

$$\eta = \frac{3T^2}{5} \frac{\langle \chi_{ij} | \tilde{p}_{ij} \rangle^2}{\langle \chi_{ij} | \hat{C} | \chi_{ij} \rangle} \tag{5.47}$$

We can then choose a suitably appropriate variational ansatz for $\chi_{ij} = \frac{p_{ij}}{\Delta^2}\tilde{g}(x)$ and expand $\tilde{g}(x) = \sum_{s=0} c_s C_s(x^2)$ as before. From this, we get a lower bound on the shear

viscosity in the high temperature limit that can be written as

$$\eta_F \geq \frac{2^{7/2}}{45} D^\eta \left(\frac{T}{T_F}\right)^{3/2} \eta_0 \tag{5.48}$$

where $D^\eta = (A^\eta)^2_{00}(M^\eta_{st})^{-1}_{00}$, $\eta_0 = (mT_F)^{3/2}$ and

$$A^\eta_{00} = \int \mathrm{d}x f^0_F(x)(1 - f^0_F(x))x^6 \tag{5.49}$$

and

$$M^\eta_{st} = \int \mathrm{d}\Gamma \frac{mTa^2X^2x^3}{1 + 2mTa^2x^2} f^0_F(x_1) f^0_F(x_2)(1 - f^0_F(x_3))(1 - f^0_F(x_4))\widehat{C}_s \cdot \widehat{C}_t \tag{5.50}$$

with

$$\widehat{C}_t = \left[C_t(x_1)x_1^{ij} + C_t(x_2)x_2^{ij} - C_t(x_3)x_3^{ij} - C_t(x_4)x_4^{ij}\right]/2 \tag{5.51}$$

In the high temperature limit, $T/T_F \to \infty$, we have

$$\eta_F = \begin{cases} \frac{5\sqrt{mT}}{32a^2\sqrt{\pi}} & |a| \to 0 \\ \frac{15(mT)^{3/2}}{32\sqrt{\pi}} & |a| \to \infty \end{cases} \tag{5.52}$$

Below T_c, the shear viscosity from binary scattering of phonons was calculated in Ref. [105] as

$$\eta_H = 5.06 \times 10^{-6} \xi^{7/2} \left(\frac{T_F}{T}\right)^5 \eta_0 \tag{5.53}$$

5.5.2 Prandtl Number

Now that we have collected the information of the thermal conductivity and shear viscosity, we are able to examine the behavior of dimensionless parameter Prandtl number,

$\mathrm{Pr} = \mathrm{c_P}\eta/(\rho\,\kappa)$ where ρ is the mass density of the fluid. For this we need the specific heat at constant pressure. This is a non-trivial calculation (when not at large or small T) and is relegated to the appendix. At high temperature, we can use our analytic results for κ and η from Eq. (5.38) and Eq. (5.52) to gain insight. In that limit, we know that $c_p = 5n/2$ and $\rho = mn$ where n is the number density. Putting this together, we find that

$$\mathrm{Pr} = 2/3 \qquad\qquad T \gg T_F \tag{5.54}$$

in both the large and small limits of scattering length. In Fig. 5.6, we plot the Prandtl number as a function of T/T_F for negative values of $k_F a$. As discussed in more detail in Appendix B.2, the virial expansion is smooth across unitarity (from $a \to -\infty$ to $a \to \infty$), but begins to break down as we approach $a \to 0^+$ due to the presence of the bound state, so we do not show those values here. Note that the Prandl number is remarkably insensitive to the value of $k_F a$ for large, negative values of the scattering length and approaches 2/3 for large values of T/T_F.

5.6 Sound Attenuation

The existence of viscosity and thermal conductivity results in the dissipation of energy in sound waves. A sound wave is propagated through a fluid, its intensity decreased according to a law $e^{-2\gamma x}$, where x is travel distance and γ is the absorption coefficient.

The expression for the sound attenuation α_1 above the critical temperature is, [51]:

$$\alpha_1 = \frac{\gamma}{\omega^2} = \frac{1}{2\rho c^3}\big[(\frac{4}{3}\eta + \zeta) + \rho\,\kappa(\frac{1}{c_V} - \frac{1}{c_P})\big] \tag{5.55}$$

where ω is the frequency of sound wave, ρ is the mass density of fluid, c is the speed of

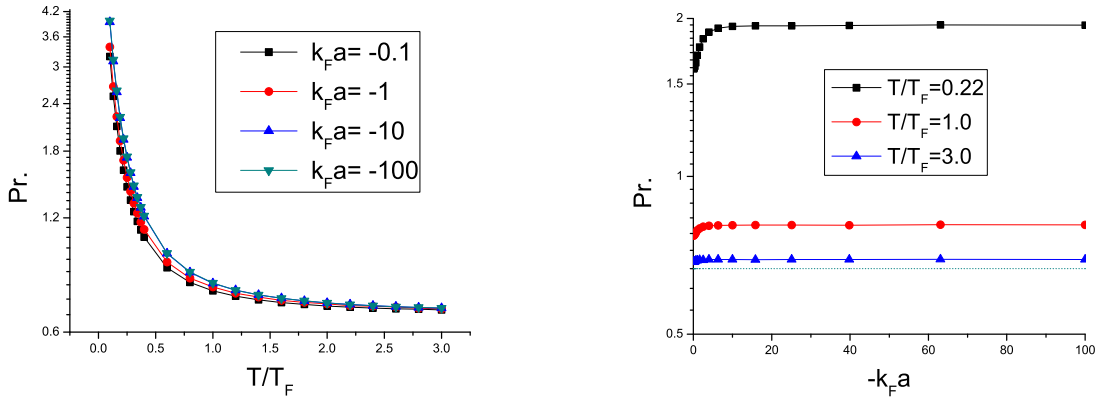

Figure 5.6: Left panel: Prandtl number as a function of T/T_F. Right panel: Prandtl number as a function of $k_F a$, the dash line is at the point 2/3. Note the convergence to Pr $\sim 2/3$ as we go to large T/T_F for all values of a.

sound wave and ζ is the bulk viscosity. Assuming that $\zeta = 0$, we can write this in a more transparent way as

$$\alpha_1 = \frac{2\eta}{3\rho c^3}\left[1 + \frac{3}{4}\frac{\Delta c_P}{Pr}\right] \equiv \frac{\eta_0}{2\rho c^3}(\alpha_\eta^* + \alpha_\kappa^*) \tag{5.56}$$

where $\Delta c_P = (c_P - c_V)/c_V$ and we have defined α_η^* and α_κ^* which we plot in Fig. 5.7.

In the normal phase at high temperature, $Pr \sim 2/3$ and $\Delta c_P \sim 2/3$, such that the contribution to the sound attenuation from the thermal conductivity is 3/4 of the contribution from the shear viscosity. Also, both Pr and Δc_P are relatively insensitive of the scattering length at high temperature, so that the results for the sound attenuation at high temperature remain qualitatively the same for any value of the scattering length, see Fig. 5.7. As we decrease in temperature, the sound absorption coefficient becomes more and more dominated by the shear viscosity.

Below T_c, we have two sound absorption coefficients. The first one is the same as above; however we know that $\Delta c_P \to 0$ rapidly as $T \to 0$. Therefore, the absorption of

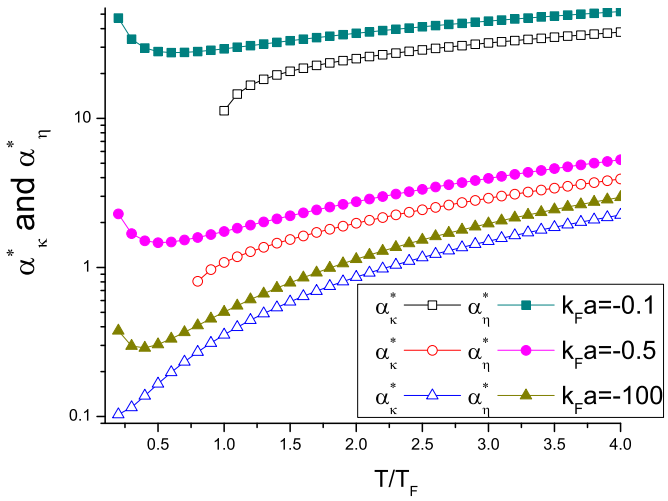

Figure 5.7: α_η^* and α_κ^* as a function of T/T_F. Note that the ratio of the two approaches a constant (3/4) as we go to larger values of T/T_F.

first sound will be dominated by the shear viscosity term. The absorption coefficient of second sound is given by, [51]

$$\alpha_2 = \frac{1}{2\rho c_2^3}\frac{\rho_s}{\rho_n}\left[\frac{4}{3}\eta + \zeta_2 - \rho(\zeta_1+\zeta_4) + \rho^2\zeta_3 + \rho\frac{\rho_n}{\rho_s}\frac{\kappa}{c_P}\right] \tag{5.57}$$

where $\rho_{n,s}$ are the normal and superfluid densities, c_2 is the speed of second sound and ζ_i are the 4 bulk viscosities in the superfluid. We can ignore the contributions from the bulk viscosities near unitarity as they are either identically zero or go to zero at low temperatures, [129]. We also know that $\eta \sim 1/T^5$ and $\kappa \sim T^2$ at low temperatures. From this, we can see that if we go to low enough temperatures, only the contribution from the shear viscosity will be important.

5.7 Conclusions

In this work we studied the thermal conductivity of a dilute Fermi gas. Our main results are summarized in Fig. (5.5). We observe that the thermal conductivity κ scales as $m^{1/2}T^{3/2}$ in the high temperature limit and as $m^{1/2}T_F^{3/2}(T/T_F)^2$ in the low temperature limit. In the high temperature limit the Prandtl ratio is 2/3, but the Prandtl number increases as the temperature is lowered. This, together with the fact that $\Delta c_p = (c_p - c_v)/c_v$ decreases at low temperature, implies that the sound attenuation length in the interesting regime $T_c < T < T_F$ is dominated by shear viscosity. In order to assess the feasibility of measuring sound attenuation we consider the ratio of to the wavelength λ of the sound wave to the sound attenuation length γ^{-1}. We have

$$\lambda\gamma = \frac{4\pi}{\sqrt{3\xi}}\Big(\frac{k}{k_F}\Big)\Big(\frac{\eta}{n}\Big)\left[1+\frac{3}{4}\frac{\Delta c_p}{Pr}\right] \simeq 11.4\Big(\frac{k}{k_F}\Big)\Big(\frac{\eta}{n}\Big)\,, \tag{5.58}$$

where we have used $\xi \simeq 0.44$ and $\Delta c_p/Pr \simeq 0$. A rough estimate of the minimum value of η/n can be obtained by extrapolating the kinetic theory result down to $T = T_c$. We get

$$\Big(\frac{\eta}{n}\Big)_{min} \simeq \frac{45\pi^{3/2}}{64\sqrt{2}}\left(\frac{T_c}{T_F}\right)^{3/2} \simeq 0.15\,. \tag{5.59}$$

Finally, we can express k/k_F in terms of the wavelength and the trap parameters. We obtain

$$\frac{k}{k_F} = \frac{R_z}{\lambda}\frac{\pi\beta^{2/3}}{(3N)^{1/3}}\,, \tag{5.60}$$

where R_z is the longitudinal cloud size, $\beta = R_\perp/R_z$ is the trap asymmetry, and N is the number of particles. For the experiment reported in [130] we get $k/k_F \simeq 0.046$ and $\lambda\gamma \simeq 0.08$. This implies that a measurement of the sound attenuation length is within reach. Higher sensitivity can be achieved by using more elongated traps or smaller

wavelengths.

There are a variety of improvements that need to be made once experimental data become available. The most important is to replace the plane wave approximation which is the basis of Eq. (5.58) by a more detailed calculation of the wave profile in a given trap geometry. It will also be interesting to study attenuation of first and second sound in the superfluid phase.

Chapter 6

Viscosity Spectral Functions of the Dilute Fermi Gas in Kinetic Theory

6.1 Introduction

The Kubo formula relates the shear viscosity to the zero momentum, zero frequency limit of the retarded stress tensor correlation function. In this chapter we will study the frequency and momentum dependence of this correlation function. We will focus on the regime of high temperature and small frequency and momentum where the methods of kinetic theory are applicable. Our study is motivated by several considerations. The first observation is that the frequency and momentum dependence of the retarded correlator encodes the time and distance scales over which the viscous contribution to the stress tensor relaxes to the Navier-Stokes expression. These scales are important for understanding how hydrodynamics breaks down in the dilute corona of a trapped Fermi gas [158, 116]. Kinetic theory predicts that in the dilute limit the shear viscosity is independent of density. This leads to a difficulty in the analysis of experiments involving scaling

flows in which the velocity field is linear in the coordinates. The Navier-Stokes equation predicts that in this case the viscous stress tensor is a function of time, but constant in space. As a consequence the dissipative force, which is proportional to gradients of the stresses, vanishes and the dissipated heat, which is governed by the volume integral of the square of the stress tensor, is infinite. This problem can be resolved if a finite relaxation time for the dissipative stresses is taken into account. In this case the dissipative stress tensor vanishes in the dilute corona, the dissipated heat is finite, and there is a viscous force that counteracts the expansion of the system.

A second motivation is to understand the physics behind nearly perfect fluidity in the unitary Fermi, in particular the question whether the unitary gas can be described in terms of quasi-particles. In kinetic theory quasi-particles manifest themselves in terms of a peak in the spectral function, but the quasi-particle peak may disappear in strong coupling. The spectral function is accessible through the behavior of the euclidean correlation function which can be computed in imaginary time Monte Carlo simulations. A calculation of the spectral function in kinetic theory serves as a useful default model for numerical calculations of the euclidean correlator.

This chapter extends and complements several recent studies of the transport properties of the dilute Fermi gas at unitarity. Calculations of transport coefficients in the context of kinetic theory can be found in [128, 155, 105, 129, 159], and a quasi-particle model is discussed in [160]. A diagrammatic calculation of the shear viscosity using the Kubo formula is described in [161]. This chapter also studies the spectral function. A sum rule for the spectral function of the stress tensor was proved in [162]. Related work on dilute Bose gases can be found in [163], and first attempts to extend the AdS/CFT correspondence to non-relativistic systems are described in [122, 123]. Finally, the spectral function of the stress tensor in QCD is studied in [164, 165, 166, 167, 168].

6.2 Preliminaries

The retarded correlation function of the stress tensor is defined by

$$G_R^{ijkl}(\omega, \mathbf{k}) = -i \int \mathrm{d}t \int \mathrm{d}\mathbf{x}\, e^{i\omega t - i\mathbf{k}\cdot\mathbf{x}} \Theta(t) \langle [\Pi^{ij}(t, \mathbf{x}), \Pi^{kl}(0, \mathbf{0})] \rangle \,. \tag{6.1}$$

A careful definition of the stress tensor $\Pi^{\alpha\beta}(t, \mathbf{x})$ in terms of the Hamiltonian of the dilute Fermi gas was given in [169, 161]. In the following, we only need the definition of the stress tensor in terms of hydrodynamic and kinetic variables, see Sec. 6.3 and 6.4. The spectral function is defined by

$$\rho^{ijkl}(\omega, \mathbf{k}) = -2\mathrm{Im}\, G^{ijkl}(\omega, \mathbf{k}) \,. \tag{6.2}$$

In the following, we will focus on the longitudinal and transverse shear channels ρ^{xyxy}, ρ^{xzxz} and ρ^{zzzz} where the z-direction is the direction defined by the external momentum $\mathbf{k}$. We will compute the retarded correlation function using linear response theory. The external field that couples to the stress tensor is the metric $g_{ij}(t, \mathbf{x})$. A formalism for coupling an interacting theory of non-relativistic particles to an external metric in a way that exhibits a non-relativistic version of general coordinate invariance was recently developed in [138]. The response to a small perturbation $g_{ij}(t, \mathbf{x}) = \delta_{ij} + h_{ij}(t, \mathbf{x})$ around the flat metric is given by

$$\delta\Pi^{ij} = \frac{\delta \Pi_{ij}^{eq}}{\delta h_{ij}} h^{ij} - \tfrac{1}{2} G_R^{ijkl} h_{kl} \tag{6.3}$$

where Π_{ij}^{eq} is the expectation value of the stress tensor in equilibrium.

6.3 Hydrodynamics

At very low frequency and momentum the retarded correlation function is governed by hydrodynamics. The hydrodynamic limit provides an important constraint for the kinetic description of the system. In this section we will derive these constraints in the case of correlations functions of the stress tensor. We note that hydrodynamics breaks down for frequencies $\omega \gtrsim (\eta/n)T$ and momenta $k \gtrsim (\eta/n)(mT)^{1/2}$, where n is the density and T is the temperature. In the unitary limit and in the vicinity of T_c we have $\eta/n \sim 1$ and the range of validity of hydrodynamics is very large. In the weak coupling limit $\eta \sim (mT)^{1/2}/a^2$, where a is the scattering length, and the range of validity of hydrodynamics is much smaller.

In order to study linear response theory we consider hydrodynamics in a curved background $g_{ij}(\mathbf{x}, t)$. Non-relativistic fluid dynamics in a non-trivial metric was studied in [47]. The continuity equation and the equations of momentum and energy conservation are given by

$$\begin{aligned} \frac{1}{\sqrt{g}}\partial_t\left(\sqrt{g}\rho\right) + \nabla_i\left(\rho v^i\right) &= 0\,, \\ \frac{1}{\sqrt{g}}\partial_t\left(\sqrt{g}\rho v^i\right) + \nabla_j \Pi^{ji} &= 0\,, \\ \frac{1}{\sqrt{g}}\partial_t\left(\sqrt{g}\rho s\right) + \nabla_i\left(\rho s v^i - \frac{\kappa}{T}\partial^i T\right) &= \frac{2R}{T}\,, \end{aligned} \tag{6.4}$$

where $\rho = mn$ is the mass density, v^i is the fluid velocity, and $g = \det(g_{ij})$. The covariant derivative of a vector field is given by $\nabla_i v_j = \partial_i v_j - \Gamma^k_{ij} v_k$, where Γ^k_{ij} is the Christoffel symbol associated with g_{ij}. The stress tensor is

$$\Pi^{ij} = \rho v^i v^j + P g^{ij} - \sigma^{ij}, \tag{6.5}$$

where the viscous term, σ_{ij}, is given by

$$\sigma_{ij} = \eta\Big(\nabla_i v_j + \nabla_j v_i + \dot{g}_{ij}\Big) + \left(\zeta - \frac{2}{3}\eta\right) g_{ij}\left(\nabla_k v^k + \frac{\dot{g}}{2g}\right) . \tag{6.6}$$

The dissipative function R is given by

$$\begin{aligned} 2R &= \frac{\eta}{2}\left(\nabla_i v_j + \nabla_j v_i - \tfrac{2}{3} g_{ij}\nabla_k v^k + \dot{g}_{ij} - \tfrac{1}{3} g_{ij}\frac{\dot{g}}{g}\right)^2 \\ &\quad + \zeta\left(\nabla_i v^i + \frac{\dot{g}}{2g}\right)^2 + \frac{\kappa}{T}\partial_i T \partial^i T, \end{aligned} \tag{6.7}$$

where κ is the thermal conductivity. We are interested in small deviations from equilibrium. For this purpose we write $g_{ij} = \delta_{ij} + h_{ij}$, and $\rho = \rho_0 + \delta\rho$, $P = P_0 + \delta P$ etc. and linearize the equations in h_{ij}, v_i, δP, δs, $\delta\rho$ and δT. After going to Fourier space we find

$$\begin{aligned} \frac{\mathrm{i}}{2}\omega\rho_0 h + \mathrm{i}\omega\delta\rho + \rho_0(-\mathrm{i}k)v_z &= 0\,, \\ \mathrm{i}\omega\rho_0 v^i + (-\mathrm{i}k)\delta P\delta^{iz} + \mathrm{i}k\sigma^{iz} &= 0\,, \\ \mathrm{i}\omega\rho_0\delta s + \frac{\kappa k^2}{T}\delta T &= 0\,, \end{aligned} \tag{6.8}$$

where $h = \mathrm{Tr}(h_{ij})$ and we have chosen the direction of k to be the z-axis. The fluctuations in thermodynamic variables are related by thermodynamic identities. We will consider $\delta\rho$ and δs to be the independent variable and use

$$\begin{aligned} \delta P &= \frac{\partial P}{\partial\rho}\Big|_s \delta\rho + \frac{\partial P}{\partial s}\Big|_\rho \delta s = c_s^2\delta\rho + \frac{\partial P}{\partial s}\Big|_\rho \delta s\,, \\ \delta T &= \frac{\partial T}{\partial\rho}\Big|_s \delta\rho + \frac{\partial T}{\partial s}\Big|_\rho \delta T = \frac{\partial T}{\partial\rho}\Big|_s \delta\rho + \frac{T}{c_V}\delta s\,, \end{aligned} \tag{6.9}$$

where c_s is the speed of sound and c_V is specific heat at constant volume.

We can now solve for the hydrodynamic variables in terms of the external field h_{ij} and compute Π_{ij} from Eq. (6.5). We then determine G_R using Eq. (6.3). We are particularly interested in the transverse shear correlators G_R^{xyxy} and G_R^{xzxz}, as well as the longitudinal correlator G_R^{zzzz}. We find

$$G_R^{xyxy} = -\mathrm{i}\eta\omega\,, \tag{6.10}$$

$$G_R^{xzxz} = -\frac{\mathrm{i}\eta\omega^2}{\omega - \mathrm{i}k^2(\eta/\rho_0)}\,, \tag{6.11}$$

$$G_R^{zzzz} = -\frac{\omega^2\rho_0(c_s^2 + \mathrm{i}\omega\alpha)}{\omega^2 - c_s^2k^2 - \mathrm{i}\omega k^2\alpha}\,. \tag{6.12}$$

We note that G_R^{xzxz} has a diffusive pole, where η/ρ_0 is the momentum diffusion coefficient, and G_R^{zzzz} has a sound pole where α is the sound attenuation coefficient,

$$\alpha\rho_0 = \frac{4}{3}\eta + \zeta + \frac{\kappa c_s^2k^2}{\omega^2}\left(\frac{1}{c_V} - \frac{1}{c_P}\right)\,. \tag{6.13}$$

Finally, we can take the imaginary parts and compute the spectral functions. In the Kubo limit $k = 0$, $\omega \to 0$ we find

$$\lim_{\omega,k\to 0}\frac{\rho_T}{2\omega} = \eta\,, \tag{6.14}$$

$$\lim_{\omega,k\to 0}\frac{\rho_L}{2\omega} = \frac{4}{3}\eta + \zeta\,, \tag{6.15}$$

where T, L labels the transverse and longitudinal components of the spectral functions, $\rho_T = \rho^{xyxy}, \rho^{xzxz}$ and $\rho_L = \rho^{zzzz}$.

6.4 Kinetic Theory in Curved Space

In this section we calculate the spectral function using kinetic theory in curved sapace. The basic object in kinetic theory is the distribution function $f(\mathbf{x}, \mathbf{p}, t)$ where $f = f_\uparrow = f_\downarrow$. The distribution function satisfies the Boltzmann equation. The kinetic equation in a curved background can be found by starting from the Boltzmann equation in general relativity [170, 171]

$$\frac{1}{p^0}\left(p^\mu \frac{\partial}{\partial x^\mu} - \Gamma^i_{\alpha\beta} p^\alpha p^\beta \frac{\partial}{\partial p^i}\right) f(t, \mathbf{x}, \mathbf{p}) = C[f]\,, \tag{6.16}$$

where i, j, k are three-dimensional indices and μ, α, β are four-dimensional indices. In the non-relativistic limit $p^0 \simeq m$, $\Gamma^i_{00} \simeq 0$, and $\Gamma^i_{0j} \simeq \frac{1}{2} g^{ik} \dot{g}_{kj}$ [138]. We get

$$\left(\frac{\partial}{\partial t} + \frac{p^i}{m}\frac{\partial}{\partial x^i} - \left(g^{il}\dot{g}_{lj}p^j + \Gamma^i_{jk}\frac{p^j p^k}{m}\right)\frac{\partial}{\partial p^i}\right) f(t, \mathbf{x}, \mathbf{p}) = C[f]\,, \tag{6.17}$$

We consider small deviations from equilibrium and write $f = f_0 + \delta f$ with $f_0(\mathbf{p}) = f_0(p^i p^j g_{ij}/(2mT))$. We also write $g_{ij} = \delta_{ij} + h_{ij}$ and linearize in h_{ij} and δf. We get

$$\left(\partial_t + \frac{p^i}{m}\partial_i\right)\delta f + \frac{f_0(1-f_0)}{2mT} p^i p^j \dot{g}_{ij} = C[\delta f]\,. \tag{6.18}$$

We will solve the linearized Boltzmann equation by making an ansatz for δf. We go to Fourier space and restrict ourselves to quadratic terms in p and write

$$\delta f(\omega, \mathbf{k}, \mathbf{p}) = \omega f_0(1-f_0)\frac{p^i p^j}{2mT}\frac{\xi_T h^T_{ij} + \xi_L h^L_{ij}}{\omega - \mathbf{v}_p \cdot \mathbf{k} + \mathrm{i}\epsilon}\,, \tag{6.19}$$

where $\xi_{T,L} = \xi_{T,L}(\omega, \mathbf{k})$ and

$$h_{ij}^T = h_{ij} - \frac{1}{3}\delta_{ij}h\,, \quad h_{ij}^L = \frac{1}{3}\delta_{ij}h\,. \tag{6.20}$$

Using this ansatz the LHS of the linearized Boltzmann equation becomes

$$LHS = \frac{\mathrm{i}\omega f_0(1-f_0)}{2mT}\left\{(\xi_T+1)p^ip^jh_{ij}^T + (\xi_L+1)p^ip^jh_{ij}^L\right\}\,. \tag{6.21}$$

The RHS of the Boltzmann equation involves the linearized collision integral

$$RHS = \int \mathrm{d}\Gamma_{234}\, r(1,2;3,4)\frac{\omega}{2mT}\left[g_{ij}(\mathbf{p}_1) + g^{ij}(\mathbf{p}_2) - g^{ij}(\mathbf{p}_3) - g^{ij}(\mathbf{p}_4)\right]\left(\xi_T h_{ij}^T + \xi_L h_{ij}^L\right)\,, \tag{6.22}$$

where we have defined $g^{ij}(\mathbf{q}) \equiv g^{ij}(\mathbf{q};\omega,\mathbf{k}) = q^iq^j/(\omega - \mathbf{v}_q\cdot\mathbf{k} + \mathrm{i}\epsilon)$ and we have labeled the momenta such that $\mathbf{p}_1 = \mathbf{p}$. We have also defined the phase space measure $\mathrm{d}\Gamma_{234} = \mathrm{d}\Gamma_1\mathrm{d}\Gamma_2\mathrm{d}\Gamma_2$ with $\mathrm{d}\Gamma_i = \mathrm{d}^3p_i/(2\pi)^3$ and the transition rate $r(1,2;3,4) = w(1,2;3,4)D(1,2;3,4)$. The factor $D(1,2;3,4)$ contains the distribution functions

$$D(1,2;3,4) = f_0(\mathbf{p}_1)f_0(\mathbf{p}_2)\left(1-f_0(\mathbf{p}_3)\right)\left(1-f_0(\mathbf{p}_4)\right)\,, \tag{6.23}$$

and $w(1,2;3,4)$ is the collision probability

$$w(1,2;3,4)\mathrm{d}\Gamma_{34} = v_{rel}\left(\frac{\mathrm{d}\sigma}{\mathrm{d}\Omega'}\right)\mathrm{d}\Omega'\,. \tag{6.24}$$

Here, $v_{rel} = |\mathbf{v}_1 - \mathbf{v}_2|$ is the relative velocity, $\mathrm{d}\Omega'$ is the solid angle along $2\mathbf{q}' = \mathbf{p}_3 - \mathbf{p}_4$ and $(\mathrm{d}\sigma)/(\mathrm{d}\Omega')$ is the differential cross section. We also define $2\mathbf{q} = \mathbf{p_1} - \mathbf{p_2}$ where $|\mathbf{q}| = |\mathbf{q}'|$. We will consider a dilute Fermi gas in which the scattering amplitude is

completely characterized by the s-wave scattering length a. The differential cross section is

$$\frac{\mathrm{d}\sigma}{\mathrm{d}\Omega'} = \frac{1}{4\pi}\frac{a^2}{1+a^2q^2}\,. \tag{6.25}$$

In order to solve for $\xi_{T,L}$ we will take moments of the linearized Boltzmann equation. The quadratic moments of the LHS are given by

$$L^{ab} = \int \mathrm{d}\Gamma_p \,\frac{\mathrm{i}\omega f_0(1-f_0)}{2mT} p^a p^b p^i p^j \sum_{T,L} h_{ij}^{T,L}(\xi_{T,L}+1)\,, \tag{6.26}$$

where $L^{ab} = L^{ab}(\omega,\mathbf{k})$. The moments of the RHS are given by

$$\begin{aligned} R^{ab} &= \frac{\omega}{2mT}\int \mathrm{d}\Gamma_{tot}\, r(1,2;3,4)\, p_1^a p_1^b \left[g_{ij}(\mathbf{p}_1) + g^{ij}(\mathbf{p}_2) - g^{ij}(\mathbf{p}_3) - g^{ij}(\mathbf{p}_4)\right] \sum_{T,L}\xi_{T,L}h_{ij}^{T,L} \\ &= \frac{\omega}{2mT}\int \mathrm{d}\Gamma_{tot}\, r(1,2;3,4)\, \left[p_1^a p_1^b + p_2^a p_2^b - p_3^a p_3^b - p_4^a p_4^b\right] g^{ij}(\mathbf{p}_1) \sum_{T,L}\xi_{T,L}h_{ij}^{T,L} \\ &= \frac{2\omega}{m^2T}\int \frac{\mathrm{d}^3p\mathrm{d}^3q}{(2\pi)^6}\,\mathrm{d}\Omega_{q'}\,\frac{a^2q}{1+a^2q^2}\,D_{2\leftrightarrow 2}\,\left(q^a q^b - q'^a q'^b\right) g^{ij}(\mathbf{p}_1)\sum_{T,L}\xi_{T,L}h_{ij}^{T,L}\,, \end{aligned} \tag{6.27}$$

with $D_{2\leftrightarrow 2} = D(1,2;3,4)$ and $R^{ab} = R^{ab}(\omega,\mathbf{k})$.

6.4.1 Transverse Channel

We can now determine $\xi_{T,L}$ by solving $L^{ab} = R^{ab}$. We begin by considering $h_{xy} = h_{yx} \neq 0$ with all other components of h_{ij} vanishing. In this case $h = 0$ and only ξ_T contributes.

We find

$$\begin{aligned} L^{xy} &= \int \mathrm{d}\Gamma_p \frac{\mathrm{i}\omega f_0(1-f_0)}{2mT}\left(\xi_T+1\right) p^x p^y p^i p^j h_{ij}^T \\ &= \frac{\mathrm{i}\omega\left(\xi_T+1\right)h_{xy}}{30\pi^2 mT}\int \mathrm{d}p\, p^6 f_0(1-f_0) \\ &\equiv \frac{\mathrm{i}\omega\left(\xi_T+1\right)h_{xy}}{15} I_{xy} \end{aligned} \tag{6.28}$$

and

$$\begin{aligned} R^{xy} &= \frac{2\omega\xi_T h_{xy}}{m^2 T}\int \frac{\mathrm{d}^3p\mathrm{d}^3q}{(2\pi)^6}\,\mathrm{d}\Omega_{q'}\,\frac{a^2 q}{1+a^2q^2}\,D_{2\leftrightarrow 2}\,\left(q^x q^y - q'^x q'^y\right) g^{ij}(\mathbf{p}_1) \\ &= \frac{2\omega\xi_T h_{xy}}{\pi^3 mT}\int \mathrm{d}p\,\mathrm{d}q\,\mathrm{d}\alpha\,\mathrm{d}\beta\,\frac{a^2 q}{1+a^2q^2}\,D_{2\leftrightarrow 2}\,\frac{p^2q^2q^xq^yq^xq^y}{2m\omega - pk\alpha - 2qk\beta + \mathrm{i}\epsilon} \equiv \frac{\omega\xi_T h_{xy}}{15} C_{xy} \end{aligned} \tag{6.29}$$

Setting $L^{xy} = R^{xy}$ gives

$$\xi_T^{(xy)}(\omega,\mathbf{k}) = -\frac{I_{xy}}{I_{xy} + \mathrm{i}C_{xy}(\omega,\mathbf{k})}\,. \tag{6.30}$$

The superscript (xy) indicates that we have obtained ξ_T by projecting on the Π^{xy} channel. In the limit $\mathbf{k}\to 0$ our ansatz Eq. (6.19) is complete, and there is no dependence on the channel. At finite $\mathbf{k}$, however, additional tensor structures in Eq. (6.19) are possible and there is some dependence of $\xi_{L,T}$ on the channel.

In kinetic theory the stress tensor is given by

$$\delta\Pi^{ij} = 2\int \frac{\mathrm{d}^3p}{(2\pi)^3}\frac{p^i p^j}{m}\delta f\,, \tag{6.31}$$

where the factor 2 is the spin degeneracy. Using the ansatz Eq. (6.19) we get

$$\delta\Pi^{xy} = \frac{\omega\xi_T^{(xy)}h_{xy}}{mT}\int\frac{\mathrm{d}^3p}{(2\pi)^3}f_0(1-f_0)\frac{p^xp^yp^xp^y}{m\omega - p^zk + \mathrm{i}\epsilon} \equiv \xi_T^{(xy)}h_{xy}J_{xy}\,. \tag{6.32}$$

We can now extract the retarded correlation function and the spectral function using Eq. (6.3) and Eq. (6.2). We find

$$\rho^{xyxy}(\omega,\mathbf{k}) = 2\mathrm{Im}\big(\xi_T^{(xy)}(\omega,\mathbf{k})\big)\mathrm{Re}\big(J_{xy}(\omega,\mathbf{k})\big) + 2\mathrm{Re}\big(\xi_T^{(xy)}(\omega,\mathbf{k})\big)\mathrm{Im}\big(J_{xy}(\omega,\mathbf{k})\big)\,. \tag{6.33}$$

In general the functions C_{xy} and J_{xy} have to computed numerically. The limit $\mathbf{k}\to 0$ can be studied analytically. We may consider two cases. In the free case the collision integral C_{xy} vanishes and $\xi_T = -1$. The spectral function is then given by $\rho^{xyxy}(\omega,\mathbf{k}) = -2\mathrm{Im}\,J_{xy}(\omega,\mathbf{k})$. The function $J_{xy}(\omega,\mathbf{k})$ can be computed analytically for all values of ω and $\mathbf{k}$. The collisionless spectral function is

$$\frac{\rho^{xyxy}(\omega,\mathbf{k})}{2\omega} = \frac{1}{16\pi}\frac{(2mT)^2}{k}\,Li_2\left(\zeta_F^{-1}\exp\left(-\frac{m\omega^2}{2Tk^2}\right)\right)\,, \tag{6.34}$$

where $Li_2(x)$ is a polylogarithm and $\zeta_F = \exp(-\mu/T)$ is the fugacity. In the limit $\mathbf{k}\to 0$ we find

$$\lim_{\mathbf{k}\to 0}\frac{\rho^{xyxy}(\omega,\mathbf{k})}{2\omega} = \frac{\varepsilon}{3}\pi\delta(\omega)\,, \tag{6.35}$$

where ε is the energy density

$$\varepsilon = 2\int\frac{\mathrm{d}^3p}{(2\pi)^3}f_0\frac{p^2}{2m}\,. \tag{6.36}$$

At finite momentum the delta function is spread out over the regime $\omega \lesssim |\mathbf{k}|(T/m)^{1/2}$. In the collisional case we find that in the limit $\mathbf{k}\to 0$ the collision integral is real and scales

as $C_{xy}(\omega, \mathbf{k} \to 0) \sim 1/\omega$. This means that the spectral function is dominated by the $\mathrm{Im}(\xi_T^{(xy)}(\omega, \mathbf{k}))\mathrm{Re}(J_{xy}(\omega, \mathbf{k}))$ term. We also find that in this limit $\mathrm{Re}(J_{xy}) \simeq I_{xy}/(15m)$. This implies that

$$\eta(\omega) \equiv \lim_{\mathbf{k}\to 0} \frac{\rho^{xyxy}(\omega, \mathbf{k})}{2\omega} = \frac{I_{xy}^2}{15m\omega} \frac{\mathrm{Re}(C_{xy}(\omega, \mathbf{0}))}{I_{xy}^2 + \mathrm{Re}(C_{xy}(\omega, \mathbf{0}))^2} \,. \tag{6.37}$$

The zero frequency limit is

$$\eta \equiv \lim_{\omega\to 0} \eta(\omega) = \frac{I_{xy}^2}{15m\omega \mathrm{Re}(C_{xy}(\omega, \mathbf{0}))} = \frac{15(mT)^{3/2}}{32\sqrt{\pi}} \begin{cases} 1 & a \to \infty \\ 1/(3mTa^2) & a \to 0 \end{cases} , \tag{6.38}$$

where in the last step we have evaluated the integrals in the high temperature limit. This result agrees with the hydrodynamic limit given in Eq. (6.10) and the known formula for the shear viscosity of a dilute Fermi gas in kinetic theory [128]. We can now write the frequency dependence as

$$\eta(\omega) = \frac{\eta}{1 + \omega^2\tau^2} \tag{6.39}$$

where $\tau = I_{xy}/(\omega \mathrm{Re}(C_{xy})) = 15m\eta/I_{xy}$ is a relaxation time. In the high temperature limit τ agrees with the result obtained in [158]. We can also evaluate the sum rule

$$\frac{1}{\pi}\int_0^\infty \mathrm{d}\omega\, \eta(\omega) = \frac{\eta}{2\tau} = \frac{I_{xy}}{30m} = \frac{\varepsilon}{3} \,. \tag{6.40}$$

We note that the sum rule agrees with the integral of the free spectral function given in Eq. (6.35). The sum rule also agrees with the general sum rule obtained in [162] if we take account the fact that kinetic theory does not reproduce the short distance contribution $\eta(\omega) \sim C/\sqrt{m\omega}$, where C is Tan's contact [172].

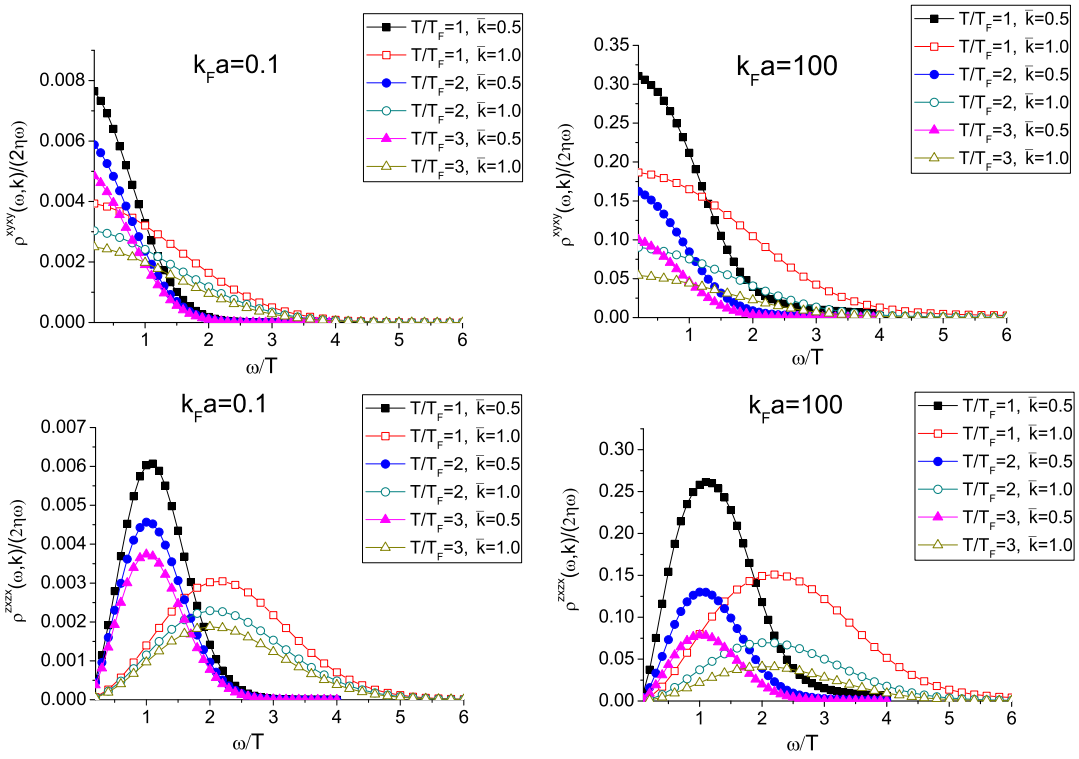

Figure 6.1: Stress tensor spectral functions in the xy and xz channels. We plot the spectral function $\rho(\omega, k)$ normalized to the value in the Kubo limit, $\rho(\omega \to 0, 0) = 2\eta\omega$, as a function of ω/T for different values of $\bar{k} = k/(2mT)^{1/2}$ and T/T_F. The panels on the left show the result for $k_F a = 0.1$, which corresponds to weak coupling, and the panels on the right show the spectral function close to unitarity, for $k_F a = 100$.

The spectral function in the xz channel can be computed in the same fashion. The spectral function $\rho^{xzxz}(\omega, \mathbf{k})$ is given by Eq. (6.33) with the obvious replacement $(xy) \to (xz)$. In the Kubo limit we find

$$\lim_{\omega,\mathbf{k}\to 0} \frac{\rho^{xzxz}(\omega, \mathbf{k})}{2\omega} = \eta \tag{6.41}$$

as expected from hydrodynamics, see Eq. (6.11). Numerical results for the spectral function in the xy and xz channel are shown in Fig. 6.1. We consider two different

scattering length, one corresponding to weak coupling, $k_F a = 0.1$, and one close to unitarity, $k_F a = 100$. We plot the spectral function as a function of ω/T for several values of $\bar{k} = k/\sqrt{2mT}$ and T/T_F.

We first discuss $\rho^{xyxy}(\omega, \mathbf{k})$. At zero momentum the spectral function normalized to $2\eta\omega$ is a Lorentzian with a width proportional to $1/\eta$. This implies that the peak in the spectral function is narrow in weak coupling, but very broad in strong coupling. As the momentum k grows the width of the peak increases and it becomes less sensitive on the strength of the coupling. In this regime the spectral function is close to the free spectral function. We also find numerically that the spectral function satisfies the sum rule Eq. (6.40) even at non-zero momentum k. In the xz channel the normalized spectral function $\rho^{xzxz}(\omega, \mathbf{k})/(2\eta\omega)$ vanishes in the limit $\omega \to 0$ for any non-zero value of k. For $k = 0$ the normalized spectral function approaches unity as $\omega \to 0$. This is in agreement with the hydrodynamic prediction Eq. (6.11). We find that the spectral function has a peak which, like the peak in the xy channel, corresponds to a diffusive mode. The width of the mode is controlled by k except in the limit of small momenta where the width is controlled by the shear viscosity.

6.4.2 Longitudinal Case

In this section we study the longitudinal spectral function $\rho^{zzzz}(\omega, \mathbf{k})$. The calculation is more involved because both ξ_T and ξ_L contribute. We consider a perturbation $h_{zz} \neq 0$ with all other $h_{ij} = 0$. In this case $h^L_{ij} = \frac{h_{zz}}{3}\delta_{ij}$ and $h^T_{zz} = h_{ij} - \frac{h_{zz}}{3}\delta_{ij} = -\frac{h_{zz}}{3}\,\mathrm{diag}(1, 1, -2)$. The LHS of the Boltzmann equations is $L^{zz} = L^{zz}_T + L^{zz}_L$ with

$$L^{zz}_{T,L} = \int \mathrm{d}\Gamma\, \frac{\mathrm{i}\omega f_0(1-f_0)}{2mT}(\xi_{T,L}+1)p^z p^z p^i p^j h^{T,L}_{ij} \equiv \frac{\mathrm{i}\omega(\xi_{T,L}+1)h_{zz}}{3} I^{zz}_{T,L}\,. \tag{6.42}$$

The collision integrals can be written as

$$
\begin{aligned}
R_T^{zz} &= \frac{2\omega\xi_T}{m^2T}\int\frac{\mathrm{d}^3p\mathrm{d}^3q}{(2\pi)^6}\,\mathrm{d}\Omega_{q'}\,D_{2\leftrightarrow 2}\,\frac{a^2q}{1+a^2q^2}\,(q^zq^z-q'^zq'^z)\,g^{ij}(\mathbf{p_1})h_{ij}^T \\
&= -\frac{\omega\xi_T h_{zz}}{12\pi^3mT}\int\mathrm{d}p\,\mathrm{d}q\,\mathrm{d}\alpha\,\mathrm{d}\beta\,D_{2\leftrightarrow 2}\,\frac{a^2q}{1+a^2q^2}\,p^2q^4\,\frac{(\beta^2-\frac{1}{3})(p^2(1-3\alpha^2)-8pq\alpha\beta+4q^2(1-3\beta^2))}{2m\omega-pk\alpha-2qk\beta+\mathrm{i}\epsilon} \\
&\equiv \frac{\omega\xi_T h_{zz}}{3}C_T^{zz}\,, \qquad (6.43) \\
R_L^{zz} &= \frac{2\omega\xi_T}{m^2T}\int\frac{\mathrm{d}^3p\mathrm{d}^3q}{(2\pi)^6}\,\mathrm{d}\Omega_{q'}\,D_{2\leftrightarrow 2}\,\frac{a^2q}{1+a^2q^2}\,(q^zq^z-q'^zq'^z)\,g^{ij}(\mathbf{p_1})h_{ij}^L \\
&= -\frac{\omega\xi_L h_{zz}}{3\pi^3mT}\int\mathrm{d}p\,\mathrm{d}q\,\mathrm{d}\alpha\,\mathrm{d}\beta\,D_{2\leftrightarrow 2}\,\frac{a^2q}{1+a^2q^2}\,p^2q^4\,\frac{(\beta^2-\frac{1}{3})(p^2/4+pq\alpha\beta+q^2)}{2m\omega-pk\alpha-2qk\beta+\mathrm{i}\epsilon} \\
&\equiv \frac{\omega\xi_L h_{zz}}{3}C_L^{zz}\,. \qquad (6.44)
\end{aligned}
$$

We can now solve for $\xi_{T,L}$. We find

$$
\xi_{T,L}^{(zz)}(\omega,\mathbf{k}) = -\frac{I_{T,L}^{zz}}{I_{T,L}^{zz}+\mathrm{i}C_{T,L}^{zz}(\omega,\mathbf{k})}\,. \qquad (6.45)
$$

The zz component of the stress tensor is given by

$$
\begin{aligned}
\delta\Pi^{zz} &= 2\omega\int\frac{\mathrm{d}^3p}{(2\pi)^3}\,f_0(1-f_0)\frac{p^zp^z}{m}\frac{p^ip^j}{2mT}\frac{\xi_T^{(zz)}h_{ij}^T+\xi_L^{(zz)}h_{ij}^L}{\omega-\mathbf{v}_p\cdot\mathbf{k}+\mathrm{i}\epsilon} \\
&= \frac{\omega h_{zz}}{12\pi^2mT}\int\mathrm{d}p\,\mathrm{d}\alpha\,\frac{f_0(1-f_0)p^6\alpha^2}{m\omega-pk\alpha+\mathrm{i}\epsilon}\left[\xi_T^{(zz)}(3\alpha^2-1)+\xi_L^{(zz)}\right] \\
&\equiv \omega h_{zz}\left(\xi_T^{(zz)}(\omega,\mathbf{k})J_T^{zz}(\omega,\mathbf{k})+\xi_L^{(zz)}(\omega,\mathbf{k})J_L^{zz}(\omega,\mathbf{k})\right)\,. \qquad (6.46)
\end{aligned}
$$

We can now extract the retarded correlators and the spectral function using Eq. (6.3) and Eq. (6.2). We get

$$
\frac{\rho^{zzzz}(\omega,\mathbf{k})}{2\omega} = \mathrm{Im}\left(\xi_T^{(zz)}(\omega,\mathbf{k})J_T^{zz}(\omega,\mathbf{k})+\xi_L^{(zz)}(\omega,\mathbf{k})J_L^{zz}(\omega,\mathbf{k})\right)\,. \qquad (6.47)
$$

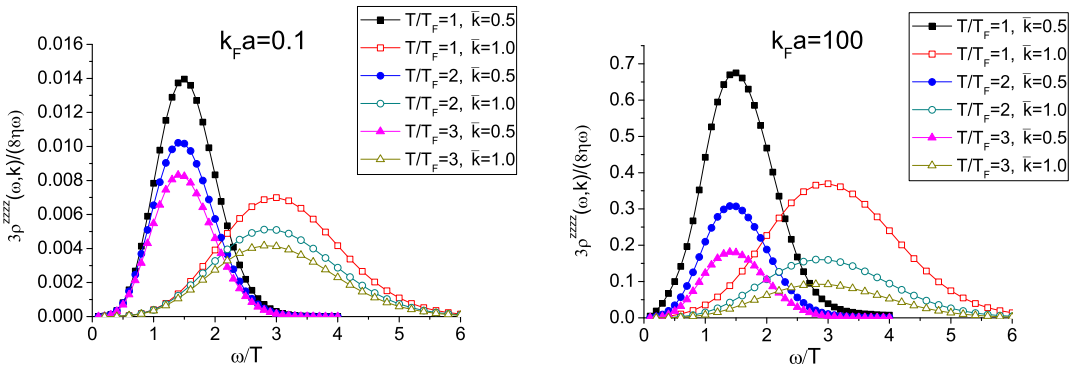

Figure 6.2: Viscosity spectral function in the zz channel. We plot the spectral function $\rho(\omega, k)$ normalized to the value in the Kubo limit, $\rho(\omega \to 0, 0) = \frac{8}{3}\eta\omega$, as a function of ω/T for different values of $\bar{k} = k/(2mT)^{1/2}$ and T/T_F.

The result again simplifies in the limit $\mathbf{k} \to 0$. In the collisional case we find that the function J is dominated by its real part. Also, one can show that the $\mathbf{k} \to 0$ limit of $\mathrm{Re}(C_L^{zz}) = 0$ and therefore $\mathrm{Im}(\xi_L^{(zz)}) = 0$. We find

$$\lim_{\mathbf{k}\to 0} \frac{\rho^{zzzz}(\omega, \mathbf{k})}{2\omega} = \lim_{\mathbf{k}\to 0} \mathrm{Im}\big(\xi_T^{(zz)}(\omega, \mathbf{k})\big)\mathrm{Re}\big(J_T^{zz}(\omega, \mathbf{k})\big) = \frac{I_T^{zz}\mathrm{Re}(J_T^{zz}(\omega, \mathbf{0}))}{(I_T^{zz})^2 + \mathrm{Re}(C_T^{zz}(\omega, \mathbf{0}))^2} \tag{6.48}$$

The transverse and longitudinal integrals that we have done are obviously related to each other. In the limit $\mathbf{k} \to 0$ we have

$$I_T^{zz} = \frac{2}{15} I_{xy} \qquad J_T^{zz}(\omega, \mathbf{0}) = \frac{4}{3} J_{xy}(\omega, \mathbf{0}) = \frac{4}{45m\omega} I_{xy} \qquad C_T^{zz} = \frac{2}{15} C_{xy}\,. \tag{6.49}$$

This shows that as $\mathbf{k} \to 0$ the ansatz Eq. (6.19) is complete and $\xi_T^{(zz)}(\omega) = \xi_T^{(xy)}(\omega)$. We can also show that

$$\lim_{\omega,\mathbf{k}\to 0} \frac{\rho^{zzzz}(\omega, \mathbf{k})}{2\omega} = \frac{4}{3}\eta\,. \tag{6.50}$$

Comparing this result with the hydrodynamic prediction (6.12) we find that the bulk viscosity ζ vanishes. This follows from scale invariance at unitarity [47]. The fact that we also find $\zeta = 0$ away from unitarity is related to the fact that we only take into account elastic $2 \leftrightarrow 2$ collisions. Numerical results for $\rho^{zzzz}(\omega, \mathbf{k})$ normalized to the hydrodynamic limit $\frac{8}{3}\omega\eta$ are shown in Fig. 6.2. We observe that the spectral function shows a sound peak at $\omega = c_s k$. At the largest temperature considered, $T/T_F = 3$, the speed of sound differs from the asymptotic high temperature value $c_s^2 = (5T)/(3m)$ by about 10%. The width of the sound peak is close to that of the free spectral function. This is at variance with hydrodynamics which predicts that the sound peak is narrow in strong coupling, and in the limit of small momentum. At zero momentum hydrodynamics predicts that $\rho(\omega)/\omega$ is constant. Higher order effects will turn this part of the spectrum into a broad peak with a width inversely proportional to the relaxation time. This implies that at small momentum we expect a narrow peak with a width proportional to $(k/c_s)(\eta/\rho)$ superimposed on a broad peak with a width proportional $\varepsilon/(T\eta)$. Our ansatz correctly reproduces the $k \to 0$ limit as well as the existence of a sound peak, but it appears to be too simple to reproduce the two-peak structure at small k.

6.5 Summary and Discussion

We have computed the viscosity spectral function using kinetic theory in a non-trivial background metric. We find that a simple quadratic ansatz for the non-equilibrium distribution function δf satisfies the main constraints on the spectral function, in particular the existence of a diffusive peak and a sound peak (although it misses the interplay between these two features in the longitudinal channel), the correct Kubo limit, and the viscosity sum rule. Kinetic theory misses the non-analytic high frequency tail of the

spectral function $\eta(\omega) \sim C/\sqrt{m\omega}$. We find that the width of the diffusive peak at zero momentum is inversely proportional to the viscosity. This implies that the relaxation time for the shear stress is $\tau \simeq 3\eta/(2\varepsilon)$, in agreement with [158]. We also find that at large momentum the spectral function is close to the free spectral function, and the width of the transport peak is of order $k(T/m)^{1/2}$.

There are at least two important questions that we have not addressed in this chapter. The first is a systematic matching to second order hydrodynamics. For this purpose it is important to understand the structure of second order hydrodynamics in the conformal limit along the lines of the analysis in the relativistic case performed in [173]. The second is a detailed study of the imaginary time correlation functions, with an emphasis on finding the optimal strategy for extracting transport coefficients from Quantum Monte Carlo calculations. The main difficulty is that the imaginary time correlation function is mainly sensitive to the spectral weight of the transport peak, and that the sum rule implies that the weight is independent of the shear viscosity. This problem can be addressed by utilizing the information contained in the momentum dependence of the correlation function, and by considering not only the shear channel but also the sound channel [164, 167].

Chapter 7

Outlook

Strictly speaking, the kinetic approach is applicable only to rarefied gas and not reliable in practice for calculating the transport coefficients for finite density systems. To address a dense and strongly coupled system, it is conceivable that, one reasonable approach is taking into account the three or four bodies interactions. Another issue is the problem of extending hydrodynamic theories to include dissipative terms beyond first order in gradients of velocity and temperature. Both methods have been received a great accomplishment in recent works [55, 138, 174, 175]. In this chapter, we will briefly introduce some newly developments in these two approaches.

7.1 Three Body Interaction

In dilute gas, as we have showed, both the shear viscosity and thermal conductivity are independent of density. This is because that the Boltzmann equation is the lowest order approximation of the BBGKY hierarchy equation and does not contain the information of multiple collisions. To know the density dependence of the transport coefficients,

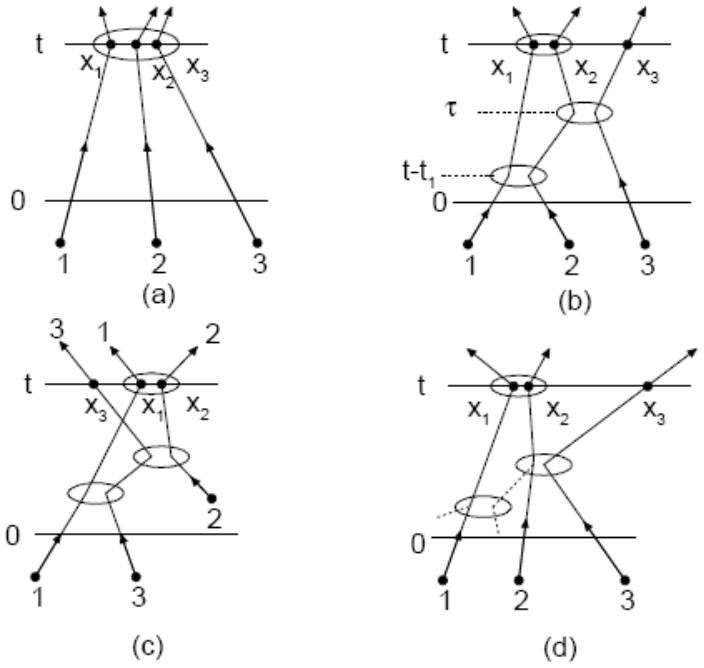

Figure 7.1: Genuine triple collisions (a) and ring collisions: recollision (b), cyclic (c) and hypothetical (d) collision [10].

according to Eq. 3.6, we must go to the second equation, which involved in three body collisions. We write the second sequence of BBKGY equation again,

$$\left(\frac{\partial}{\partial t}+\mathbf{v}_1\cdot\nabla_{\mathbf{r}_1}+\mathbf{F}_1\cdot\nabla_{p_1}+\mathbf{v}_2\cdot\nabla_{\mathbf{r}_2}+\mathbf{F}_2\cdot\nabla_{p_2}+\frac{1}{2}\mathbf{K}_{12}\cdot(\nabla_{p_1}-\nabla_{p_2})\right)f_2(\mathbf{p}_2,\mathbf{r}_2,t)$$
$$=-\int \mathrm{d}\Gamma_3\left(\mathbf{K}_{13}\cdot\nabla_{p_1}+\mathbf{K}_{23}\cdot\nabla_{p_2}\right)f_3(\mathbf{p}_1,\mathbf{r}_1,\mathbf{p}_2,\mathbf{r}_2,\mathbf{p}_3,\mathbf{r}_3,t) \tag{7.1}$$

The basic assumption to obtain a higher accurate but truncated kinetic equation is,

$$f_3(\mathbf{p}_1,\mathbf{r}_1,\mathbf{p}_2,\mathbf{r}_2,\mathbf{p}_3,\mathbf{r}_3,t)=f_1^0f_2^0f_3^0$$
$$f_2(\mathbf{p}_2,\mathbf{r}_2,t)=J_{12}f_1^0f_2^0+\int \mathrm{d}\Gamma_3\left(S_{123}-J_{12}J_{23}-J_{12}J_{13}+J_{12}\right)f_1^0f_2^0f_3^0 \tag{7.2}$$

where J_{12} accounts for pair collision, S_{123} is the genius triplet correlation and all other higher terms have been neglected. It is an important new result, that generalizes the Boltzmann equation to include triple collisions [50, 65]. Note that the function J_{12} and J_{23} are noticeable different from zero only within the range of interaction, r_0. It leads to a straightness estimation that the order of correction is $\sim r_0^3$. Substituting the expression of f_2 and f_3, we have the transport equation in the form

$$\frac{\partial f}{\partial t} + \mathbf{v} \cdot \frac{\partial f}{\partial \mathbf{r}} = C^{(2)}[f] + C^{(3)}[f] \tag{7.3}$$

where we ignore the script of 1 because of the closure. And

$$\begin{aligned} C^{(2)} &= \int \mathrm{d}\Gamma_2 J_{12} f_1^0 f_2^0 \\ C^{(3)} &= \int \mathrm{d}\Gamma_2 \mathrm{d}\Gamma_3 \left(S_{123} - J_{12} J_{23} - J_{12} J_{13} + J_{12} \right) f_1^0 f_2^0 f_3^0 \end{aligned} \tag{7.4}$$

For example, in a hard sphere model, assuming the short repulsive potential range is d. It is instructive to analyze the different types of contributions from S_{123}, illustrated in Figure 7.1 [10]. They contain genuine triple collisions, where three particles are simultaneously in each others interaction sphere. Once they have collided, the particles will separate and never re-collide again in the relaxation time scale. In hard sphere systems, where interactions are instantaneous, this term is quite small. Moreover, S_{123} contains sequences of two uncorrelated successive binary collisions (12) (13) and (12) (23). Such collisions have already been accounted for in the Boltzmann collision term J_{12}. So, they are subtracted out from the possible sequences of binary collisions among three particles in Eq. 7.4. Finally S_{123} contains sequences of three correlated successive binary collisions, such as the recollision (12)(13)(12) and the cyclic collision (12)(23)(13), generally

referred to as ring collisions. In the model of hard spheres, the density expansion of the shear viscosity and thermal conductivity is given by [176]

$$\kappa = \kappa_0(1 + 1.2nd^3), \qquad \eta = \eta_0(1 + 0.35nd^3) \tag{7.5}$$

where κ_0 and η_0 is the low density Boltzmann result and n is the particle density.

7.2 Higher Order of Dissipative Fluid Dynamics

To date, the most commonly used second-order dissipative fluid dynamics are introduced by Israel and Stewart [52, 53, 54], based on the Grad's momentum expansion method. This theory does not have the unphysical problems that are encountered in the first order theory of relativistic fluids. In recent years, theoreticians have begun to apply this theory for the description of collective flow in heavy-ion collisions [55, 177, 117, 178]. On the other hand, the Müller-Israel-Stewart theory could miss some terms of second order in gradients. A variation of the second order approaches have been built up to classify all possible terms completely.

7.2.1 Results from Baier-Romatschke-Son-Starinets-Stephanov

An elegant way of obtaining $T^{\mu\nu}$ builds upon the conformally invariant theories [173], the action $S[\phi, g_{\mu\nu}]$, viewed as a functional of the external metric $g_{\mu\nu}$. $g_{\mu\nu}$ is invariant under local dilatations, or Weyl transformations:

$$g_{\mu\nu} \to \mathrm{e}^{-2\omega} g_{\mu\nu} \tag{7.6}$$

where ω is the function of space-time coordinates. Rescaling in four dimensions, if the energy momentum tensor $T^{\mu\nu}$ under Weyl transformations

$$T^{\mu\nu} \to \mathrm{e}^{(d+2)\omega} T^{\mu\nu} \tag{7.7}$$

and $T^{\mu}_{\mu} = 0$, therefore, the hydrodynamic equation $\nabla_{\mu} T^{\mu\nu} = 0$ is Weyl invariant. If one assumes that the conformal invariance is preserved throughout the evolution of the system, conformal invariance imposes a constrain on the dissipative terms, formed by less than d derivatives, which here $d = 4$.

It is easy to check that the 1st order N-S equation satisfy this constraint automatically. Firstly, the traceless condition forces $\zeta = 0$, the only viscous term is the shear viscosity and velocity tensor transform as $\nabla^{\mu} u^{\nu} \to \mathrm{e}^{3\omega} \nabla^{\mu} u^{\nu}$. Secondly, $\eta = const \cdot T^{d-1}$ in a conformal fluid. Therefore, the shear stress tensor transforms as

$$\pi^{\mu\nu} \to \mathrm{e}^{6\omega} \pi^{\mu\nu} \tag{7.8}$$

To find all possible 2nd order contributions to $T^{\mu\nu}$, ones directly add 2nd order derivatives which satisfying the conformal constraint Eq. 7.7 and employ the first order equation

$$\mathcal{D} \ln T = -\frac{1}{d-1} \left(\nabla_{\perp} \cdot u^{\mu} \right), \qquad \mathcal{D} u^{\mu} = -\nabla^{\mu}_{\perp} \ln T \tag{7.9}$$

to convert temporal derivatives ($\mathcal{D} = u^{\mu} \nabla_{\mu}$) into spatial ($\nabla^{\mu}_{\perp} = \Delta^{\mu\alpha} \nabla_{\alpha}$). Additionally, tensor $\Pi_2^{\mu\nu}$ is symmetric, transverse, $u_{\mu} \Pi_2^{\mu\nu} = 0$ and traceless, $g_{\mu\nu} \Pi_2^{\mu\nu} = 0$ for a comformal fluid. The authors point out: the last two constraints allow for 8 possible 2nd order

corrections:

$$D^{\langle\mu}\ln\varepsilon D^{\nu\rangle}\ln\varepsilon,\quad D^{\langle\mu}D^{\nu\rangle}\ln\varepsilon\quad D^{\langle\mu}u^{\nu\rangle}(\nabla_\alpha u^\alpha),\quad P^{\mu\nu}_{\alpha\beta}\nabla^{\langle\alpha}u^{\gamma\rangle}g_{\gamma\delta}\nabla^{\langle\delta}u^{\beta\rangle},$$
$$P^{\mu\nu}_{\alpha\beta}\nabla^{\langle\alpha}u^{\gamma\rangle}g_{\gamma\delta}\Omega^{\beta\delta},\quad P^{\mu\nu}_{\alpha\beta}\Omega^{\alpha\gamma}g_{\gamma\delta}\Omega^{\beta\delta},\quad u_\gamma R^{\gamma\langle\mu\nu\rangle\delta}u_\delta,\quad R^{\langle\mu\nu\rangle} \tag{7.10}$$

where $R^{\alpha\mu\nu\beta}$ is the Riemann tensor, $R^{\mu\nu}$ is the Ricci tensor and $\Omega^{\mu\nu}$ is the vortex tensor. However, only 5 combinations of the above terms transform homogeneously under Weyl transformation. This determines the form of the 2nd order dissipative terms, creating 5 independent new constant. Thus, the final expression , up to second order in derivatives, is

$$\begin{aligned}\Pi^{\mu\nu} &= -\eta\sigma^{\mu\nu}-\tau_\Pi\left[{}^{\langle}D\Pi^{\mu\nu\rangle}+\frac{d}{d-1}\Pi^{\mu\nu}(\nabla\cdot u)\right]\\ &\quad+\kappa\left[R^{\langle\mu\nu\rangle}-(d-2)u_\alpha R^{\alpha\langle\mu\nu\rangle\beta}u_\beta\right]\\ &\quad+\frac{\lambda_1}{\eta^2}\Pi^{\langle\mu}_\lambda\Pi^{\nu\rangle\lambda}-\frac{\lambda_2}{\eta^2}\Pi^{\langle\mu}_\lambda\Omega^{\nu\rangle\lambda}+\lambda_3\Omega^{\langle\mu}_\lambda\Omega^{\nu\rangle}\lambda\end{aligned} \tag{7.11}$$

Note that the κ term is related to curved spaces and vanishes in flat space.

The conformal symmetry constraint approach provides the general form of the 2nd order viscous equations, however, it does not give the 2nd order coefficients τ_π, κ, λ_1, λ_2 and λ_3. Ones must determine them through explicit calculation. Such calculations were performed for weakly coupled QCD by York and Moore. We summarize their results in the next section.

7.2.2 Results from York-Moore

In the framework of kinetic theory, M. York and G. Moore [174] compute these second-order hydrodynamic coefficients in QCD to leading order in the weak coupling expansion.

They set up from the kinetic theory

$$2P^{\mu}\partial_{\mu}f^{a}(\mathbf{x},\mathbf{p}) = -\mathcal{C}[f] \tag{7.12}$$

where $p^0 = E_p = \sqrt{\mathbf{p}^2 + m^2}$ in terms of the on-shell condition. Using λ to keep track of the order in derivatives, the Boltzmann equation can be written as:

$$f(\mathbf{x},\mathbf{p}) = f_0 + \lambda f_1 + \lambda^2 f_2 + ... \tag{7.13}$$

f_0 is the equilibrium distribution function which fixed by the condition $\mathcal{C}[f_0] = 0$. The L.H.S of the Boltzmann equation has an explicit derivative so it starts at $\mathcal{O}(\lambda)$. In contrast to the collision operator was expanded to the first order before, here one has,

$$2P^{\mu}\partial_{\mu}f_1(\mathbf{x},\mathbf{p}) = -\mathcal{C}_{11}[f_1] - \mathcal{C}_{1;\mathcal{M}_1}[f_1] - \mathcal{C}_1[f_2] \tag{7.14}$$

where $\mathcal{C}_{11}$ is the collision operator expanded to quadratic order in terms of f_1, $\mathcal{C}_1[f_2]$ is the collision operator expanded to first order in f_2, and $\mathcal{C}_{1;\mathcal{M}_1}[f_1]$ is the collision operator expanded to first order in f_1 with the scattering matrix element also expanded to first order in f_1, all other higher terms have been neglects, including term $\mathcal{C}^2_{1;\mathcal{M}_1}[f_1]$, which will be higher order in the gauge coupling.

It is enough to consider the components in f_2 which contribute to the viscous stress-energy tensor, i.e. the departure source of spherical harmonic number $l = 2$. In the expression Eq. 7.14, it is obviously to show f_1 determining the terms of f_2. The expression of f_1 has been derived in literature. For weakly coupling QCD, one can refer the work, shown as,

$$f_1(\mathbf{p}) = p^{\mu}p^{\nu}\frac{\sigma_{\mu\nu}}{2}\beta^3\chi(-\beta u\cdot P) \tag{7.15}$$

where $\beta \equiv 1/T$, $\sigma_{\mu\nu}$ is the shear viscosity tensor and χ is a dimensionless function which remains to be determined. The definition of the temperature and velocity have been fixed to the first order λ under the relationship

$$\begin{aligned} u^\mu \partial_\mu \beta &= \frac{\beta}{3} \Delta^{\mu\nu} \partial_\mu u_\nu \\ \Delta^{\nu\alpha} u^\mu \partial_\mu u_\alpha &= \frac{1}{\beta} \Delta^{\nu\alpha} \partial_\alpha \beta \end{aligned} \tag{7.16}$$

After carefully evaluating, all the related second order terms are listed below:

$2p^\mu \partial_\mu f_1$ term

$$\begin{aligned} \Pi_{ij,2 \quad order} \supset & \frac{\beta^4}{30\pi^2} \left(\partial_t \sigma_{ij} + \frac{1}{3} \sigma_{ij} \partial_k u^k - \sigma_{ik} \sigma_j^k - 2\sigma_{ik} \Omega_j^k \right) \int_{\mathbf{p}} p^5 \overline{\chi}(p) \widetilde{\chi}(p) \\ & - \frac{4\beta^5}{105} \left(\sigma_{ik} \sigma_j^k - \frac{\delta_{ij} \sigma_{kl} \sigma^{kl}}{3} \right) \int_{\mathbf{p}} p^6 \overline{\chi}(p) \widetilde{\chi}(p) \end{aligned} \tag{7.17}$$

where the first term leads a negative coefficient to λ_1. However, the second term contributes to λ_1 positively and the magnitude dominates all contributions to λ_1 in weakly coupling QCD. Besides, the first term is the sole contributor to the term τ_π and λ_2 with the fixing relation $\lambda_2 = -2\eta\tau_\pi$.

$\mathcal{C}_{11}[f_1]$ term

$$\Pi_{ij,2\ \ order} \supset \frac{1}{35}\left(\sigma_{ik}\sigma^k_j - \frac{\delta_{ij}\sigma_{kl}\sigma^{kl}}{3}\right)\left(3x_{pk}x_{pp'}x_{pk'} - x^2_{pk} - x^2_{pp'} - x^2_{kp'} + \frac{2}{3}\right) \times \int \mathrm{d}\Gamma_{pkp'k'}|\mathcal{M}|^2\left\{\overline{\chi}(p)\overline{\chi}(p)\overline{\chi}(k)f_0(p)f_0(k)(\mathrm{e}^{(p+k)/T}) + 5\mathrm{perm.terms}\right\} \tag{7.18}$$

where x_{pk} is angle between the momentum $\mathbf{p}$ and $\mathbf{k}$. Obviously, this term can be classified as a source of λ_1 evaluated precisely together with results of first order. For 3 flavor QCD, the $\mathcal{C}_{11}$ contribution to λ_1 varies between -0.18 at weak to -0.45 at stronger coupling. This contribution could be positive in the toy model of $\lambda\phi^4$ theory, $\sim +0.0372$.

$\mathcal{C}_{1;}\mathcal{M}_1$ contribution

Expand the matrix element as well:

$$\mathcal{M}[f] = \mathcal{M}[f_0] + \lambda\int_{\mathbf{r}} f_1(\mathbf{r})\frac{\mathrm{d}\mathcal{M}[f]}{\mathrm{d}f(\mathbf{r})} + \mathcal{O}(\lambda^2) \tag{7.19}$$

Therefore the $\mathcal{O}(\lambda)$ correction to $\mathcal{M}$ first gives rise to a nonzero effect at second order in λ.

$$\Pi_{ij,2\ \ order} \supset \frac{A_{ab}\sigma_{rs}}{2^9\pi^5}\int \mathrm{d}\Gamma_{pkp'k'}\overline{\chi}_{ij}(p)(\mathcal{M}_0\mathcal{M}_1 + \mathcal{M}_0\mathcal{M}_1) \times [\overline{\chi}_{rs}(p) + \overline{\chi}_{rs}(k) - \overline{\chi}_{rs}(p') - \overline{\chi}_{rs}(k')] \tag{7.20}$$

where $\mathcal{M}_1$ is a function in terms of σ_{ij}, A_{ab} is $16d_f^2n_f^2C_f^2/d_A$ for fermion-fermion scattering in a $SU(N_c)$ gauge theory with n_f fermions. It is $16d_fn_fC_fC_A$ for fermion-boson

scattering and $4d_AC_A^2$ for boson-boson scattering. This term is the third source which lead a contribution to λ_1. However, even though the scatters are enhanced via soft gluon exchange, the numerical simulation demonstrate that its contribution to λ_1 is quite small, never exceeding 0.003 for 3-flavor QCD and 0.0003 for pure gluon QCD.

Table 7.2.2 summarizes the results for strongly coupled $N = 4$ SYM theory in [173] and for weakly coupled QCD given by York and Moore.

Coeffcients	τ_π	λ_1	λ_2	λ_3	κ
$N = 4$ SYM	$\frac{2-\ln 2}{2\pi T}$	$\frac{\eta}{2\pi T}$	$\frac{-\ln 2\eta}{\pi T}$	0	$\frac{\eta}{\pi T}$
Kinetic Theory	$\frac{5.0\sim5.9}{T}\frac{\eta}{s}$	$\frac{4.1\sim5.2}{T}\frac{\eta^2}{s}$	$-2\eta\tau_\pi$	0	$\mathcal{O}(g^{-4})T^2$

7.2.3 Results from Denicol-Koide-Rischke

In the work [175] of Denicol-Koide-Rischke, the authors rederive the equations of motion of dissipative relativistic fluid dynamics from kinetic theory. The original relativistic Boltzmann equation is written as

$$p^\mu \partial_\mu f = C[f] \tag{7.21}$$

To derive the equations of motion for the dissipative currents, Israel and Stewart use the second momentum of the Boltzmann eqaution

$$p^\mu p^\nu p^\lambda \partial_\mu f = p^\nu p^\lambda C[f] \tag{7.22}$$

The expression of f is expanded to second momentum and then truncated by an ansatz of 14 moments approximation. After integrating out both hands, the equations of motion are obtained by the projections $u_\nu u_\lambda \partial_\mu \langle p^\mu p^\nu p^\lambda \rangle$, $\Delta^\alpha_\lambda u_\nu \partial_\mu \langle p^\mu p^\nu p^\lambda \rangle$ and $\Delta^{\alpha\beta}_{\nu\lambda} \partial_\mu \langle p^\mu p^\nu p^\lambda \rangle$ on the both sides of Boltzmann equation. These equations determine the time evolution of

Π, n^μ and $\pi^{\mu\nu}$ through their comoving derivatives.

In contrast with above procedures, the authors directly use the definition of comoving derivatives, where

$$\begin{aligned}
\dot{\Pi} &= -\frac{m^2}{3}\int \mathrm{d}\Gamma \delta\dot{f} \\
\dot{n}^\mu &= \int \mathrm{d}\Gamma p^\mu \delta\dot{f} \\
\dot{\pi}^{\mu\nu} &= \int \mathrm{d}\Gamma p^\mu p^\nu \delta\dot{f}
\end{aligned} \tag{7.23}$$

with the expression of $\delta\dot{f}$, where

$$\delta\dot{f} = -\dot{f}_0 - \frac{1}{u\cdot p} p\cdot\nabla f + \frac{1}{u\cdot p} C[f] \tag{7.24}$$

Therefore, the equation of motion of dissipative currents are obtained,

$$\begin{aligned}
\dot{\Pi} &= -\frac{\Pi}{\tau_\Pi} - \beta_\Pi\theta - l_{\Pi n}\partial\cdot n - \tau_{\Pi n} n\cdot\dot{u} - \delta_{\Pi\Pi}\Pi\theta - \lambda_{\Pi n}\cdot\nabla\alpha_0 + \lambda_{\Pi\pi}\pi^{\mu\nu}\sigma_{\mu\nu} \\
\dot{n}^\mu &= -\frac{n^\mu}{\tau_n} + \beta_n\nabla^\mu\alpha_0 - n_\nu\omega^{\nu\mu} - \delta_{nn} n^\mu\theta - l_{n\Pi}\nabla^\mu\Pi + l_{n\pi}\Delta^{\mu\nu}\partial_\lambda\pi^\lambda_\nu \\
&\quad + \tau_{n\Pi}\Pi\dot{u}^\mu - \tau_{n\pi}\pi^\mu_\nu\dot{u}^\nu - \lambda_{nn} n^\nu\sigma^\mu_\nu + \lambda_{n\Pi}\Pi\nabla^\mu\alpha_0 - \lambda_{n\pi}\pi^{\mu\nu}\nabla_\nu\alpha_0 \\
\dot{\pi}^{\mu\nu} &= -\frac{\pi^{\mu\nu}}{\tau_\pi} + 2\beta_\pi\sigma^{\mu\nu} + 2\pi^\mu_\alpha\omega^{\alpha\nu} - \tau_{\pi n} n^\mu\dot{u}^\nu \\
&\quad + l_{\pi n}\nabla^\mu n^\nu - \delta_{\pi\pi}\pi^{\mu\nu}\theta - \tau_{\pi\pi}\pi^\mu_\alpha\sigma^{\nu\alpha} + \lambda_{\pi n} n^\mu\nabla^\nu\alpha_0 + \lambda_{\pi\Pi}\Pi\sigma^{\mu\nu}
\end{aligned} \tag{7.25}$$

And of course, the equations obtained via the two approaches are formally identical; the only difference is in the coefficients. The authors show that, in the model of a one-dimension massless Boltzmann gas, their coefficients simplify,

$$\beta_\pi = \frac{4P_0}{5}, \quad \tau_\pi^{-1} = \frac{3}{5}\sigma P_0\beta_0, \quad \lambda = \frac{124}{63} \tag{7.26}$$

which differ with the results from IS theory,

$$\beta_\pi = \frac{2P_0}{3}, \quad \tau_\pi^{-1} = \frac{5}{9}\sigma P_0 \beta_0, \quad \lambda = 2 \tag{7.27}$$

And the latter approach is better adapted than IS theory to capture the microphysics contained in the Boltzmann equation.

7.3 Conclusion

Hydrodynamic picture is an excellent tool to explore the time evolution of strongly coupled system at its initial time stage. However, considering a real physics system, the validity of hydrodynamic equation is not only limited to sufficiently early times, but also to sufficiently high density regions, for example, the low transverse momenta regions of strongly coupled QGP; the dense core of trapped unitarity gas. Correspondingly, it is important for us to completely understand the conditions when hydrodynamics breakdown and reduce to kinetic theory.

We have already know that, in kinetic theory, the two particle collisions are not sensitive to the system density and lead to the density independent transport coefficients. However, if the three body interaction is taken into account at moderated densities, it effect an positive density dependent correction on the transport coefficients. The second order hydrodynamics expand the gradients of temperature and velocity to higher orders; introduce more undetermined transport coefficients and lead negative corrections on the known transport coefficients, viscosity and thermal conductivity. It actually imposed an important question: at the moderate densities, could we obtain the consistent limitation of transport coefficients through these two approaches?

Grad's momentum expansion method and Chapman-Enskog expansions method are served as the tools to accomplish the second order hydrodynamic equations under the framework of kinetic theory. However, in contrast to the remarkable succusses of kinetic theory in which recover the Navier-Stokes equation at the first order. One hasn't obtained the fully systematic formula which match the kinetic theory to the second order hydrodynamics. At the end of this thesis, I would like to bring another interesting question: is able to recover the second order hydrodynamics equation from the kinetic theory which take into account the three body collisions?

REFERENCES

[1] J. Adams, C. Adler, MM Aggarwal, Z. Ahammed, J. Amonett, BD Anderson, M. Anderson, D. Arkhipkin, GS Averichev, SK Badyal, et al. Particle-type dependence of azimuthal anisotropy and nuclearmodification of particle production in Au+ Au collisions at $\sqrt{s_{NN}} = 200$GeV. *Phys. Rev. Lett.*, 92(LBNL–55274), 2003.

[2] J. Adams, MM Aggarwal, Z. Ahammed, J. Amonett, BD Anderson, D. Arkhipkin, GS Averichev, SK Badyal, Y. Bai, J. Balewski, et al. Multistrange Baryon Elliptic Flow in Au+ Au Collisions at $\sqrt{s_{NN}} = 200$GeV. *Phys. Rev. Lett.*, 95(12):122301, 2005.

[3] P.R. Sorensen. *Kaon and Lambda Production at Intermediate p_T: Insights into the Hadronization of the Bulk Partonic Matter Created in Au+ Au Collisions at RHIC.* PhD thesis, University of California, Los Angeles, 2003.

[4] U.W. Heinz. Thermalization at RHIC. *Arxiv preprint nucl-th/0407067*, 2004.

[5] P. Huovinen, P.F. Kolb, U. Heinz, PV Ruuskanen, and S.A. Voloshin. Radial and elliptic flow at RHIC: Further predictions. *Phys. Lett. B*, 503(1-2):58–64, 2001.

[6] http://ltl.tkk.fi/research/theory/helium.html.

[7] M.G. Alford, A. Schmitt, K. Rajagopal, and T. Schäfer. Color superconductivity in dense quark matter. *Rev. Mod. Phys.*, 80(4):1455, 2008.

[8] J. L. Roberts, N. R. Claussen, S. L. Cornish, and C. E. Wieman. Magnetic field dependence of ultracold inelastic collisions near a feshbach resonance. *Phys. Rev. Lett.*, 85(4):728–731, Jul 2000.

[9] Neil R. Claussen. *Dynamics of Bose-Einstein condensates near a Feshbach resonance in ^{85}Rb.* PhD thesis, University of Colorado, 2003. https://jilawww.colorado.edu/pubs/thesis/claussen/.

[10] M. H. Ernst. Bogoliubov Choh Uhlenbeck Theory: Cradle of Modern Kinetic Theory. *ArXiv Condensed Matter e-prints*, July 1997.

[11] LD Landau, EM Lifshitz, and L.E. Reichl. Statistical physics, part 1. *Physics Today*, 34:74, 1981.

[12] K. Adcox et al. Formation of dense partonic matter in relativistic nucleus nucleus collisions at RHIC: Experimental evaluation by the PHENIX collaboration. *Nucl. Phys.*, A757:184–283, 2005.

[13] I. Arsene et al. Quark Gluon Plasma an Color Glass Condensate at RHIC? The perspective from the BRAHMS experiment. *Nucl. Phys.*, A757:1–27, 2005.

[14] B. B. Back et al. The PHOBOS perspective on discoveries at RHIC. *Nucl. Phys.*, A757:28–101, 2005.

[15] John Adams et al. Experimental and theoretical challenges in the search for the quark gluon plasma: The STAR collaboration's critical assessment of the evidence from RHIC collisions. *Nucl. Phys. A*, 757:102–183, 2005.

[16] AJ Leggett. Modern trends in the theory of condensed matter. *Proceedings of the XVIth Karpacz Winter School of Theoretical Physics, Springer Verlag*, page 1327, 1980.

[17] P. Nozieres and S. Schmitt-Rink. Bose condensation in an attractive fermion gas: From weak to strong coupling superconductivity. *Journal of Low Temp. Physics*, 59(3):195–211, 1985.

[18] D. Vollhardt and P. Wölfle. *The superfluid phases of helium 3*. CRC, 1990.

[19] A.J. Leggett. *Quantum liquids: Bose condensation and Cooper pairing in condensed-matter systems*. Oxford University Press, USA, 2006.

[20] A. Griffin, DW Snoke, and S. Stringari. *Bose-Einstein Condensation*. Cambridge Univ Pr, 1996.

[21] A.J. Leggett. Bose-Einstein condensation in the alkali gases: Some fundamental concepts. *Rev. Mod. Phys.*, 73(2):307–356, 2001.

[22] I. Bloch, J. Dalibard, and W Zwerger. Many-body physics with ultracold gases. *Rev. Mod. Phys.*, 80:885, 2008. [arXiv:0704.3011].

[23] S. Giorgini, L. P. Pitaevskii, and S. Stringari. Theory of ultracold atomic fermi gases. *Rev. Mod. Phys.*, 80:1215, 2008. [arXiv:0706.3360].

[24] T. Alm, B.L. Friman, G. Röpke, and H. Schulz. Pairing instability in hot asymmetric nuclear matter. *Nuclear Physics A*, 551(1):45–53, 1993.

[25] M. Baldo, U. Lombardo, and P. Schuck. Deuteron formation in expanding nuclear matter from a strong coupling BCS approach. *Phys. Rev. C*, 52(2):975–985, 1995.

[26] H. Stein, A. Schnell, T. Alm, and G. Röpke. Correlations and pairing in nuclear matter within the Nozieeres-Schmitt-Rink approach. *Z. Phys. A*, 351:295, 1995.

[27] P. Boek. Superfluid nuclear matter calculations. *Nucl. Phys. A*, 657(2):187–215, 1999.

[28] L. Mestel. On the theory of white dwarf stars. I. The energy sources of white dwarfs. *Monthly Notices of the Royal Astronomical Society*, 112:583, 1952.

[29] B. Paczynski. Evolution of Single Stars. I. Stellar Evolution from Main Sequence to White Dwarf or Carbon Ignition. *Acta Astronomica*, 20:47, 1970.

[30] C. Kittel and P. McEuen. *Introduction to solid state physics*, volume 4. Wiley New York, 1986.

[31] L.D. Landau. The theory of a Fermi liquid. *Sov. Phys. JETP*, 3(6):920–925, 1957.

[32] G. Baym and C. Pethick. Landau Fermi-liquid theory: concepts and applications. *Quark-gluon plasma*, 190:193, 2004.

[33] AA Abrikosov and IM Khalatnikov. The theory of a Fermi liquid. *Rep. Prog. Phys*, 22:329–367, 1959.

[34] K. Yagi, T. Hatsuda, and Y. Miake. *Quark-Gluon Plasma*, volume 1. 2005.

[35] Arthur M. Poskanzer. Anisotropic flow at the SPS and RHIC. 2001.

[36] M. Gyulassy, I. Vitev, and X.N. Wang. High p_T Azimuthal Asymmetry in Noncentral A+ A at RHIC. *Phys. Rev. Lett.*, 86(12):2537–2540, 2001.

[37] M. Gyulassy, P. Levai, and I. Vitev. Jet tomography of Au+ Au reactions including multi-gluon fluctuations. *Phys. Lett. B*, 538(3-4):282–288, 2002.

[38] D. Molnar and S.A. Voloshin. Elliptic flow at large transverse momenta from quark coalescence. *Phys. Rev. Lett.*, 91(9):92301, 2003.

[39] R. Balian and NR Werthamer. Superconductivity with Pairs in a Relative p Wave. *Phys. Rev.*, 131(4):1553–1564, 1963.

[40] PW Anderson and WF Brinkman. Anisotropic Superfluidity in ^{3}He: A Possible Interpretation of Its Stability as a Spin-Fluctuation Effect. *Phys. Rev. Lett.*, 30(22):1108–1111, 1973.

[41] P. Kapitza. Viscosity of liquid helium below the-point. *Nature*, 141(3558):74, 1938.

[42] JF Allen and AD Misener. Flow of liquid helium II. *Nature*, 141(3558):75, 1938.

[43] L. Landau. Theory of the superfluidity of helium II. *Phys. Rev.*, 60(4):356–358, 1941.

[44] L. Tisza. Transport phenomena in helium II. *Nature*, 141(3577):913, 1938.

[45] E.M. Gosling, IR McDonald, and K. Singer. On the calculation by molecular dynamics of the shear viscosity of a simple fluid. *Molecular Physics*, 26(6):1475–1484, 1973.

[46] W.T. Ashurst and WG Hoover. Dense-fluid shear viscosity via nonequilibrium molecular dynamics. *Phys. Rev. A*, 11(2):658–678, 1975.

[47] D. T. Son. Vanishing bulk viscosities and conformal inv of unitary fermi gas. *Phys. Rev. Lett.*, 98:020604, 2007. [arXiv:cond-mat/0511721].

[48] K. Meier, A. Laesecke, and S. Kabelac. Transport coefficients of the Lennard-Jones model fluid. I. Viscosity. *The Journal of Chemical Physics*, 121:3671, 2004.

[49] D. Kharzeev and K. Tuchin. Bulk viscosity of QCD matter near the critical temperature. *JHEP*, 2008:093, 2008.

[50] E. M. Lifshitz L. D. Landau. *Physical Kinetics*, volume X of *Course of Theoretical Physics*. Pergamon Press, 1981.

[51] E. M. Lifshitz L. D. Landau. *Fluid Dynamics*, volume VI of *Course of Theoretical Physics*. Pergamon Press, 1959.

[52] J. Stewart. Non-equilibrium relativistic kinetic theory. *Non-equilibrium relativistic kinetic theory*, pages 1–113, 1971.

[53] JM Stewart. On transient relativistic thermodynamics and kinetic theory. *Proceedings of the Royal Society of London. Series A, Mathematical and Physical Sciences*, 357(1688):59–75, 1977.

[54] W. Israel and JM Stewart. Transient relativistic thermodynamics and kinetic theory. *Annals of Physics*, 118(2):341–372, 1979.

[55] A. Muronga. Second-Order Dissipative Fluid Dynamics for Ultrarelativistic Nuclear Collisions. *Phys. Rev. Lett.*, 88(6):62302, 2002. [arXiv:nucl-th/0104064v4].

[56] A. Muronga. Causal theories of dissipative relativistic fluid dynamics for nuclear collisions. *Phys. Rev. C*, 69(3):34903, 2004.

[57] C. Eckart. The thermodynamics of irreversible processes. III. Relativistic theory of the simple fluid. *Phys. Rev.*, 58(10):919–924, 1940.

[58] NN Bogoliubov. On the theory of superfluidity. *J. Phys.(USSR)*, 11(23):4–2, 1947.

[59] S.R. Groot, W.A. Leeuwen, and C.G. van Weert. *Relativistic Kinetic Theory: Principles and Applications*. North-Holland Pub. Co., 1980.

[60] K. Huang. *Statistical mechanics*. 1963.

[61] R.L. Liboff. *Kinetic theory: classical, quantum, and relativistic descriptions*. Springer Verlag, 2003.

[62] H. Grad. On the kinetic theory of rarefied gases. *Communications on Pure and Applied Mathematics*, 2(4):331–407, 1949.

[63] AV Bobylev. The Chapman-Enskog and Grad methods for solving the Boltzmann equation. In *Akademiia Nauk SSSR Doklady*, volume 262, pages 71–75, 1982.

[64] C. Cercignani and G.M. Kremer. *The relativistic Boltzmann equation: theory and applications*. Birkhauser, 2002.

[65] EGD Cohen. Fifty years of kinetic theory. *Physica A: Statistical Mechanics and its Applications*, 194(1-4):229–257, 1993.

[66] LS Garcia-Colin and A. Flores. Note on the transport coefficients of a moderately dense gas. *Physica*, 32(2):444–449, 1966.

[67] LS Garcia-Colin, RM Velasco, and FJ Uribe. Beyond the Navier-Stokes equations: Burnett hydrodynamics. *Physics Reports*, 465(4):149–189, 2008.

[68] LS Garcia-Colin and M. Löpez de Haro. The Burnett equations in extended irreversible thermodynamics. *Journal of Non-Equilibrium Thermodynamics*, 7(2):95–104, 1982.

[69] C. Manuel, A. Dobado, and F. J. Llanes-Estrada. Shear viscosity in a cfl quark star. *JHEP*, 0509:076, 2005. [arXiv:hep-ph/0406058].

[70] M.G. Alford, M. Braby, and A. Schmitt. Bulk viscosity in kaon-condensed color–flavor-locked quark matter. *Journal of Physics G: Nuclear and Particle Physics*, 35:115007, 2008.

[71] C. Manuel and F. J. Llanes-Estrada. Bulk viscosity in a cold cfl superfluid. *JCAP*, 0708:001, 2007. [arXiv:0705.3909 [hep-ph]].

[72] P. Jaikumar, M. Prakash, and T. Schäfer. Neutrino emission from goldstone modes in dense quark matter. *Phys. Rev. D*, 66:063003, 2002. [arXiv:astro-ph/0203088].

[73] S. Reddy, M. Sadzikowski, and M. Tachibana. Neutrino rates in color flavor locked quark matter. *Nucl. Phys. A*, 714:337, 2003. [arXiv:nucl-th/0203011].

[74] M. Mannarelli and C. Manuel. Transport theory for cold relativistic superfluids from an analogue model of gravity. *Phys. Rev. D*, 77:103014, 2008. [arXiv:0802.0321 [hep-ph]].

[75] N. Iwamoto. Quark beta decay and the cooling of neutron stars. *Phys. Rev. Lett.*, 44:1637, 1980.

[76] H. Heiselberg and C. J. Pethick. Transport and relaxation in degenerate quark plasmas. *Phys. Rev. D*, 48:2916, 1993.

[77] T. Schäfer and K. Schwenzer. Neutrino emission from ungapped quark matter. *Phys. Rev. D*, 70:114037, 2004. [arXiv:astro-ph/0410395].

[78] C. J. Pethick. Cooling of neutron stars. *Rev. Mod. Phys.*, 64:1133, 1992.

[79] H. M. Lattimer, K. A. van Riper, M. Prakash, and M. Prakash. Rapid cooling and the structure of neutron stars. *Astrophys. J.*, 425:802, 1994.

[80] D. G. Yakovlev and C. J. Pethick. Neutron star cooling. *Ann. Rev. Astron. Astrophys.*, 42:169, 2004. [arXiv:astro-ph/0402143].

[81] P. S. Shternin and D. G. Yakovlev. Electron thermal conductivity owing to collisions between degenerate electrons. *Phys. Rev. D*, 74:043004, 2006. [arXiv:astro-ph/0608371].

[82] C. J. Horowitz, O. L. Caballero, and D. K. Berry. Thermal conductivity of the crust of accreting neutron stars. *Phys. Rev. E*, 79:026103, 2009. [arXiv:0804.4409 [astro-ph]].

[83] D.N. Aguilera, V. Cirigliano, J.A. Pons, S. Reddy, and R. Sharma. Superfluid heat conduction and the cooling of magnetized neutron stars. *Phys. Rev. Lett.*, 102(9):91101, 2009.

[84] I. A. Shovkovy and P. J. Ellis. Thermal conductivity of dense quark matter and cooling of stars. *Phys. Rev. C*, 66:015802, 2002. [arXiv:hep-ph/0204132].

[85] F. Karsch. Lattice results on QCD thermodynamics. *Nucl. Phys. A*, 698(1-4):199–208, 2002.

[86] P.J. Siemens. Liquid–gas phase transition in nuclear matter. 1983.

[87] M. Alford, K. Rajagopal, and F. Wilczek. Color-flavor locking and chiral symmetry breaking in high density QCD. *Nucl. Phys. B*, 537(1-3):443–458, 1999.

[88] D. Bailin and A. Love. Superfluidity and superconductivity in relativistic fermion systems. *Physics Reports*, 107(6):325–385, 1984.

[89] R. Casalbuoni. Lecture notes on superconductivity: Condensed matter and QCD. *Lecture at the University of Barcelona, Spain*, 2003.

[90] M. Alford, K. Rajagopal, and F. Wilczek. QCD at finite baryon density: Nucleon droplets and color superconductivity. *Physics Letters B*, 422(1-4):247–256, 1998.

[91] R. Rapp, T. Schäfer, E. Shuryak, and M. Velkovsky. Diquark Bose condensates in high density matter and instantons. *Phys. Rev. Lett.*, 81(1):53–56, 1998.

[92] G. Hooft. Magnetic monopoles in unified gauge theories. *Nucl. Phys. B*, 79(2):276–284, 1974.

[93] W.E. Brown, J.T. Liu, and H. Ren. Transition temperature to the superconducting phase of QCD at high baryon density. *Phys. Rev. D*, 62(5):054016, 2000.

[94] D.K. Hong. Aspects of high density effective theory in QCD. *Nucl. Phys. B*, 582(1-3):451–476, 2000.

[95] D. T. Son and M. A. Stephanov. Inverse meson mass ordering in color-flavor-locking phase of high density qcd. *Phys. Rev. D*, 61:074012, 2000. [arXiv:hep-ph/9910491].

[96] T. Schaefer and F. Wilczek. Quark description of hadronic phases. *Phys. Rev. D*, 60(7):74014, 1999.

[97] R. Casalbuoni and R. Gatto. Effective theory for color-flavor locking in high density qcd. *Phys. Lett. B*, 464:111, 1999. [arXiv:hep-ph/9908227].

[98] P. F. Bedaque and T. Schäfer. High density quark matter under stress. *Nucl. Phys. A*, 697:802, 2002. [arXiv:hep-ph/0105150].

[99] T. Schäfer. Mass terms in effective theories of high density quark matter. *Phys. Rev. D*, 65:074006, 2002. [arXiv:hep-ph/0109052].

[100] M.G. Alford, M. Braby, S. Reddy, and T. Sch
"afer. Bulk viscosity due to kaons in color-flavor-locked quark matter. *Phys. Rev. C*, 75(5):055209, 2007.

[101] I. M. Khalatnikov. *Introduction to the Theory of Superfluidity.* W. .A. Benjamin, Inc., 1965.

[102] K. Zarembo. Dispersion laws for Goldstone bosons in a color superconductor. *Phys. Rev. D*, 62(5):054003, 2000.

[103] H. Jensen, H. Smith, and J. W. Wilkins. Upper and lower bounds on transport coefficients arising from a linearized boltzmann equation. *Phys. Rev*, 185:323, 1969.

[104] D. T. Son. Low-energy quantum effective action for relativistic superfluids. preprint, hep-ph/0204199.

[105] G. Rupak and T. Schäfer. Shear viscosity of a superfluid fermi gas in the unitarity limit. *Phys. Rev. A*, 76:053607, 2007. [arXiv:0707.1520 [cond-mat.other]].

[106] G. P. Lepage. Vegas: An adaptive multidimensional integration program. *J. Comp. Phys.*, 27:192–203, 1978. preprint, CLNS-80/447.

[107] E. Flowers and N. Itoh. Transport properties of dense matter. i. *Astrophys. J.*, 206:218, 1976.

[108] E. Flowers and N. Itoh. Transport properties of dense matter. ii. *Astrophys. J.*, 230:847, 1979.

[109] N. Itoh, S. Mitake, H. Iyetomi, and S. Ichimaru. Electrical and thermal conductivities of dense matter in the liquid metal phase. i. *Astrophys. J.*, 273:774, 1983.

[110] J. Wambach, T. L. Ainsworth, and D. Pines. Quasiparticle interactions in neutron matter for applications in neutron stars. *Nucl. Phys. A*, 555:128, 1993.

[111] D. A. Baiko, P. Haensel, and D. G. Yakovlev. Thermal conductivity of neutrons in neutron star cores. *A&A*, 374:151–163, 2001. [arXiv:astro-ph/0105105].

[112] T. Schäfer and D. Teaney. Nearly perfect fluidity: From cold atomic gases to hot quark gluon plasmas. *Rept. Prog. Phys.*, 72:126001, 2009. [arXiv:0904.3107 [hep-ph]].

[113] K. M. O'Hara, S. L. Hemmer, M. E. Gehm, S. R. Granade, and J. E. Thomas. Observation of a strongly-interacting degenerate fermi gas of atoms. *Science*, 298:2179, 2002. [cond-mat/0212463].

[114] T. Schäfer. The shear viscosity to entropy density ratio of trapped fermions in the unitarity limit. *Phys. Rev. A*, 76:063618, 2007. [arXiv:cond-mat/0701251].

[115] A. Turlapov, J. Kinast, B. Clancy, L. Luo, J. Joseph, and J. E. Thomas. Is a gas of strongly interacting atomic fermions a nearly perfect fluid. *J. Low Temp. Phys*, 150:567, 2008. [arXiv:0707.2574].

[116] T. Schäfer and C. Chafin. Scaling flows and dissipation in the dilute fermi gas at unitarity. [arXiv:0912.4236 [cond-mat.quant-gas]].

[117] K. Dusling and D. Teaney. Simulating elliptic flow with viscous hydrodynamics. *Phys. Rev. C*, 77:034905, 2008. [arXiv:0710.5932 [nucl-th]].

[118] P. Romatschke and U. Romatschke. Viscosity information from relativistic nuclear collisions: How perfect is the fluid observed at rhic? *Phys. Rev. Lett.*, 99:172301, 2007. [arXiv:0706.1522 [nucl-th]].

[119] G. Policastro, DT Son, and AO Starinets. Shear viscosity of strongly coupled N= 4 supersymmetric Yang-Mills plasma. *Phys. Rev. Lett.*, 87(8):81601, 2001.

[120] D. T. Son and A. O. Starinets. Viscosity, black holes, and quantum field theory. *Ann. Rev. Nucl. Part. Sci.*, 57:95, 2007. [arXiv:0704.0240 [hep-th]].

[121] J.M. Maldacena. The large N limit of superconformal field theories and. *Adv. Theor. Math. Phys.*, 2:231–252.

[122] D. T. Son. Toward an ads/cold atoms correspondence: a geometric realization of the schroedinger symmetry. *Phys. Rev. D*, 78:046003, 2008. [arXiv:0804.3972 [hep-th]].

[123] K. Balasubramanian and J. McGreevy. Gravity duals for non-relativistic cfts. *Phys. Rev. Lett.*, 101:061601, 2008. [arXiv:0804.4053 [hep-th]].

[124] C. Cao, E. Elliott, J. Joseph, H. Wu, J. Petricka, T. Schäfer, and J. E. Thomas. Universal quantum viscosity in a unitary fermi gas. *Science*, 331:58–61, 2011. [arXiv:1007.2625 [cond-mat.quant-gas]].

[125] T. Schäfer. Dissipative fluid dynamics for the dilute fermi gas at unitarity: Free expansion and rotation. [arXiv:1008.3876 [cond-mat.quant-gas]].

[126] H. Song and U. W. Heinz. Causal viscous hydrodynamics in 2+1 dimensions for relativistic heavy-ion collisions. *Phys. Rev. C*, 77:064901, 2008. [arXiv:0712.3715 [nucl-th]].

[127] P. Kovtun, D. T. Son, and A. O. Starinets. Viscosity in strongly interacting quantum field theories from black hole physics. *Phys. Rev. Lett.*, 94:111601, 2005. [arXiv:hep-th/0405231].

[128] G. M. Bruun and H. Smith. Viscosity and thermal relaxation for a resonantly interacting fermi gas. *Phys. Rev. A*, 72:043605, 2005. [cond-mat/0504734].

[129] M. A. Escobedo, M. Mannarelli, and C. Manuel. Bulk viscosities for cold fermi superfluids close to the unitary limit. *Phys. Rev. A*, 79:063623, 2009. [arXiv:0904.3023 [cond-mat.quant-gas]].

[130] J. Joseph, B. Clancy, L. Luo, J. Kinast, A. Turlapov, and J. E. Thomas. Sound propagation in a fermi gas near a feshbach resonance. *Phys. Rev. Lett.*, 98:170401, 2007. [cond-mat/0612567].

[131] E. Taylor, H. Hu, X.-J. Liu, L. P. Pitaevskii, A. Griffin, and S. Stringari. First and second sound in a strongly interacting fermi gas. *Phys. Rev. A*, 80:053601, 2009. [arXiv:0905.0257v3 [cond-mat.quant-gas]].

[132] H. Feshbach. Unified theory of nuclear reactions* 1. *Annals of Physics*, 5(4):357–390, 1958.

[133] S. Inouye, MR Andrews, J. Stenger, H.J. Miesner, DM Stamper-Kurn, and W. Ketterle. Observation of Feshbach resonances in a Bose–Einstein condensate. *Nature*, 392(6672):151–154, 1998.

[134] M. Greiner, C.A. Regal, and D.S. Jin. Emergence of a molecular Bose–Einstein condensate from a Fermi gas. *Nature*, 426(6966):537–540, 2003.

[135] C.A. Regal, C. Ticknor, J.L. Bohn, and D.S. Jin. Creation of ultracold molecules from a Fermi gas of atoms. *Nature*, 424(6944):47–50, 2003.

[136] MW Zwierlein, CA Stan, CH Schunck, SMF Raupach, AJ Kerman, and W. Ketterle. Condensation of pairs of fermionic atoms near a Feshbach resonance. *Phys. Rev. Lett.*, 92(12):120403, 2004.

[137] AJ Moerdijk, BJ Verhaar, and A. Axelsson. Resonances in ultracold collisions of 6Li, 7Li, and 23Na. *Phys. Rev. A*, 51(6):4852–4861, 1995.

[138] D. T. Son and M. Wingate. General coordinate invariance and conformal invariance in nonrelativistic physics: Unitary fermi gas. *Annals Phys*, 321:197, 2006. [arXiv:cond-mat/0509786].

[139] D. Lee and T. Schäfer. Cold dilue neutron matter on the lattice i: Lattice virial coefficients and large scattering lengths. *Phys. Rev. C*, 73:015201, 2006. [nucl-th/0509017].

[140] J. Bardeen, L.N. Cooper, and J.R. Schrieffer. Theory of superconductivity. *Phys. Rev.*, 108(5):1175–1204, 1957.

[141] H.K. Onnes. Further experiments with liquid helium. C. On the change of electric resistance of very pure metals at very low temperatures, etc. iv The resistance of pure mercury at helium temperatures. In *Proceedings, Akademie der Wetenschappen, Amsterdam*, volume 13, pages 1274–1276, 1911.

[142] N.M. Plakida. *High-temperature superconductivity: experiment and theory.* Springer-Verlag, 1994.

[143] JI Kapusta. Neutrino superfluidity. *Phys. Rev. Lett.*, 93(25):251801, 2004.

[144] J. Margueron, H. Sagawa, and K. Hagino. BCS-BEC crossover of neutron pairs in symmetric and asymmetric nuclear matter. *Phys. Rev. C*, 76(6):64316, 2007.

[145] Y. Ohashi and A. Griffin. BCS-BEC crossover in a gas of Fermi atoms with a Feshbach resonance. *Phys. Rev. Lett.*, 89(13):130402, 2002.

[146] A. Perali, P. Pieri, L. Pisani, and GC Strinati. BCS-BEC crossover at finite temperature for superfluid trapped Fermi atoms. *Phys. Rev. Lett.*, 92(22):220404, 2004.

[147] GE Astrakharchik, J. Boronat, J. Casulleras, and S. Giorgini. Equation of state of a Fermi gas in the BEC-BCS crossover: A quantum Monte Carlo study. *Phys. Rev. Lett.*, 93(20):200404, 2004.

[148] Q. Chen, J. Stajic, S. Tan, and K. Levin. BCS-BEC crossover: From high temperature superconductors to ultracold superfluids. *Physics Reports*, 412(1):1–88, 2005.

[149] E. Burovski, N. Prokof'ev, B. Svistunov, and M. Troyer. Critical temperature and thermodynamics of attractive fermions at unitarity. *Phys. Rev. Lett.*, 96:160402, 2006. [cond-mat/0602224].

[150] J. Carlson, S.-Y. Chang, V. R. Pandharipande, and K. E. Schmidt. Superfluid fermi gases with large scattering length. *Phys. Rev. Lett.*, 91:050401, 2003. [physics/0303094].

[151] G. Rupak and T. Schäfer. Density functional theory for non-relativistic fermions in the unitarity limit. *Phys. Rev. A*, 816:52, 2009. [arXiv:0804.2678 [nucl-th]].

[152] A. M. J. Schakel. Derivation of the effective action of a dilute fermi gas in the unitary limit of the bcs-bec crossover. *Ann. Phys.*, 326:193–206, 2011. [arXiv:0912.1955v2 [cond-mat.quant-gas]].

[153] R. Haussmann, M. Punk, and W. Zwerger. Spectral functions and rf response of ultracold fermionic atoms. *Phys. Rev. A*, 80:063612, 2009. [arXiv:0904.1333v3 [cond-mat.quant-gas]].

[154] M. Braby, J. Chao, and T. Schäfer. Thermal conductivity of color-flavor locked quark matter. *Phys. Rev. C*, 81:045205, 2010. [arXiv:0909.4236 [hep-ph]].

[155] G. M. Bruun and H. Smith. Shear viscosity and damping for a fermi gas in the unitarity limit. *Phys. Rev. A*, 75:043612, 2007. [cond-mat/0612460].

[156] T. R. Kirkpatrick and J. R. Dorfman. Transport in a dilute but condensed nonideal bose gas: Kinetic equations. *J. Low Temp. Phys*, 58:301, 1985.

[157] P. C. Hohenberg and B. I. Halperin. Theory of dynamic critical phenomena. *Rev. Mod. Phys.*, 49:435, 1977.

[158] G. M. Bruun and H. Smith. Frequency and damping of the scissors mode of a fermi gas. *Phys. Rev. A*, 76:045602, 2007. [arXiv:0709.1617].

[159] M. Braby, J. Chao, and T. Schäfer. Thermal conductivity and sound attenuation in dilute atomic fermi gases. *Phys. Rev. A*, 82:033619, 2010. [arXiv:1003.2601 [cond-mat.quant-gas]].

[160] H. Guo, D. Wulin, C. C. Chien, and K. Levin. Microscopic approach to viscosities in superfluid fermi gases: From bcs to bec. [arXiv:1008.0423 [cond-mat.quant-gas]].

[161] T. Enss, R. Haussmann, and W. Zwerger. Viscosity and scale invariance in the unitary fermi gas. *Annals Phys.*, 326:770–796, 2011. [arXiv:1008.0007 [cond-mat.quant-gas]].

[162] E. Taylor and M. Randeria. Viscosity of strongly interacting quantum fluids: spectral functions and sum rules. *Phys. Rev. A*, 81:053610, 2010. [arXiv:1002.0869 [cond-mat.quant-gas]].

[163] T. Nikuni and A. Griffin. Frequency and damping of hydrodynamic modes in a bose-condensed gas. *Phys. Rev. A*, 69:023604, 2004. [arXiv:cond-mat/0309269].

[164] G. Aarts and J.M.M. Resco. Transport coefficients, spectral functions and the lattice. *Journal of High Energy Physics*, 2002:053, 2002.

[165] D. Teaney. Finite temperature spectral densities of momentum and r-charge correlators in $n = 4$ yang mills theory. *Phys. Rev. D*, 74:045025, 2006. [arXiv:hep-ph/0602044].

[166] G. D. Moore and O. Saremi. Bulk viscosity and spectral functions in qcd. *JHEP*, 0809:015, 2008. [arXiv:0805.4201 [hep-ph]].

[167] H. B. Meyer. Energy-momentum tensor correlators and spectral functions. *JHEP*, 0808:031, 2008. [arXiv:0806.3914 [hep-lat]].

[168] J. Hong and D. Teaney. Spectral densities for hot qcd plasmas in a leading log approximation. arXiv:1003.0699 [nucl-th].

[169] Y. Nishida and D. T. Son. Nonrelativistic conformal field theories. *Phys. Rev. D*, 76:086004, 2007. [arXiv:0706.3746].

[170] H. Andréasson. The Einstein-Vlasov system/kinetic theory. *Living Rev. Relativ*, 8(2):2005–2, 2005.

[171] Y. Choquet-Bruhat. *General Relativity and the Einstein Equations*. Oxford University Press, 2009.

[172] S. Tan. Energetics of a strongly correlated fermi gas. *Annals Phys.*, 323:2952, 2008. [arXiv:cond-mat/0505200].

[173] R. Baier, P. Romatschke, D. T. Son, A. O. Starinets, and M. A. Stephanov. Relativistic viscous hydrodynamics, conformal invariance, and holography. *JHEP*, 04:100, 2008. [arXiv:0712.2451 [hep-th]].

[174] M. York and G. Moore. Second order hydrodynamic coefficients from kinetic theory. *Phys. Rev. D*, 79:054011, 2009. [arXiv:0811.0729 [hep-ph]].

[175] GS Denicol, T. Koide, and DH Rischke. Dissipative relativistic fluid dynamics: a new way to derive the equations of motion from kinetic theory. *Phys. Rev. Lett.*, 105:162501, 2010. [arXiv:1004.5013].

[176] JV Sengers. Density expansion of the viscosity of a moderately dense gas. *Phys. Rev. Lett.*, 15(12):515–517, 1965.

[177] U. Heinz, H. Song, and AK Chaudhuri. Dissipative hydrodynamics for viscous relativistic fluids. *Phys. Rev. C*, 73(3):34904, 2006.

[178] M. Luzum and P. Romatschke. Conformal relativistic viscous hydrodynamics: Applications to RHIC results at $\sqrt{s_{NN}} = 200GeV$. *Phys. Rev. C*, 78(3):34915, 2008. [arXiv:0804.4015v4 [nucl-th]].

APPENDICES

Appendix A

A.1 Streaming Terms in the Boltzmann Equation

A.1.1 Superfluid Phonon

In this appendix we compute the quantity α_p, which is related to the streaming terms (the left-hand side) of the Boltzmann equation. We will use the dispersion relation for the phonon given by

$$E_p = vp\left(1+\gamma p^2\right) \equiv vp\left(1+\epsilon\frac{v^2\,p^2}{T^2}\right)\,. \tag{A.1}$$

The left-hand side of the Boltzmann equation can be written as

$$\frac{df_p}{dt} = \frac{\partial f_p}{\partial t} + \boldsymbol{v}_p\cdot\boldsymbol{\nabla} f_p\,, \tag{A.2}$$

where $\mathbf{v}_p$ is the particle velocity. In local thermal equilibrium the time dependence of f_p arises from the time dependence of the local temperature and fluid velocity. We have

$$\frac{\partial f_p}{\partial t} = \frac{f_p^0(1+f_p^0)}{T}\left(\frac{E_p}{T}\frac{\partial T}{\partial t} + \boldsymbol{p}\cdot\frac{\partial \boldsymbol{u}}{\partial t}\right)\,, \tag{A.3}$$

where we have used the fact that by going to the local rest frame we can set the local fluid velocity (but not its derivatives to zero). We have also used that the number of phonons is not conserved, and the phonon chemical potential is zero. The spatial derivatives can be written as

$$\boldsymbol{v}_p \cdot \boldsymbol{\nabla} f_p = \frac{f_p^0(1+f_p^0)}{T}\left(\frac{E_p}{T}\boldsymbol{v}_p \cdot \boldsymbol{\nabla} T + \boldsymbol{v}_p \cdot \boldsymbol{\nabla}(\boldsymbol{p}\cdot\boldsymbol{u})\right) . \tag{A.4}$$

We can simplify these expressions using the Euler equation

$$\frac{\partial \boldsymbol{u}}{\partial t} = -\frac{1}{\rho_n}\boldsymbol{\nabla} P = -\frac{1}{\rho_n}\frac{dP}{dT}\boldsymbol{\nabla} T \tag{A.5}$$

where P is the pressure and ρ_n is the density of the normal component of the fluid which is defined by

$$\boldsymbol{\pi} = \rho_n \boldsymbol{u} \,, \tag{A.6}$$

where $\boldsymbol{\pi}$ is the momentum density of the fluid. We can now collect all terms that contain a gradients of T. We find

$$\frac{df_p}{dt} = \frac{f_p^0(1+f_p^0)}{T}\left(\frac{E_p}{T}\boldsymbol{v}_p \cdot \boldsymbol{\nabla} T - \frac{1}{\rho_n}\frac{dP}{dT}\boldsymbol{p}\cdot\boldsymbol{\nabla} T\right) . \tag{A.7}$$

Noting that $\boldsymbol{v}_p = (v_p/p)\boldsymbol{p}$ and using our definition of α_p in Eq. (4.57), we can write

$$\alpha_p = \frac{E_p\, v_p}{p} - \frac{T}{\rho_n}\frac{dP}{dT} \,. \tag{A.8}$$

The pressure of the phonon gas is given by

$$P = -T\int d\Gamma \ln\left(1 - e^{-E_p/T}\right) , \tag{A.9}$$

leading to

$$\frac{dP}{dT} = \frac{1}{3T}\int d\Gamma(3E_p + v_p\, p) f_p^0 \simeq \frac{2\pi^2 T^3}{45 v^3}\left(1 - \frac{60\epsilon\pi^2}{7}\right) , \tag{A.10}$$

where we have kept terms up to linear order in ϵ. The effective mass density, defined in Eq. (A.6), is given by

$$\rho_n = \frac{1}{3T}\int d\Gamma p^2 f_p^0(1 + f_p^0) \simeq \frac{2\pi^2 T^4}{45 v^5}\left(1 - 20\epsilon\pi^2\right) . \tag{A.11}$$

Inserting these results into Eq. (A.8) we get

$$\alpha_p^{(P)} = 4\epsilon v^2 \left[\frac{v^2\, p^2}{T^2} - \frac{20\pi^2}{7}\right] . \tag{A.12}$$

We note that $\alpha_p = 0$ for $\epsilon = 0$. This result is consistent with Eq. (4.48). In the case of phonons with an exactly linear dispersion relation, the LHS side (the streaming term) of the Boltzmann equation is zero. The RHS (the collision term) is zero if δf_p is a zero mode of the linearized collision operator. The zero mode associated with momentum conservation satisfies the constraints in Eq. (4.47) and, because of Eq. (4.48), gives a vanishing thermal conductivity. For $\epsilon \neq 0$ both the LHS and the RHS are not zero, and the corresponding solution of the linearized Boltzmann equation leads to a finite thermal conductivity.

A.1.2 Massive Kaon

In this section we compute the streaming term for kaons. There are two important differences as compared to the phonon case: kaons are massive, and they carry conserved charges (hypercharge and isospin) which couple to chemical potentials. For simplicity we consider only the neutral kaon, which couples to a single chemical potential (a linear

combination of isopsin and hypercharge). We will also consider the limit of low temperature, such that $T \ll m, \mu, \delta m \equiv m - \mu$, where $m \equiv m_K$ and $\mu \equiv \mu_K$. The left-hand side of the Boltzmann equation can be written as

$$\frac{df_p}{dt} = \frac{\partial f_p}{\partial \boldsymbol{u}} \cdot \frac{d\boldsymbol{u}}{dt} + \frac{\partial f_p}{\partial T}\frac{dT}{dt} + \frac{\partial f_p}{\partial \mu}\frac{d\mu}{dt} + \boldsymbol{v}_p \cdot \text{gradient terms} \tag{A.13}$$

The time derivatives of the temperature and the chemical potential can be converted to spatial derivatives using the the continuity equation. These terms do not contribute to the thermal conductivity. The derivative of the velocity field can be rewritten using the Euler equation

$$\frac{d\boldsymbol{u}}{dt} = -\frac{1}{\rho_K}\boldsymbol{\nabla} P. \tag{A.14}$$

where ρ_K is the mass density of the kaon fluid. Spatial derivatives of the velocity field only contribute to the shear viscosity. The spatial derivative of the chemical potential can be rewritten using the Gibbs-Duhem relation $dP = nd\mu + sdT$, where n is the density and s is the entropy density. We get

$$\boldsymbol{\nabla}\mu = \frac{1}{n}\boldsymbol{\nabla} P - \frac{s}{n}\boldsymbol{\nabla} T\,. \tag{A.15}$$

Collecting gradients of the temperature and pressure we find

$$\frac{df_p}{dt} = \left(\frac{\partial f_p}{\partial T} - \frac{s}{n}\frac{\partial f_p}{\partial \mu}\right)\boldsymbol{v}_p \cdot \boldsymbol{\nabla} T + \left(\frac{\boldsymbol{v}_p}{n}\frac{\partial f_p}{\partial \mu} - \frac{1}{\rho_K}\frac{\partial f_p}{\partial \boldsymbol{u}}\right) \cdot \boldsymbol{\nabla} P\,. \tag{A.16}$$

At this point we need to specify explicit expressions for the thermodynamic quantities. The pressure of an ideal gas of massive bosons is given by

$$P = -T \int d\Gamma \ln\left(1 - e^{-(E_p-\mu)/T}\right) . \tag{A.17}$$

The entropy density, particle density, and mass density are

$$\begin{aligned} s &= \frac{1}{3T}\int d\Gamma\, f_p^0 \left(3\left(E_p-\mu\right)+v_p p\right) \simeq \left(\frac{\delta m}{T}+\frac{5}{2}\right) n\,, \\ n &= \int d\Gamma\, f_p^0 \simeq \left(\frac{m\,T}{2\pi v^2}\right)^{3/2} e^{-\delta m/T}\,, \\ \rho_K &= \frac{1}{3T}\int d\Gamma\, p^2\, f_p^0(1+f_p^0) \simeq \frac{m}{v^2} n\,, \end{aligned} \tag{A.18}$$

where we have given analytical results in the low temperature limit. We also need the derivatives of the distribution function with respect to the thermodynamic quantities,

$$\begin{aligned} \frac{\partial f}{\partial T} &= \frac{f_p^0(1+f_p^0)}{T}\frac{E_p-\mu}{T} \\ \frac{\partial f}{\partial \mu} &= \frac{f_p^0(1+f_p^0)}{T} \\ \frac{\partial f}{\partial \boldsymbol{u}} &= \frac{f_p^0(1+f_p^0)}{T}\boldsymbol{p}. \end{aligned} \tag{A.19}$$

The coefficient of the $\boldsymbol{\nabla} P$ term in Eq. (A.16) is given by

$$\frac{\boldsymbol{v}_p}{n}\frac{\partial f}{\partial \mu} - \frac{1}{\rho_K}\frac{\partial f}{\partial \boldsymbol{u}} = \frac{f_p^0(1+f_p^0)}{T}\left(\frac{\boldsymbol{v}_p}{n} - \frac{\mathbf{p}}{\rho_K}\right). \tag{A.20}$$

Using $v_p = v^2 p/E_p \sim v^2 p/m$ we can see that $v_p/p \sim v^2/m$. We can also show that $n/\rho_K = v^2/m$. This implies that the coefficient of $\boldsymbol{\nabla} P$ is zero. The $\boldsymbol{\nabla} T$ term is

$$\frac{df}{dt} = \left(\frac{\partial f}{\partial T} - \frac{s}{n}\frac{\partial f}{\partial \mu}\right) \boldsymbol{v}_p \cdot \boldsymbol{\nabla} T = \frac{f_p^0(1+f_p^0)}{T}\left(\frac{E_p - \mu}{T} - \frac{s}{n}\right) \boldsymbol{v}_p \cdot \boldsymbol{\nabla} T \,. \tag{A.21}$$

We can then read off the coefficient α_p. We find

$$\alpha_p^{(K)} = \frac{v^2}{m}\left[E_p - \mu - \frac{Ts}{n}\right] \simeq \frac{v^4 p^2}{2m^2} - \frac{5v^2 T}{2m} \,. \tag{A.22}$$

A.2 Orthogonal Polynomials

In this appendix we collect some explicit expressions for the orthogonal polynomials $B_s(p^2)$ introduced in section 4.7. The starting point is Eq. (4.68)

$$\int d\Gamma f_p^0(1+f_p^0) p^2 B_s(p^2) B_t(p^2) \equiv A_s \delta_{st} \,, \tag{B.23}$$

together with $B_0 = 1$. We write

$$\begin{aligned} B_0 &= 1 \\ B_1 &= p^2 + c_{10} \\ B_2 &= p^4 + c_{22} p^2 + c_{20} \\ B_3 &= p^6 + c_{34} p^4 + c_{32} p^2 + c_{30} \\ &\vdots \end{aligned} \quad , \tag{B.24}$$

and iteratively determine the coefficients c_{st}. For example, we find

$$c_{10} = \begin{cases} -\frac{20\pi^2 T^2}{7v^2} & \text{phonons,} \\ -\frac{5mT}{v^2} & \text{kaons.} \end{cases} \tag{B.25}$$

which implies that $B_1 \propto \alpha_p$. This relation plays a role in ensuring the consistency of the linearized Boltzmann equation. The variational function $g(p) = B_0$ is a zero mode of the linearized collision operator. We already showed that a term $g(p) \propto B_0$ is eliminated by the constraints, Eq. (4.48), and that it does not contribute to the thermal conductivity. The collision operator acting on any function $g(p)$ is orthogonal to B_0, because B_0 is a zero mode, and the collision operator is hermitean. This implies that the streaming term must be orthogonal to B_0 also. The streaming term is proportional to α_p, and orthogonality to B_0 follows from the relation $\alpha_p \propto B_1$.

The final result for the thermal conductivity requires the normalization constant A_1. Using the result for B_1 we get

$$A_1 = \int d\Gamma\, f_p^0(1+f_p^0)p^2(p^2+c_{10})^2 = \begin{cases} \frac{256\pi^6}{245v^9}T^9 & \text{phonons,} \\ \frac{15}{32\pi^{3/2}}\left(\frac{2mT}{v^2}\right)^{9/2} e^{-\delta m/T} & \text{kaons.} \end{cases} \tag{B.26}$$

Appendix B

B.1 Trial Functions

We expand on the definitions of the trial funcion polynomials as defined in Eq. (5.32),

$$A_s^{(F,H)}\delta_{st} = \int \mathrm{d}x\, f^0(x)(1 \pm f^0(x))x^4 B_s^{(F,H)}(x^2)B_t^{(F,H)}(x^2)\,. \tag{A.1}$$

where

$$B_s^{(F,H)}(x^2) = x^{2s} + \sum_{i=0}^{s-1} a_{si}^{(F,H)} x^{2i} \tag{A.2}$$

such that $B_0^{(F,H)}(x^2) = 1$. Defining

$$c_n^{(F,H)} = \int \mathrm{d}x\, f^0(x)(1 \pm f^0(x))x^{4+n}, \tag{A.3}$$

we see that $A_0 = c_0$. We can then proceed to find

$$\begin{aligned} a_{10} &= -c_2/c_0 \\ a_{20} &= (c_2c_6 - c_4^2)/(c_0c_4 - c_2^2) \\ a_{21} &= (c_0c_6 - c_2c_4)/(c_0c_4 - c_2^2) \\ &\vdots \end{aligned} \tag{A.4}$$

We can then calculate that

$$A_1 = c_4 - c_2^2/c_0 \tag{A.5}$$

Evaluating the integrals for c_n in the two cases of fermions with $E_p = p^2/(2m)$ and phonons with $E_p = vp$, we find

$$\begin{aligned} A_1^F &= \frac{512}{245}\pi^8 \\ A_1^H &= 1.31152, \end{aligned} \tag{A.6}$$

which we can then use to evaluate the expressions for the thermal conductivity.

B.2 Thermodynamic Properties

B.2.1 Virial Expansion

In the high temperature limit, $T \gg T_F$, it is convenient to use a virial expansion to rewrite the pressure and other thermodynamical quantities, such as c_V and c_P. We begin

with an expansion of the pressure as,

$$P(\mu, T) = \frac{\nu T}{\lambda^3} \sum_{l=1}^{\infty} b_l z^l \tag{B.7}$$

where $\lambda = \sqrt{2\pi/mT}$ is thermal wave length, ν is the egeneracy factor and $z = \mathrm{e}^{\mu/T}$ is the fugacity. b_1 is 1 always (and corresponds to the ideal gas), but we are interested in the first-order corrections which have been previous calculated, [**?**, 139]. There are two sources for b_2; one is from quantum corrections to the classical statistics, which becomes important as $n\lambda^3 \sim 1$; another one is related to atomic interaction. The correction of due to quantum statistics is

$$b_l^0 = \begin{cases} l^{-\frac{5}{2}} & \text{for ideal Bose gas} \\ (-1)^{l+1} l^{-\frac{5}{2}} & \text{for ideal Fermi gas} \end{cases} \tag{B.8}$$

From the standard cluster expansion, we can write down the expression of the effect of due to non-zero scattering length,

$$b_2 - b_2^0 = \sqrt{2} \sum_n (\mathrm{e}^{-\epsilon_n/T} - \mathrm{e}^{-\epsilon_n^0/T}) \tag{B.9}$$

where ϵ_n is the energy spectrum for the interacting system in the center of mass frame and ϵ_n^0 is the energy for the non-interacting system. This has been calculated in Ref. [139] as

$$b_2 - b_2^0 = \begin{cases} \frac{1}{\sqrt{2}} \mathrm{e}^{x^2} [1 - \mathrm{erf}(|x|)] & x < 0 \\ \sqrt{2} e^{x^2} - \frac{1}{\sqrt{2}} \mathrm{e}^{x^2} [1 - \mathrm{erf}(x)] & x > 0, \end{cases}$$

where erf(x) is the error function, $x = \lambda/(a\sqrt{2\pi})$ and the bound state energy in the $x > 0$ case was assumed to be $E_b = 1/(ma^2)$. We can write down the asymptotic forms in the

limits of zero and infinite scattering lengths as

$$b_2 - b_2^0 = \begin{cases} -\frac{a}{\lambda} & a \to 0^- \\ \sqrt{2}\, e^{1/(mTa^2)} & a \to 0^+ \\ \frac{1}{\sqrt{2}}(1 + \frac{\sqrt{2}}{\pi}\frac{\lambda}{|a|}) & a \to \pm\infty \end{cases} \tag{B.10}$$

Not surprisingly, the interaction part of b_2 approaches a finite number as $a \to \infty$, and is the same order as the effects of quantum statistics. One can also see that the total b_2 will start off negative for small and negative scattering length, but eventually becomes positive as $a \to -\infty$. Interestingly, that means there is a value for the scattering length where the quantum correction and the interaction correction cancel and $b_2 = 0$. For positive scattering length, the contribution from the atomic interaction is always larger (and positive) than the quantum correction, so that $b_2 > 0$ for all $a > 0$. Also, as we approach smaller values of the scattering length ($a \to 0^+$), the bound state energy becomes larger and b_2 starts becoming very large. In this regime, our expansion does not make sense anymore, so we will limit ourselves to the $a < 0$ regime or the large positive scattering lengths.

B.2.2 Specific Heat

Given that our thermodynamic variables are (μ, T), we must use some thermodynamic identities to calculate the specific heats at constant temperature and pressure. The typical derivatives of the pressure are

$$s = \frac{\partial P}{\partial T}\Big|_\mu \quad \text{and} \quad n = \frac{\partial P}{\partial \mu}\Big|_T \tag{B.11}$$

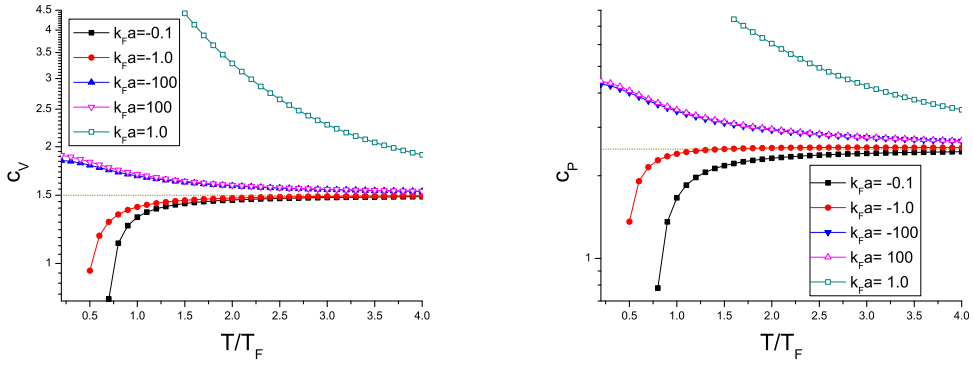

Figure B.1: The left panel shows c_V in units of n_0 as a function of T/T_F n_0. Here, $n_0 = \nu z/\lambda^3$ is the density of the free gas. The right panel shows the temperature dependence of c_P.

To calculate the specific heat at constant volume using the thermodynamical variables, (μ, T), we write down

$$c_V = T\frac{\partial s}{\partial T}\Big|_V = \frac{\partial(s,V)}{\partial(T,V)} = \frac{\partial(s,V)/\partial(T,\mu)}{\partial(T,V)/\partial(T,\mu)} = T\Big[\frac{\partial s}{\partial T}\Big|_\mu - \frac{(\partial n/\partial T)^2_\mu}{(\partial n/\partial \mu)_T}\Big] \tag{B.12}$$

where $V = N/n$ with N being the total number and we have used the definition of the Jacobian,

$$\frac{\partial(a,b)}{\partial(c,d)} = \mathrm{Det}\begin{pmatrix} \partial a/\partial c\big|_d & \partial a/\partial d\big|_c \\ \partial b/\partial c\big|_d & \partial b/\partial d\big|_c \end{pmatrix}$$

We do not express c_P directly, but use the formula for the difference between the specific heats,

$$c_P - c_V = -T\frac{\big[(\partial V/\partial T)_P\big]^2}{(\partial V/\partial P)_T} \tag{B.13}$$

Transforming to the variables (μ, T), we have

$$\frac{\partial V}{\partial T}|_P = \frac{s}{n}\frac{\partial n}{\partial \mu}\Big|_T - \frac{\partial n}{\partial T}\Big|_\mu \tag{B.14}$$

and

$$\frac{\partial V}{\partial P}|_T = \frac{\partial n}{\partial \mu}\Big|_T \tag{B.15}$$

which gives us

$$c_P = c_V + T\frac{\left[\frac{s}{n}(\partial n/\partial \mu)\big|_T - (\partial n/\partial T)\big|_\mu\right]^2}{(\partial n/\partial \mu)\big|_T} \tag{B.16}$$

High Temperature Phase

Using the high temperature expressions for pressure including the first virial correction as $P = \frac{\nu T}{\lambda^3}(z + b_2 z^2)$, we can then derive

$$\begin{aligned} c_V &= \frac{\nu z}{\lambda^3}\left[\frac{3}{2} + \frac{15}{4}z b_2 - zT\frac{\partial b_2}{\partial T} + zT^2\frac{\partial^2 b_2}{\partial^2 T}\right] \\ c_P &= c_V + \frac{\nu z}{\lambda^3}\left[1 + 5z b_2 - 2zT\frac{\partial b_2}{\partial T}\right] \end{aligned} \tag{B.17}$$

Obviously, we arrive at the answers for a classical free gas if $b_2 = 0$ with $n_0 = \frac{\nu z}{\lambda^3}$ being the density for a free gas. We show the results for the specific heats in Fig. B.2.1. Note that the small positive scattering length ($k_F a = 1$) already gives a large deviation from the ideal gas at temperatures of a few times the Fermi temperature, indicating the breakdown of the Virial expansion. Also, note the smoothness of the transition across unitarity, from $a \to -\infty$ to $a \to \infty$.

Superfluid Phase

At zero temperature, the pressure from the fermions, P_F, is given by

$$P_F = \frac{4\sqrt{2}}{15\pi^2\xi^{3/2}} m^{3/2}\mu^{5/2} \tag{B.18}$$

from which we find the zero temperature fermionic density is

$$n_F = \frac{\partial P_F}{\partial \mu}\Big|_T = \frac{2\sqrt{2}m^{3/2}}{3\pi^2\xi^{3/2}}\mu^{3/2} \tag{B.19}$$

In order to calculate second derivatives of the pressure (as needed in the specific heat), we need to thermal contribution from the phonons as well,

$$P_H = \frac{\pi^2 T^4}{90}\Big(\frac{3m}{2\mu}\Big)^{3/2} \tag{B.20}$$

Putting these together and taking the appropriate derivatives, we find

$$\begin{aligned} c_V &= \frac{24\zeta[5]}{\pi^2} T^3 \Big(\frac{3m}{2\mu}\Big)^{3/2} \\ c_P &= c_V + \mathcal{O}(T^7)\ . \end{aligned} \tag{B.21}$$

These equations obviously verify Nernst's theorem, the difference of two type specific heat, $c_P - c_v$ tends to zero more rapidly than specific heats themselves as $T \to 0$. Generally, if entropy $s \sim T^n$ for $T \to 0$, then $c_P - c_v \sim T^{2n+1}$.